# INFLAMMATORY MICROENVIRONMENT ALTERS THE REGENERATIVE CAPACITY OF ADIPOSE-DERIVED MESENCHYMAL STEM CELLS

**Ph.D. THESIS**

Diána Szűcs, M.Sc.

Supervisor:
Zoltán Veréb, PhD


**DOCTORAL SCHOOL OF CLINICAL MEDICINE**
**DEPARTMENT OF DERMATOLOGY AND ALLERGOLOGY**
**FACULTY OF MEDICINE,**
**INTERDISCIPLINARY RESEARCH DEVELOPMENT AND INNOVATION,**
**CENTER OF EXCELLENCE,**
**UNIVERSITY OF SZEGED,**
**2024**
**SZEGED**

**TABLE OF CONTENTS**

LIST OF ABBREVIATIONS ..... 4
LIST OF PUBLICATIONS ..... 6
Scientific papers included in the thesis ..... 6
Publications not related to the thesis ..... 6
1. INTRODUCTION ..... 8
1.1 Wound healing ..... 8
1.2. Chronic wounds ..... 9
1.3. Clinical treatment and regenerative medicine ..... 10
1.4. Mesenchymal stem cells ..... 11
1.5. Adipose-derived mesenchymal stem cells ..... 11
2. AIMS ..... 13
3. MATERIALS AND METHODS ..... 15
3.1. Sample Collection ..... 15
3.2. Stromal Vascular Fraction Isolation ..... 15
3.3. Mesenchymal Stem Cell Differentiation ..... 15
3.4. Surface Antigen Expression Analysis by Flow Cytometry ..... 16
3.5. Treatment of AD-MSC for RNA Isolation/Wound Healing Assay ..... 16
3.6. Assessment of Cytotoxic Effects of Inflammatory Agents on AD-MSCs ..... 16
3.7. Cell Proliferation and Metabolism ..... 17
3.8. Cellular Impedance Measurement ..... 17
3.9. RNA Isolation for RNA Sequencing ..... 17
3.10. RNA Sequencing ..... 18
3.11. RNA-Seq Analysis ..... 18
3.12. RNA Isolation for qPCR ..... 19
3.13. RT-PCR ..... 19
3.14. qPCR ..... 19
3.15. Protein Array ..... 19
3.16. Enzyme-Linked Immunosorbent Assay (ELISA) ..... 20
3.17. Quanterix Multiplex Enzyme-Linked Immunosorbent Assay (ELISA) ..... 20
3.18. In vitro scratch (wound healing) Assay ..... 20
3.19. Statistical analysis ..... 21
4. RESULTS ..... 22

4.2. Comprehensive Transcriptomic Profiling of Treated Cells ..... 30
4.3. ViSEAGO Analysis and Clustered Pathways ..... 30
4.4. Cellular Characterization and Safety Evaluation of Treatment ..... 34
4.5. Influence of treatments on cell proliferation and migration ..... 37
4.6. Analysis of Gene and Protein Expression using qPCR and ELISA ..... 40
5. DISCUSSION ..... 42
6. SUMMARY ..... 47
7. FUNDING ..... 48
8. ACKNOWLEDGMENTS ..... 49
9. REFERENCES ..... 50

## LIST OF ABBREVIATIONS

| | |
|---|---|
| **AD-MSC** | Adipose-tissue-derived mesenchymal stem cells |
| **BDNF** | Brain-derived neurotrophic factor |
| **BrdU** | 5-bromo-2'-deoxyuridine |
| **CXCL10** | Chemokine (C-X-C motif) ligand 10 |
| **CXCL2** | Chemokine (C-X-C motif) ligand 2 |
| **CXCL3** | Chemokine (C-X-C motif) ligand 3 |
| **CXCL6** | Chemokine (C-X-C motif) ligand 6 |
| **CXCL8** | Chemokine (C-X-C motif) ligand 8 |
| **CXCL9** | Chemokine (C-X-C motif) ligand 9 |
| **DCs** | Dendritic cells |
| **DEG** | Differentially expressed genes |
| **DMEM-HG** | Dulbecco's Modified Eagle Medium – High Glucose |
| **EtOH-DEPC** | Ethanol - Diethyl Pyrocarbonate |
| **FACS** | Fluorescence-activated cell sorting |
| **FBS** | Fetal bovine serum |
| **FGF** | Fibroblast growth factor |
| **GSEA** | Gene set enrichment analysis |
| **HGF** | Hepatocyte growth factor |
| **ICAM-1** | Intercellular Adhesion Molecule-1 |
| **IDO** | Indoleamine 2,3-dioxygenase |
| **IFNγ** | Interferon-γ |
| **IGF-1** | Insulin-like growth factor 1 |
| **IL-10** | Interleukin-10 |
| **IL-11** | Interleukin-11 |
| **IL-15** | Interleukin-15 |
| **IL-16** | Interleukin-16 |
| **IL-1Ra** | Interleukin-1 receptor antagonist |
| **IL-1β** | Interleukin-1β |
| **IL-6** | Interleukin-6 |
| **IL-7** | Interleukin-7 |
| **IL-8** | Interleukin-8 |
| **IL-8** | Interleukin-8 |
| **IL1RN** | Interleukin-1 Receptor Antagonist |
| **IP-10** | Interferon gamma-induced protein 10 |
| **KEGG** | Kyoto Encyclopedia of Genes and Genomes |
| **KYNU** | Kynureninase |
| **LPS** | Lipopolysaccharide |
| **MCP-1** | Monocyte chemoattractant protein-1 |
| **MSC** | Mesenchymal stem cells |
| **MTT** | 3-(4,5-Dimethylthiazol-2-yl)-2,5-Diphenyltetrazolium Bromide |
| **NKs** | Natural killer cells |
| **PBS** | Phosphate buffered saline |
| **PCA** | Principal component analysis |
| **PGE2** | Prostaglandin E2 |

| | |
|---|---|
| **PolyIC** | Polyinosinic-polycytidylic acid |
| **SVF** | Stromal vascular fraction |
| **TGFB3** | Transforming growth factor beta-3 |
| **TGFβ** | TGF-beta-1 protein |
| **TNF-α** | Tumor Necrosis Factor-α |
| **VCAM-1** | Vascular cell adhesion protein-1 |
| **VEGF** | Vascular Endothelial Growth Factor |

**LIST OF PUBLICATIONS**
**Scientific papers included in the thesis**

i. **Szűcs D**, Miklós V, Monostori T, Guba M, Kun-Varga A, Póliska S, Kis E, Bende B, Kemény L, Veréb Z. Effect of Inflammatory Microenvironment on the Regenerative Capacity of Adipose-Derived Mesenchymal Stem Cells. Cells. 2023 Jul 29;12(15):1966. doi: 10.3390/cells12151966. PMID: 37566046; PMCID: PMC10416993.; IF: 6.0; Journal specialization: *Scopus* – General Biochemistry, Genetics, and Molecular Biology, Location: *Q1*; *SJR*- Biochemistry, Genetics and Molecular Biology (miscellaneous)

ii. **Szűcs D**, Monostori T, Miklós V, Páhi ZG, Póliska S, Kemény L and Veréb Z (2024), Licensing effects of inflammatory factors and TLR ligands on the regenerative capacity of adipose-derived mesenchymal stem cells. Front. Cell Dev. Biol. 12:1367242. doi: 10.3389/fcell.2024.1367242; IF: 5.5; Journal specialization: *Scopus* - Cell Biology, Developmental Biology, Location: *Q1*; *SJR*- Developmental Biology

Total IF: 11.5

**Publications not related to the thesis**

I. Tamás Monostori, **Diána Szűcs**, Borbála Lovászi, Lajos Kemény, Zoltán Veréb. Advances in tissue engineering and 3D bioprinting for corneal regeneration. IJB null, 0(0), 1669. https://doi.org/10.36922/ijb.1669; IF: 7.422; (Journal specialization: *Scopus* Biotechnology, Industrial and Manufacturing Engineering, Materials Science (miscellaneous); Location: *Q1, SJR*- Biochemistry, Genetics and Molecular Biology, Engineering, Materials Science

II. Kun-Varga A, Gubán B, Miklós V, Parvaneh S, Guba M, **Szűcs D**, Monostori T, Varga J, Varga Á, Rázga Z, Bata-Csörgő Z, Kemény L, Megyeri K, Veréb Z. Herpes Simplex Virus Infection Alters the Immunological Properties of Adipose-Tissue-Derived Mesenchymal-Stem Cells. Int J Mol Sci. 2023 Jul 26;24(15):11989. doi: 10.3390/ijms241511989. PMID: 37569367; PMCID: PMC10418794.; IF:5.6 (Journal specialization: *Scopus* – Biochemistry, Genetics and Molecular Biology, Location: *Q1*; *SJR*- Biochemistry, Genetics and Molecular Biology, Chemical Engineering, Chemistry, Computer Science, Medicine

III. **Szűcs D**, Fekete Z, Guba M, Kemény L, Jemnitz K, Kis E, Veréb Z. Toward better drug development: Three-dimensional bioprinting in toxicological research. Int J Bioprint. 2023 Jan 6;9(2):663. doi: 10.18063/ijb.v9i2.663. PMID: 37065668; PMCID: PMC10090537; IF: 7.422; (Journal specialization: *Scopus* Biotechnology, Industrial and Manufacturing Engineering, Materials Science (miscellaneous); Location: *Q1*, *SJR*- Biochemistry, Genetics and Molecular Biology, Engineering, Materials Science

IV. Páhi ZG, Kovács L, **Szűcs D**, Borsos BN, Deák P, Pankotai T. Usp5, Usp34, and Otu1 deubiquitylases mediate DNA repair in Drosophila melanogaster. Sci Rep. 2022 Apr 7;12(1):5870. doi: 10.1038/s41598-022-09703-x. PMID: 35393473; PMCID: PMC8990000.; IF: 4.6; Journal specialization: *Scopus*: General; Location: *Q1*, *SJR*- Multidisciplinary

V. Guba M, **Szűcs D**, Kemény L, Veréb Z. Mesterséges bőrszövetek a kutatásban és a gyógyításban [Tissue engineered skin products in research and therapeutic applications]. Orv Hetil. 2022 Mar 6;163(10):375-385. Hungarian. doi: 10.1556/650.2022.32330. PMID: 35249001.; IF: 0.707

VI. Bálint A, Farkas K, Méhi O, Kintses B, Vásárhelyi BM, Ari E, Pál C, Madácsy T, Maléth J, Szántó KJ, Nagy I, Rutka M, Bacsur P, **Szűcs D**, Szepes Z, Nagy F, Fábián A, Bor R, Milassin Á, Molnár T. Functional Anatomical Changes in Ulcerative Colitis Patients Determine Their Gut Microbiota Composition and Consequently the Possible Treatment Outcome. Pharmaceuticals (Basel). 2020 Oct 28;13(11):346. doi: 10.3390/ph13110346. PMID: 33126430; PMCID: PMC7692875.; IF: 5.215; Journal specialization: *Scopus*: Molecular Medicine, Pharmaceutical Science; Location: *Q1*; *SJR*- Biochemistry, Genetics and Molecular Biology, Pharmacology, Toxicology and Pharmaceutics

Total IF: 30.966

# 1. INTRODUCTION

## 1.1 Wound healing

The process of wound healing is complex and meticulously controlled, with its duration varying depending on the underlying cause. Chronic wounds, typically taking approximately 12 weeks to heal, exhibit a slowed or halted healing process due to underlying pathophysiological factors. Often, different phases of wound healing overlap. Adequate blood circulation within the wound area is essential for effective healing, as reduced oxygen and nutrient supply can result in ischemic or necrotic tissue formation, thereby impeding the healing process. Venous leg ulcers, prevalent among individuals with chronic venous insufficiency, commonly manifest around the ankle and lower leg. The annual prevalence of venous leg ulcers in adults aged 65 and older ranges from 1.65% to 1.74%, while in Europe, it ranges from 0.2% to 1% of the general population. Recent studies suggest that approximately 1% of the population will experience at least one episode of a venous ulcer during their lifetime, with a higher prevalence among older individuals. (1–9)

The molecular mechanisms underlying wound healing are intricate and multifaceted. **(Figure 1.)** When tissue damage occurs, a cascade of events initiates the healing response, typically involving inflammation, proliferation, and tissue remodeling. On a molecular level, tissue injury prompts the release of inflammatory mediators such as cytokines and chemokines, which attract immune cells to facilitate debris removal and protect against potential infections. Additionally, growth factors are released to stimulate cell proliferation and migration, promoting the generation of new tissue. During the proliferation phase, various cell types—including fibroblasts, endothelial cells, and keratinocytes—undergo proliferation and migration towards the wound site. Fibroblasts play a crucial role in synthesizing extracellular matrix components like collagen, thereby enhancing the structural integrity of the healing tissue. Simultaneously, endothelial cells stimulate angiogenesis, forming new blood vessels vital for ensuring sufficient nutrient and oxygen delivery to the wound area. Keratinocytes migrate across the wound surface to form a new epithelial layer, effectively sealing the wound and restoring the skin's protective barrier. In the final stage of wound healing, tissue remodeling occurs, involving the breakdown and rearrangement of the extracellular matrix by enzymes such as matrix metalloproteinases (MMPs) and other proteases. Maintaining a delicate balance between matrix synthesis and degradation is crucial for achieving proper wound closure and

minimizing scar formation. The molecular mechanisms orchestrating wound healing are tightly regulated and involve a sophisticated interplay of diverse cell types, signaling molecules, and extracellular matrix constituents. Any disruption in these processes can lead to impaired wound healing and the development of chronic wounds. (1–5,7–11)

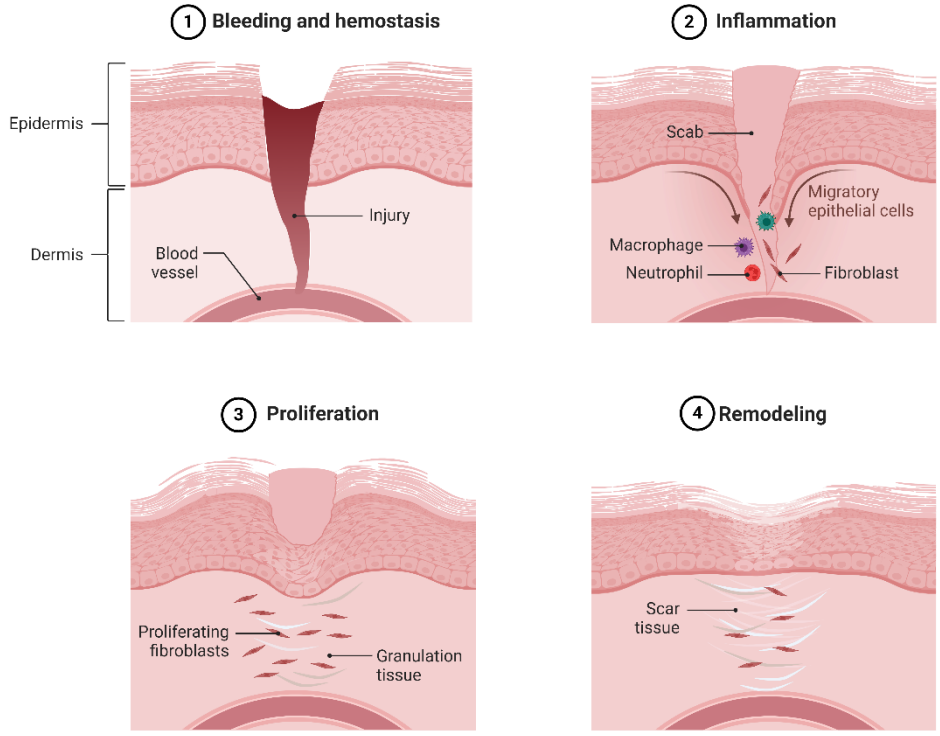


**Figure 1.** Illustrative Overview of Wound Healing Phases (Created with BioRender.com)

### 1.2. Chronic wounds

The molecular foundation of chronic wounds involves a sophisticated interplay among various biological elements. In contrast to acute wounds, which typically proceed through healing stages rapidly, chronic wounds are characterized by a prolonged and disturbed healing process. This complexity arises from several factors, including persistent inflammation, compromised cellular responses, and abnormal remodeling of the extracellular matrix (ECM). On a molecular scale, chronic wounds often exhibit prolonged inflammation, marked by elevated levels of pro-inflammatory cytokines and chemokines within the wound environment. This sustained inflammatory state disrupts the usual healing cascade, resulting in prolonged tissue damage and delayed wound closure. (12–17)

Furthermore, impaired cellular responses exacerbate the persistence of chronic wounds. Dysfunction in critical cell types involved in wound healing, such as fibroblasts, endothelial

cells, and immune cells, can hinder tissue repair processes. For instance, fibroblasts may undergo reduced proliferation and ECM synthesis, while endothelial cells may encounter difficulties in forming new blood vessels through angiogenesis. Dysfunctional ECM remodeling represents another characteristic feature of chronic wounds. The ECM, crucial for providing structural support to the wound bed and facilitating cell migration and tissue repair, undergoes abnormal composition and organization in chronic wounds. This disruption compromises cell function and obstructs the formation of new tissue. A thorough understanding of these molecular mechanisms is essential for devising effective therapies aimed at promoting the healing and resolution of chronic wounds. (12–16)

### 1.3. Clinical treatment and regenerative medicine

Chronic wounds impose significant morbidity due to the demanding treatment regimen required for leg ulcers, involving frequent visits for topical dressings, debridement, and compression therapy, with potential hospitalization for complications, notably leg infections. Healing may be protracted or unattainable in certain patients, with a considerable recurrence rate post-complete healing. Managing challenging wounds remains a considerable concern, often entailing months or even years of treatment, with uncertain outcomes, necessitating a multidisciplinary wound-healing team and specialized medical aids, along with increased costs, including those covered by National Health Insurance. Streamlining the healing process could alleviate costs and complications, thereby reducing the disease burden significantly.(2,10,18,19)

Regenerative medicine holds promise in addressing chronic wounds by leveraging the body's innate healing mechanisms and fostering tissue regeneration, encompassing approaches such as cell/stem cell therapy, growth factor therapy, and tissue-engineered products. However, implementing cell and stem cell therapy presents challenges, as injected cells must navigate non-physiological environments to regenerate tissue, particularly in the context of non-healing wounds often associated with bacterial infections, notably in diabetic patients. Stem cells must withstand and proliferate within inflammatory microenvironments. Despite the growing interest in stem cell therapies, inconsistent outcomes and the absence of pretreatment protocols for injected cells may compromise efficacy. Literature suggests that pretreating— or "licensing"—

stem cells could augment their regenerative potential and expedite wound closure. (2,7,10,17,18,20–23)

### 1.4. Mesenchymal stem cells

In adult organisms, hematopoietic stem cells (HSC) are instrumental in replenishing blood components, while mesenchymal stem cells (MSC) play a role in the regeneration of tissues and organs. Although primarily obtained from bone marrow, MSCs can be harvested from virtually any tissue or organ. Since 2006, the International Society for Cellular Therapy (ISCT) has established criteria for identifying MSCs, which include adherence to specific markers (CD73, CD90, and CD105), absence of certain surface markers (CD14, CD34, CD133, and CD117), and the ability to differentiate into bone, adipose, and cartilage tissues in laboratory settings. These adaptable MSCs possess the capacity for self-renewal and differentiation into various cell types under appropriate conditions, making them promising candidates for cell therapy applications. Additionally, MSCs display immunosuppressive properties, making them useful in organ transplantation, treating graft versus host disease (GVHD), and reducing inflammation. In recent years, stem cells sourced from the umbilical cord and adipose tissue have gained therapeutic significance, alongside MSCs from bone marrow, particularly given the significant contribution of stem cells from these tissue sources. (7,17,21,24–29)

### 1.5. Adipose-derived mesenchymal stem cells

Adipose tissue is distributed across various anatomical sites in the human body, including subcutaneous and visceral locations, intra-articular and intramuscular regions, intra-hepatic depots, and bone marrow. As an energy reservoir and an endocrine organ, adipose tissue produces various mediators impacting metabolism and cellular function. Three distinct types of adipose tissue are recognized: (I) white adipose tissue, primarily serving in energy storage but also producing adipokines; (II) brown adipose tissue, involved in thermogenesis regulation and energy storage; and (III) beige adipose tissue, contributing to both thermogenesis and energy storage. (30–39) The adipose-tissue-derived mesenchymal stem cells (AD-MSC) reside within adipose tissue, predominantly in the stromal vascular fraction (SVF), which can be obtained through minimally invasive methods. AD-MSCs, characterized by multipotency and self-renewal capabilities, exhibit multilineage differentiation potential into mesodermal lineage

cells, including adipocytes, chondrocytes, and osteoblasts. AD-MSCs and their secretome hold promise in regenerative medicine for immune-related disorders because they possess notable proliferation and immunosuppressive attributes. Their interaction with various immune cells, such as T cells, B cells, macrophages, natural killer cells (NKs), dendritic cells (DCs), neutrophils, and mast cells, underscores their potential in modulating immune responses. (6,34–38,31,39,30,3,33,40–45)

AD-MSCs exert immunomodulatory effects through interactions with T cells, involving cell adhesion molecules and alterations in the secretion of mediators (IDO, TGFβ, IL-10, and PGE2). Their response to T cells is influenced by the production of chemokines, with studies demonstrating that in the presence of high pro-inflammatory cytokines, AD-MSCs induce Treg generation and inhibit T cell proliferation, activation, and differentiation, thus suppressing the immune response. Conversely, under low pro-inflammatory cytokine conditions, AD-MSCs inhibit Treg generation while activating T-cell proliferation, activation, and differentiation. AD-MSCs also impact B cells by regulating their proliferation, activation, differentiation, chemotaxis, and Breg induction. Additionally, they modulate NK cells, DCs, macrophages, and neutrophils, highlighting their diverse immunoregulatory potential. (3,40,30,33,46,47,34,48,42,35,36,41,49,37,38,43,44,31,50,39,51) Given their immunomodulatory effects, angiogenic properties, and differentiation capacity, AD-MSCs offer opportunities for tissue replacement, repair, and regeneration, making them applicable in various diseases associated with tissue damage. Potential therapeutic applications include wound healing, skin regeneration, autoimmune disorders, hematological disorders, graft-versus-host disease, bone and cartilage repair, cardiovascular and muscular diseases, neurodegenerative diseases, and radiation injuries. However, for the safe and successful application of AD-MSCs, their purity and potency must be rigorously determined. (3,10,30,31,33–40,42–45,47–62) This study explores the wound healing and skin regeneration capabilities of AD-MSCs, particularly in highly inflamed environments that may influence their gene and protein expression profiles.

## 2. AIMS

Our studies aimed to conduct a preclinical trial of an effective cell therapy procedure and to investigate the response of adipose-derived mesenchymal stem cells (AD-MSCs) to an inflammatory milieu. In the context of non-healing chronic wounds and ulcers, the imperative for stem cells is not only to endure an inflammatory environment but also to undergo proliferation and harness their regenerative and immunomodulatory capabilities for tissue repair. Recent studies suggest that pretreatment and licensing of cells before therapeutic administration may enhance the efficacy of the therapy; therefore, it is crucial to investigate cellular functionality under physiological conditions and within an inflammatory microenvironment before clinical application.

In our initial Project I, we aimed to establish an in vitro model of chronic non-healing ulcers in which we could investigate the regenerative potential of AD-MSC.

1. Examine whether AD-MSC retains its tissue regenerative capacity, especially wound closure, in inflammatory microenvironments.
2. Define the MSCs secretome in the microenvironment typical of chronic non-healing
3. Analyze the gene expression pattern of the AD-MSC upon inflammatory conditions.
4. Investigate the gene expression changes for the biological pathways related to stemness and regenerative and immunological properties of the cells.
5. Identify new signaling processes and biological pathways that may be important for future therapeutic developments.

In the next project (Project II), our aims were

1. Build an extended model based on our previous results to study the effects of licensing on AD-MSC,
2. Employ a more sensitive cytokine detection method to measure difficult-to-detect, low-concentration cytokines.
3. Upgrade a more robust wound-healing assay.

4. Investigate the gene expression changes for the biological pathways related to stemness and regenerative and immunological properties of the cells.
5. Identify new signaling processes and biological pathways that may be important for future therapeutic developments.
6. Compare the gene expression changes caused by different treatments from a therapeutic point of view.

## 3. MATERIALS AND METHODS

### 3.1. Sample Collection

Adipose tissue collection followed the principles of the Declaration of Helsinki. It was approved by the National Public Health and Medical Officer Service (NPHMOS) and the National Medical Research Council (16821-6/2017/EÜIG, STEM-01/2017), aligning with Directive 2004/23/CE of EU Member States regarding presumed written consent for tissue collection. Tissues were obtained from patients undergoing plastic surgery. (Sex: 2/3 F/M, Age: 50.2 ± 11.7 years),

### 3.2. Stromal Vascular Fraction Isolation

Adipose tissue was isolated promptly after surgery. Following homogenization, the tissue was washed with $Ca^{2+}$ and $Mg^{2+}$ free PBS (Biosera, Nuaille, France) and centrifuged at 600 rpm for 8 minutes at room temperature. After centrifugation, the stromal vascular fraction (SVF), which contains mesenchymal stem cells, was found in the upper fraction. After two washes, tissue digestion was performed using Collagenase Type IA (Merck KGaA, Darmstadt, Germany) at a concentration of 0.25 mg/ml for 1 hour at 37°C on a tube rotator. Subsequently, the cells were washed, and the upper layer was discarded, retaining only the SVF fraction at the base of the tube. The cell pellet was suspended in $Ca^{2+}$ and $Mg^{2+}$ free PBS (Biosera, Nuaille, France) filtered using a 100 μm Corning® cell strainer. After several washes, the yellowish upper layer was preserved and suspended in 1 ml of medium. Cell counting was conducted using the EVE automatic cell counter, NanoEntek (NanoEntek, Seoul, Korea), followed by seeding in a T25 $cm^2$ flask. The maintenance medium consisted of DMEM-HG medium supplemented with 10% FBS, 1% L-glutamine, and 1% Antibiotic–Antimycotic Solution (all from Biosera, Nuaille, France) for subsequent experiments.

### 3.3. Mesenchymal Stem Cell Differentiation

Validation of AD-MSCs differentiation involved seeding $5 \times 10^4$ cells/well in a 24-well plate. Following 24 hours, the medium was replaced with a differentiation medium, employing commercially available Gibco's StemPro® Adipogenesis, Osteogenesis, and Chondrogenesis differentiation kits according to the manufacturer's guidelines (Gibco, Thermo Fisher Scientific, Waltham, MA, USA). After 21 days, cells were fixed with 4% methanol-free formaldehyde

(Molar Chemicals, Hungary) for 20 minutes at RT. AD-MSC differentiation was confirmed through various staining methods: Nile red staining for lipid-laden particles, Alizarin red staining for mineral deposits during osteogenesis, and Toluidine blue staining for chondrogenic mass labeling.

### 3.4. Surface Antigen Expression Analysis by Flow Cytometry

Surface antigen expression patterns were characterized using three-color flow cytometry with fluorochrome-conjugated antibodies and isotype-matching controls. The BD FACSAria™ Fusion II flow cytometer (BD Biosciences Immunocytometry Systems, Franklin Lakes, NJ, USA) measured fluorochrome signals, and Flowing Software (Cell Imaging Core, Turku Centre for Biotechnology, Finland) facilitated data analysis.

### 3.5. Treatment of AD-MSC for RNA Isolation/Wound Healing Assay

AD-MSCs from abdominal adipose tissue were cultured in T25 $cm^2$ flasks ($2.8 \times 10^5$ cells/flask) for 24 hours in the cell culture medium. Subsequently, the medium was replaced for treatment with either (A) LPS [100 ng/mL] (tlrl-peklps, ultrapure, Invivogen, San Diego, CA, USA), (B) TNFα [100 ng/mL] (300-01A, Peprotech, London, UK), and in case of our second project with (C) IL-1β [10 ng/mL] (200-01B, Peprotech, London, UK), (D) IFNγ [10 ng/mL] (300-02, Peprotech, London, UK), or (E) PolyI:C [25 ng/mL] (tlrl-pic, Invivogen, San Diego, CA, USA) as well. Cells were incubated for 24 hours under standard conditions (37 °C, 5% $CO_2$), with untreated cells serving as controls. Cells were collected for RNA isolation, or a wound healing assay was performed after treatment.

### 3.6. Assessment of Cytotoxic Effects of Inflammatory Agents on AD-MSCs

To evaluate the cytotoxic impact of the administered treatment, the Cytotoxicity Detection Kit (LDH) (REF: 11644793001, Roche, Basel, Switzerland) was employed according to the manufacturer's instructions. Cell supernatants were collected after 24 hours of inflammation induction (as described above), and the colorimetric absorbance measurement was conducted using the Synergy HTX multi-plate reader (Agilent/BioTek, Santa Clara, CA, USA) at 490 nm, with a reference wavelength of 620 nm.

### 3.7. Cell Proliferation and Metabolism

Proliferation effects were evaluated using the BrdU Cell Proliferation ELISA Kit (Ref: 11647229001, Roche, Basel, Switzerland). 5-bromo-2'-deoxyuridine (BrdU), a thymidine analog, was incorporated into DNA to assess the impact on activator molecule proliferation. Cells were seeded at a density of 1.5 × 104 cells per well in a 96-well plate. The inflammatory environment was simulated with specified materials and concentrations for 24 hours. Measurements were conducted on the Synergy HTX multi-plate reader (Agilent/BioTek, Santa Clara, CA, USA) at 550 nm, with a reference at 650 nm for the MTT assay and at 450 nm, with a reference at 690 nm. Additionally, changes in metabolism due to inflammation were investigated using the Cell Proliferation Kit (MTT) (Ref: 11465007001, Roche, Basel, Switzerland). Cells were incubated for 24 hours under standard conditions (37 °C, 5% CO2), followed by colorimetric absorbance measurement at 550 nm, with a reference at 650 nm, using the same multi-plate reader after induction of inflammation.

### 3.8. Cellular Impedance Measurement

Label-free cellular impedance measurements were performed with an Agilent xCELLingence Real-Time Cell Analysis (RTCA) DP (dual-purpose) instrument (Agilent/BioTek, Santa Clara, CA, USA). In total, $1 \times 10^4$ AD-MSCs were seeded per well of E-Plate 16. Cells were incubated overnight under standard conditions (37 °C, 5% $CO_2$) for attachment. The cells were then treated with LPS and TNFα (described above), and the cellular impedance was measured for 24 h (37 °C, 5% $CO_2$).

### 3.9. RNA Isolation for RNA Sequencing

Cells were collected, and the pellet was suspended in 1 mL TRI Reagent® (Genbiotech Argentina, Buenos Aires, Argentina) before storage at -80 °C for 24 hours. Upon thawing, 200 µL chloroform was added, and after thorough mixing, samples were incubated at RT for 10 minutes. Centrifugation at 13,400 g at 4 °C for 20 minutes facilitated phase separation, with the aqueous phase transferred to clean tubes. Addition of 500 µL 2-propanol and repeated incubation and phase separation steps followed. The resulting supernatants were discarded, and the pellets were washed with 750 µL 75% EtOH-DEPC. After centrifugation at 7500 g at 4 °C for 5 minutes, supernatants were removed, and pellets were dried at 45 °C for 20 minutes.

Pellets were dissolved in RNase-free water incubated at 55 °C for 10 minutes, and the RNA concentration was determined using an IMPLEN N50 UV/Vis nanophotometer (Implen GmbH, Munich, Germany). RNA samples were stored at -80 °C until use.

### 3.10. RNA Sequencing

High-throughput mRNA sequencing was performed on the Illumina sequencing platform to obtain global transcriptome data. Quality assessment of total RNA samples utilized Agilent BioAnalyzer with the eukaryotic Total RNA Nano Kit. Samples with an RNA integrity number (RIN) value >7 were accepted for library preparation. Following the manufacturer's protocol, RNA-Seq libraries were prepared using the Ultra II RNA Sample Prep kit (New England BioLabs). Briefly, poly-A RNAs were captured fragmented at 94 °C, and double-stranded cDNA was generated. Adapter ligation, end repair, and A-tailing steps were followed by PCR amplification, resulting in sequencing libraries. Illumina NextSeq 500 instrument executed the sequence runs with single-end 75-cycle sequencing.

### 3.11. RNA-Seq Analysis

Gene expression analysis was conducted in R (version 4.2.0). Genes with low expression values (rows with only 10 counts across all samples) were removed in a prefiltering step. Principal component analysis (PCA) visualized sample-to-sample distances created using the R package PCAtools without significant batch effects. Differential expression analysis utilized DESeq2 (63), defining significantly differentially expressed genes (DEG) based on adjusted p values < 0.05 and log2-fold change threshold = 0. The DEG heat map was generated using the R package ComplexHeatmap (64), Pearson correlation in rows and columns, and z scores calculated from normalized count data. Volcano plots were created using the EnhancedVolcano package. Gene set enrichment analysis (GSEA) ordered DEGs by log2-fold changes, with the R package ClusterProfiler for GO and KEGG GSEA using pvalueCutoff = 0. In the second part of our work, we compared all treatments using the ViSEAGO package (65). The analysis utilized a ranked list of differentially expressed genes with a p-value < 0.05 and a log2foldchange > |1| as input. Functional Gene Ontology enrichment analysis was conducted using the fgsea package (66) with the ViSEAGO::runfgsea command employing the "fgseaMultilevel" method and parameters: scoreType = "std" and minSize = 5. The obtained enrichment results were

consolidated (Supplementary Table 1), and semantic similarity measures were computed using Wang distance measures, which are grounded in graph topology. The clustering of enrichment results was performed using the Ward D2 method, and the resulting dendrogram was categorized into 20 groups (67).

### 3.12. RNA Isolation for qPCR

Upon LPS and TNFα treatment (described above), the Macherey–Nagel NucleoSpin RNA Mini kit (Dueren, Germany) was applied according to the manufacturer's instructions. After this, all work with RNA and cDNA samples was performed in a BioSan UVT-B-AR DNA/RNA UV-Cleaner box (Riga, Latvia).

### 3.13. RT-PCR

After extracting RNA and checking their quality and quantity with IMPLEN N50 UV/Vis nanophotometer, cDNA synthesis was carried out using High-Capacity cDNA Reverse Transcription Kit (Applied Biosystems$^{TM}$, Thermo Fisher Scientific, Waltham, MA, USA) according to the manufacturer's guidelines. Analytik Jena qTOWER$^3$ G Touch Real-Time Thermal Cycler (Jena, Germany) was applied for reverse transcription.

### 3.14. qPCR

The Xceed 2x Mix No-ROX kit (Institute of Applied Biotechnologies, Prague, Czech Republic) and TaqMan probes (250 rxns, FAM-MGB, Thermo Fisher Scientific, Waltham, MA, USA) were applied for quantitative PCR. Three technical and three biological replicates were used in all cases, and data were analyzed using the $2^{-\Delta\Delta Ct}$ method. The protocol was performed according to the manufacturer's instructions, and the following probes were selected for the experiment: Hs00427620, Hs99999903, Hs00153133, Hs00361185, Hs 00194611, Hs00747615, Hs00174103, Hs00164932, Hs01001602, Hs 00171042, Hs00598625, Hs00265033, Hs00985639, Hs00165814, Hs01003372.

### 3.15. Protein Array

Three AD-MSC donors were treated with LPS and TNFα, as described above. Supernatants were collected and stored at -80 ° C until use. After thawing the samples, the supernatants were

pooled by type of treatment and applied to the Human XL cytokine array Kit Proteome Profiler (R&D Systems, Biotechne, McKinley Place NE, Minneapolis, MN, USA) to determine secreted factors. The array was carried out according to the manufacturer. The images were quantified using Fiji (Image J 1.53S) with an embedded Protein Array Analyzer (Version:1.1.c) macro.

### 3.16. Enzyme-Linked Immunosorbent Assay (ELISA)

To validate the protein array results and quantify cytokine/chemokine levels in cells following induction of inflammation, the Human IL-6 ELISA set (555220), Human IL-8 ELISA set (555244), Human IP-10 ELISA set (550926), and Reagent Set B (550534) were utilized from BD OptEIA™ (BD Biosciences, Franklin Lakes, NJ, USA), following the manufacturer's guidelines.

### 3.17. Quanterix Multiplex Enzyme-Linked Immunosorbent Assay (ELISA)

For the cytokine analysis, the Quanterix SP-X digital biomarker analyzer was employed. This system facilitated the simultaneous detection of 10 cytokines through a multiplex assay employing the Simoa Corplex Cytokine Panel 1 10-Plex Kit (REF: 85-0329, Quanterix). The assay procedures were carried out following the manufacturer's protocol. Supernatants were thawed, centrifuged, and subjected to a fourfold dilution with assay diluent. Freshly prepared calibration standards were measured in triplicates, with sample measurements performed in duplicates. Following the assay, the obtained results were analyzed and visualized using GraphPad.

### 3.18. In vitro scratch (wound healing) Assay

In our first project for the wound healing assay, 5 × 10^4 cells were seeded per well in 24-well plates and cultured for 24 hours under standard conditions. The protocol diverged into two approaches: (I) where a scratch was made after 24 hours and inflammatory agents were immediately added, followed by 48 hours of time-lapse microscopy; (II) where inflammatory agents were added first, then after 24 hours, a scratch was made, and the medium was changed to agents-free maintenance media, followed by 48 hours of microscopy. Scratches were made using the AutoScratch Wound Making Tool (Agilent/BioTek, Santa Clara, CA, USA). An Olympus IX83 inverted microscope took microscopic images with an Olympus ScanR high-

content imaging screening platform (Olympus, Tokyo, Japan) equipped with an Orca2 (Hamamatsu Photonics K.K., Shizuoka, Japan) camera and analyzed by Fiji/ImageJ (v.1.53m 28 September 2021).

For more robust high-content wound healing measurements requiring more samples, $1.5 \times 10^4$ cells per well were seeded in E-Plate WOUND 96 plates (REF: 300600970, Agilent/BioTek, Santa Clara, CA, USA) and incubated for 24 hours. The protocol contained the same two procedures as described above. Scratches were made using the AccuWound 96 Scratch Tool (Agilent/BioTek, Santa Clara, CA, USA), and impedance measurements were conducted using the xCELLigence Real-Time Cell Analyzer (RTCA) device (Agilent/BioTek, Santa Clara, CA, USA).

### 3.19. Statistical analysis

The normality of data distribution was assessed through Kolmogorov-Smirnov and Lilliefors tests. Parameters exhibiting non-normal distribution were logarithmically transformed to address skewness. Each experiment was replicated at least three times, with each sample analyzed in triplicate. Data are expressed as mean ± standard deviation (SD) or standard error of the mean (SEM). Statistical significance was determined employing two-way ANOVA analysis for comparisons involving more than two groups, and paired Student t-test for comparisons between two groups. A significance level of 0.95 was applied, with p-values below 0.05 ($*p < 0.05$, $**p < 0.01$, $***p < 0.001$) considered significant. Data analysis and visualization were conducted using GraphPad 8 software (version 8.0.2, Graphpad Software Inc., San Diego, California, USA).

## 4. RESULTS

The isolated primary cell lines of adipose tissue-derived mesenchymal stem cells (AD-MSCs) underwent characterization through trilineage differentiation and fluorescence-activated cell sorting (FACS) analysis, thereby confirming their specific cell type properties

We conducted a differential gene expression analysis of the RNA sequence data to delineate the alterations in gene expression and related pathways concurrent with the preconditioning of AD-MSCs using lipopolysaccharide (LPS) and tumor necrosis factor-alpha (TNFα). Our approach involved two distinct methodologies for exploring signaling pathways: a hypothesis-driven investigation of preselected terms and a hypothesis-free gene set enrichment analysis (GSEA) utilizing Gene Ontology (GO) and Kyoto Encyclopedia of Genes and Genomes (KEGG) databases. RNA samples were collected following a 24-hour conditioning of AD-MSCs with inflammatory factors. Both LPS and TNFα treatments exerted discernible effects on the overall gene expression profile, revealing 2752 differentially expressed genes (DEGs) in response to TNFα and 1613 DEGs in cells treated with LPS. The normalized expression values of these genes were subjected to clustering based on Pearson's correlation, visually represented on a heatmap **(Figure 2A)**. To further elucidate distinctions between the two treatments, we scrutinized the overlap of genes exhibiting up- and down-regulation **(Figure 2B)**. A noteworthy convergence in the impact of treatments was observed, with 607 genes exhibiting increased expression and 449 genes displaying a decreased expression. While the LPS treatment affected a comparable number of genes in both up- and down-regulation, TNFα treatment slightly skewed the number of up-regulated genes **(Figure 2C)**.

Adipose tissue-derived mesenchymal stem cells (AD-MSCs) have been demonstrated to express cytokines, chemokines, and growth factors, imparting wound-microenvironment-modulating capabilities and promoting the processes associated with wound healing. (68) Notably, several Differentially Expressed Genes (DEGs) related to these processes were identified following preconditioning. Among the immunomodulatory factors released by AD-MSCs, elevated expression was observed for IL1B, IL1RN, IL11, IL6, and IL15 in a tumor necrosis factor-alpha (TNFα) environment, whereas IL16 and TGFB3 exhibited decreased expression. In contrast, lipopolysaccharide (LPS) demonstrated a lesser impact on immunomodulatory gene expression, specifically reducing the expression of IL1RN and TGFB3. Furthermore, alterations in the expression of IDO and KYNU, associated with T cell

apoptosis, were noted; these genes were up-regulated in response to TNFα, while their expression remained largely unaltered in LPS-treated stem cells.(36) Additionally, the expression of ICAM and VCAM, implicated in lymphocyte recruitment to the injured site, was up-regulated under TNFα conditioning. (36) This observation suggests that both treatments induced immunomodulatory responses in AD-MSCs, potentially altering the behavior of these cells at the damaged tissue site to facilitate the healing process.

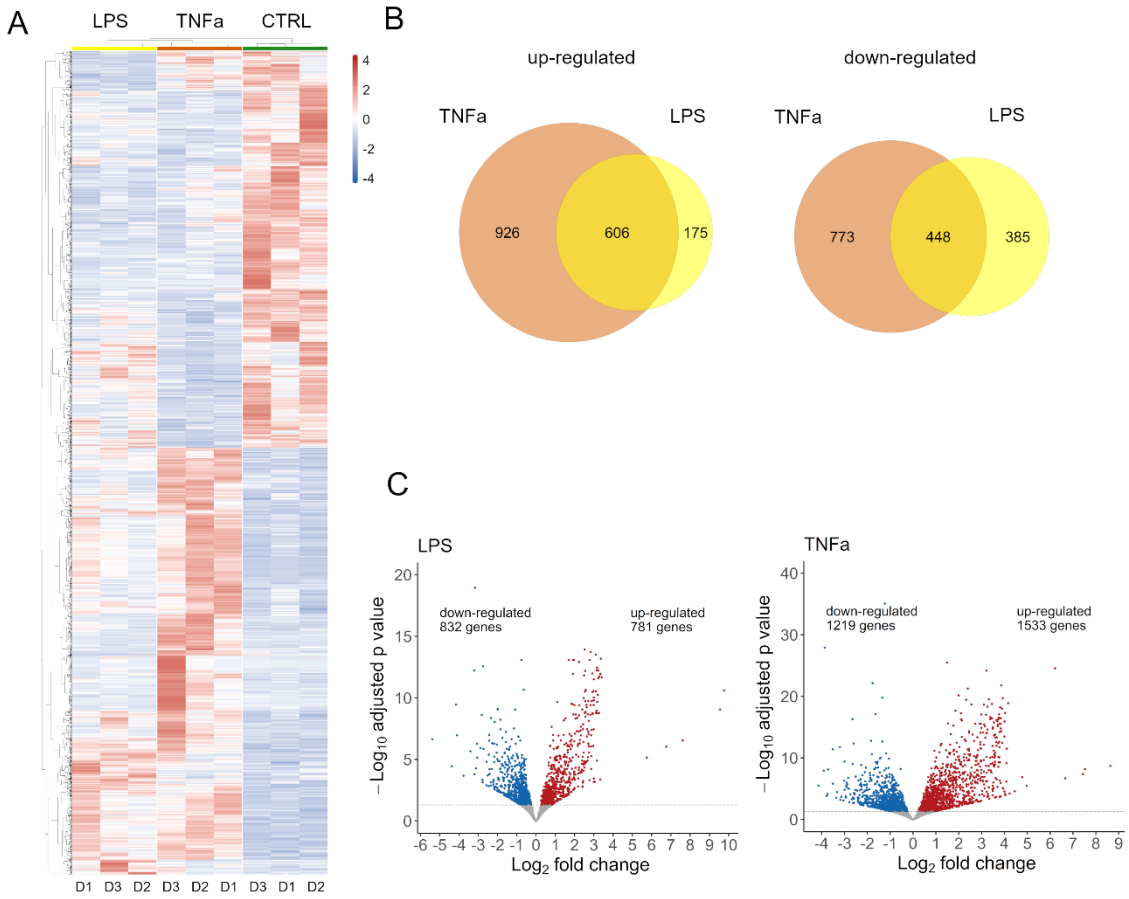


**Figure 2.** The outcomes of RNA sequencing analysis are depicted in the heat map, Venn-diagrams and Volcano plots

In addition to these immunomodulatory molecules, chemokines with roles in cell migration and immune regulation were significantly affected. (43,52,69) The expression of chemokines belonging to the CXCL family (CXCL2, CXCL3, CXCL6, CXCL8, CXCL9, CXCL10, CXCL11) and the CCL chemokine ligand family (CCL1, CCL2, CCL5, CCL7, CCL20, CCL28) underwent substantial alterations in response to TNFα treatment. At the same time, LPS exhibited minimal effects on these chemokines.

Moreover, growth factors crucial in wound healing processes, including cell migration, proliferation, differentiation, and extracellular matrix synthesis (69), demonstrated altered expression in response to both treatments. Both LPS and TNFα treatments resulted in decreased expression of VEGFB and TGFB3, coupled with up-regulation of VEGFC and FGF2. Additionally, TNFα specifically up-regulated TGFA. These changes indicate that LPS and TNFα influence MSC homing and tissue regeneration. The reparative processes executed by AD-MSCs in tissue damage necessitate coordinated interactions involving inflammation, proliferation, cell migration, and re-epithelization, often implicating common genetic elements. Leveraging previously assembled gene sets associated with stem cell behavior in wound healing, we scrutinized AD-MSCs' responses to treatments and the overlap of these responses across different gene sets. Genes were selected from the differentially expressed gene sets under at least one of the treatments, and connecting lines were drawn between sets whenever identical genes were identified **(Figure 3.)**. The widths of these lines reflected the number of similar genes, while the size of each dot denoted the fraction of Differentially Expressed Genes (DEGs) within the entire gene set. Broadly, each set of genes demonstrated connections to at least five other sets, with "wound healing migration," "cellular senescence," "cytokines growth factors," "immune response," and "stem cell EMT TEM" interconnected with every other set, indicating a dense network of interactions.

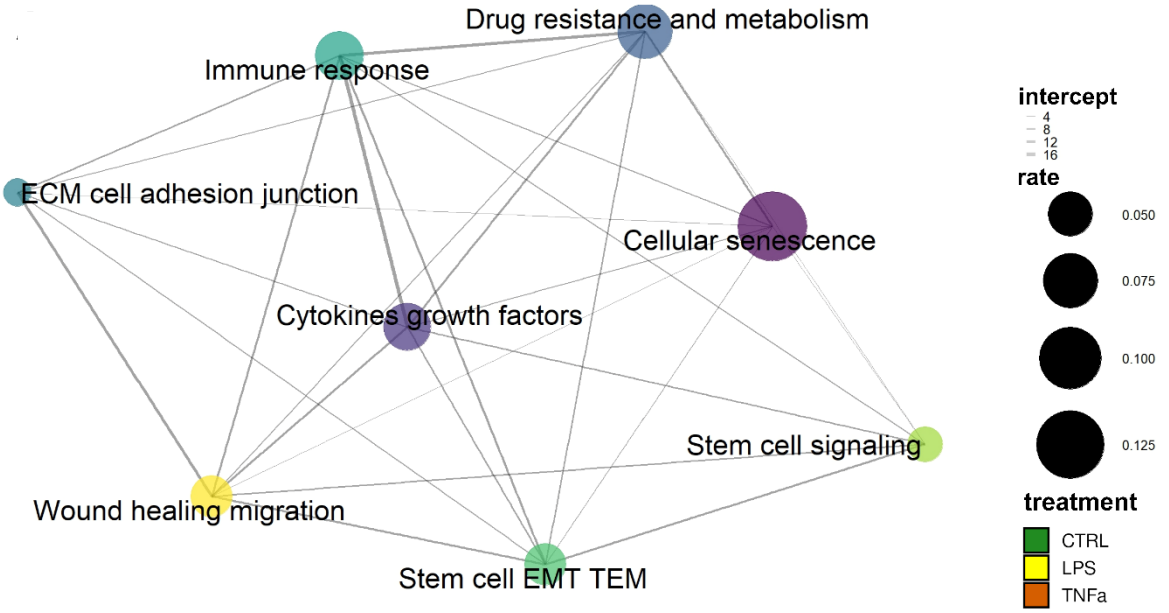


**Figure 3.** Gene set enrichment analysis illustrates the percentage of genes in the wound healing-related pathway affected by the treatments. Circle size correlates directly with the proportion of altered genes, and line thickness represents the overlap of genes.

Examining DEGs across most gene sets revealed comparable effects induced by LPS and TNFα treatments. Consequently, hierarchical clustering illustrated that the two treatments formed a distinct cluster separate from the control samples. However, within three gene sets—specifically "cellular senescence," "immune response," and "cytokine growth factors"—clustering indicated that LPS-treated AD-MSCs exhibited an expression pattern more akin to the control samples. Consequently, genes associated with these terms displayed more pronounced expressional changes in response to TNFα conditioning, while LPS exhibited a comparatively lesser effect. To comprehensively explore alterations in global gene expression, we executed Gene Set Enrichment Analysis (GSEA) employing two databases, namely Gene Ontology (GO) and Kyoto Encyclopedia of Genes and Genomes (KEGG). **(Figure 4.)** Comparable outcomes were discerned across both databases. Notably, the GSEA utilizing GO terms yielded redundant pathway terms attributed to the hierarchical nature of the database.

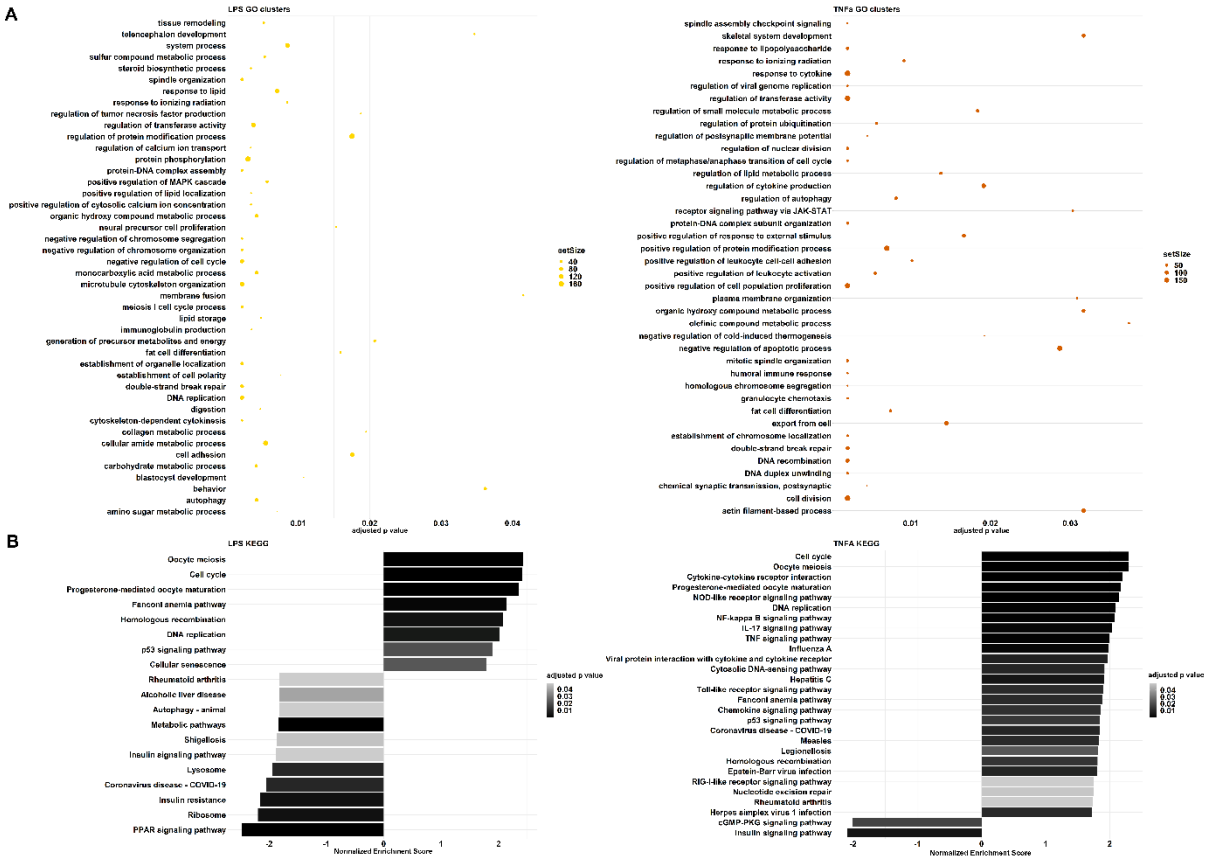


**Figure 4.** Gene ontology and KEGG analysis results summarize the pathways altered by LPS and TNFα treatment.

We performed further clustering based on semantic similarity to address this redundancy. Adjusted p-values guided the selection of parent terms within each cluster. The treatments

involving lipopolysaccharide (LPS) and tumor necrosis factor-alpha (TNFα) exhibited parallel effects on cellular processes encompassing cell division, differentiation, cytoskeleton organization, and cell-cycle-related activities **(Figure 4)**. Consequently, these treatments conferred an augmented capacity for cell proliferation, differentiation, and migration, presenting potential advantages in wound healing. While the processes above exhibit concurrent alterations, noteworthy distinctions arise in immune-related pathways resulting from the two treatments. Within the Gene Ontology (GO) clusters, lipopolysaccharide (LPS) treatment showcases the regulation of tumor necrosis factor (TNF) production **(Figure 4A)**. This cluster encompasses terms such as tumor necrosis factor production, tumor necrosis factor superfamily cytokine production, and related regulatory terms. Gene Set Enrichment Analysis (GSEA) yielded negative normalized enrichment scores (NESs) for these pathways, indicating a down-regulation of cytokine production from TNF and the TNF superfamily.

Conversely, TNFα preconditioning influenced various GO groups associated with immune system processes, such as response to LPS, response to cytokines, regulation of cytokine production, receptor signaling through JAK-STAT, positive regulation of response to external stimulus, positive regulation of leukocyte cell–cell adhesion, positive regulation of leukocyte activation, negative regulation of cold-induced thermogenesis, humoral immune response, and granulocyte chemotaxis—all exhibiting up-regulation, indicative of an enhanced immune response. Similar trends are discerned in the Kyoto Encyclopedia of Genes and Genomes (KEGG) results **(Figure 4B)**. In the case of TNFα, notable signaling pathways include NOD-like receptor, NF-kappa B, IL-17, TNF, Toll-like receptor, Chemokine, and RIG-I-like receptor signaling pathways—all integral components of an immune response, demonstrating positive NESs. Moreover, significant NESs were observed in disease pathways such as influenza A, Hepatitis C, COVID-19, Measles, Legionellosis, Epstein–Barr virus infection, and Herpes simplex virus 1 infection, encompassing Toll-like receptor, RIG-I-like receptor, TNF, Jak-STAT, or NF-kappa B signaling pathways. In contrast, LPS treatment induced distinct changes, down-regulating COVID-19 and Shigellosis pathways, while the immune pathways activated by TNFα treatment remained relatively stable. Similar outcomes were obtained through analysis using the QIAGEN IPA platform. In both treatments, the inflammatory milieu primarily influenced cell cycle regulation, impacting cell division and migration. Other

biological functions exhibited patterns reminiscent of tumor cells, possibly owing to the shared stages of tumor formation and wound healing.

The expression of specific genes was validated through quantitative real-time PCR, revealing treatment-induced changes in various gene groups, including STAT6, pivotal in signaling cascades; diverse cytokines such as IL-6, CXCL-8, CXCL-10; regeneration-associated factors like TDO2, PTGS2, ICAM-1, and VCAM-1; and alterations in the expression of CCR4, implicated in migration. Both treatments elicited elevated CXCL8, IL-6, and PTGS2 proteins and reduced STAT6 levels. Inflammatory factors induced opposing changes in the production of specific proteins; for instance, LPS treatment increased KRT14 and decreased CCR4, TDO2, and VCAM-1, whereas TNFα treatment led to increased CXCL10 and decreased Apolipoprotein A1, IL-4, and angiogenin synthesis.

Cellular impedance measurements demonstrated that cell viability remained unaltered following inflammatory agent addition, with consistent cell indices before (12 h) and after (24 h, 36 h) treatment **(Figure 5A)**. Protein production in AD-MSC supernatants was measured post-LPS and TNFα treatments to underscore the findings from gene expression analysis. The protein array revealed increased expression of various proteins, including Angiopoietin-2, CD40 ligand, Dkk1, FGF-19, HGF, ICAM-1, IGFBP-3, IL-17A, IL-22, IL-23, IL-24, LIF, MCP-3, MMP-9, RANTES, SDF-1α, Thrombospondin-1, uPAR, VEGF, Cystatin C, IL-6, IL-8, MIF, Osteopontin, and Pentraxin 3 with both treatments compared to the control. However, the treatments exhibited opposing effects on the production of specific proteins; for instance, LPS treatment decreased DDPIV and GDF-15 expression, while TNFα treatment decreased Apolipoprotein A1, IL-4, and angiogenin synthesis **(Figure 5B–C)**.

Mesenchymal stem cells derived from adipose tissue (AD-MSCs) actively participate in all stages of wound healing, namely the inflammation, proliferation, and remodeling phases. The wound healing assay conducted in this study reveals that AD-MSCs contribute to an expedited closure of wounds following treatment with lipopolysaccharide (LPS) and tumor necrosis factor-alpha (TNFα) compared to untreated controls **(Figure 6A)**. Specifically, when the therapy preceded wound creation, the wounds in the control group closed approximately 40 hours post-injury. At the same time, the treated samples exhibited accelerated wound healing, with closure occurring around 34.67 hours after LPS treatment and 37.67 hours after TNFα

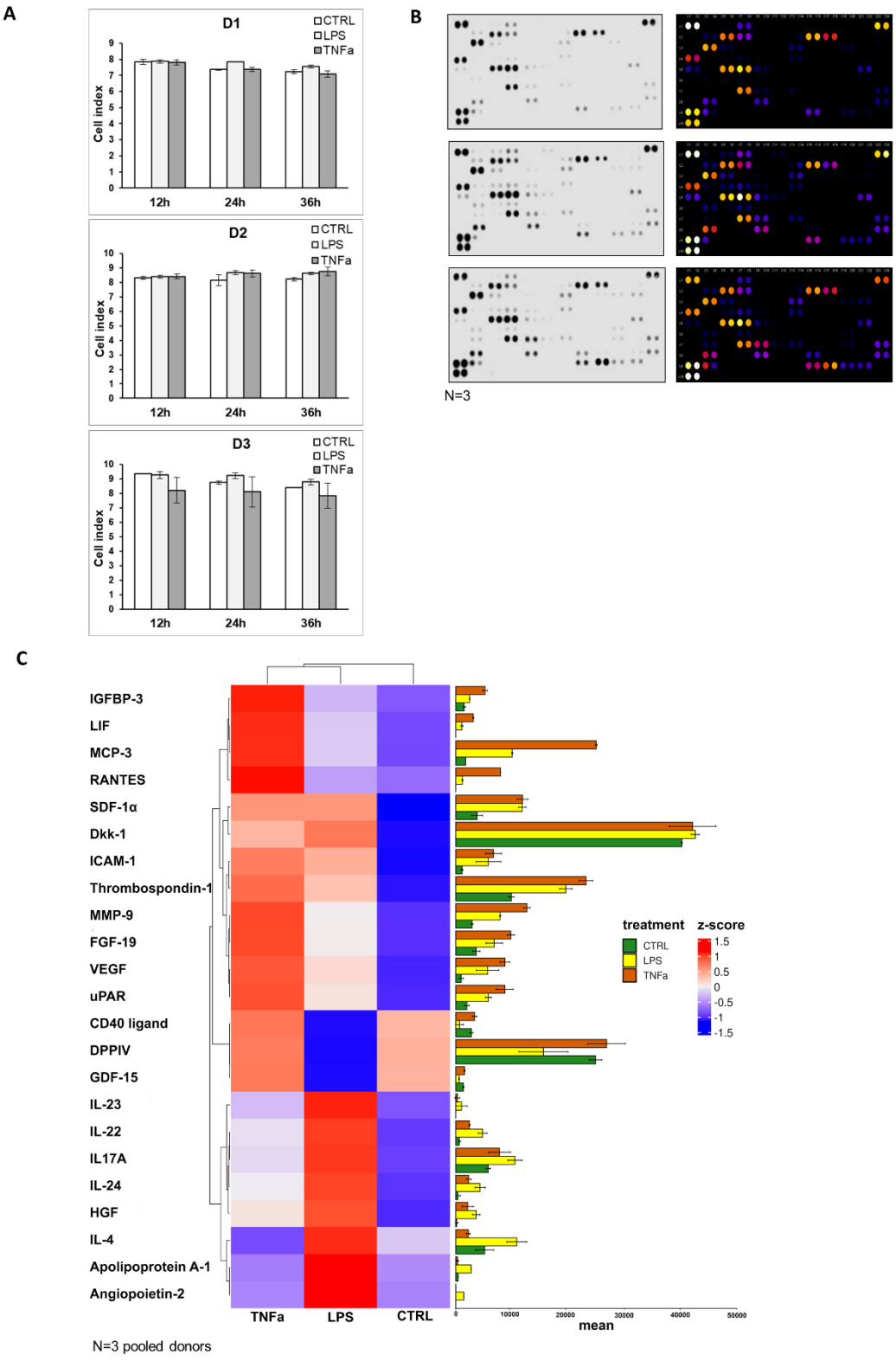


**Figure 5.** Impedance measurements show unchanged cell viability post-treatment. Visual representations, including heat maps, original membrane photos, and a bar chart, highlight significant protein-level changes observed in the protein array results.

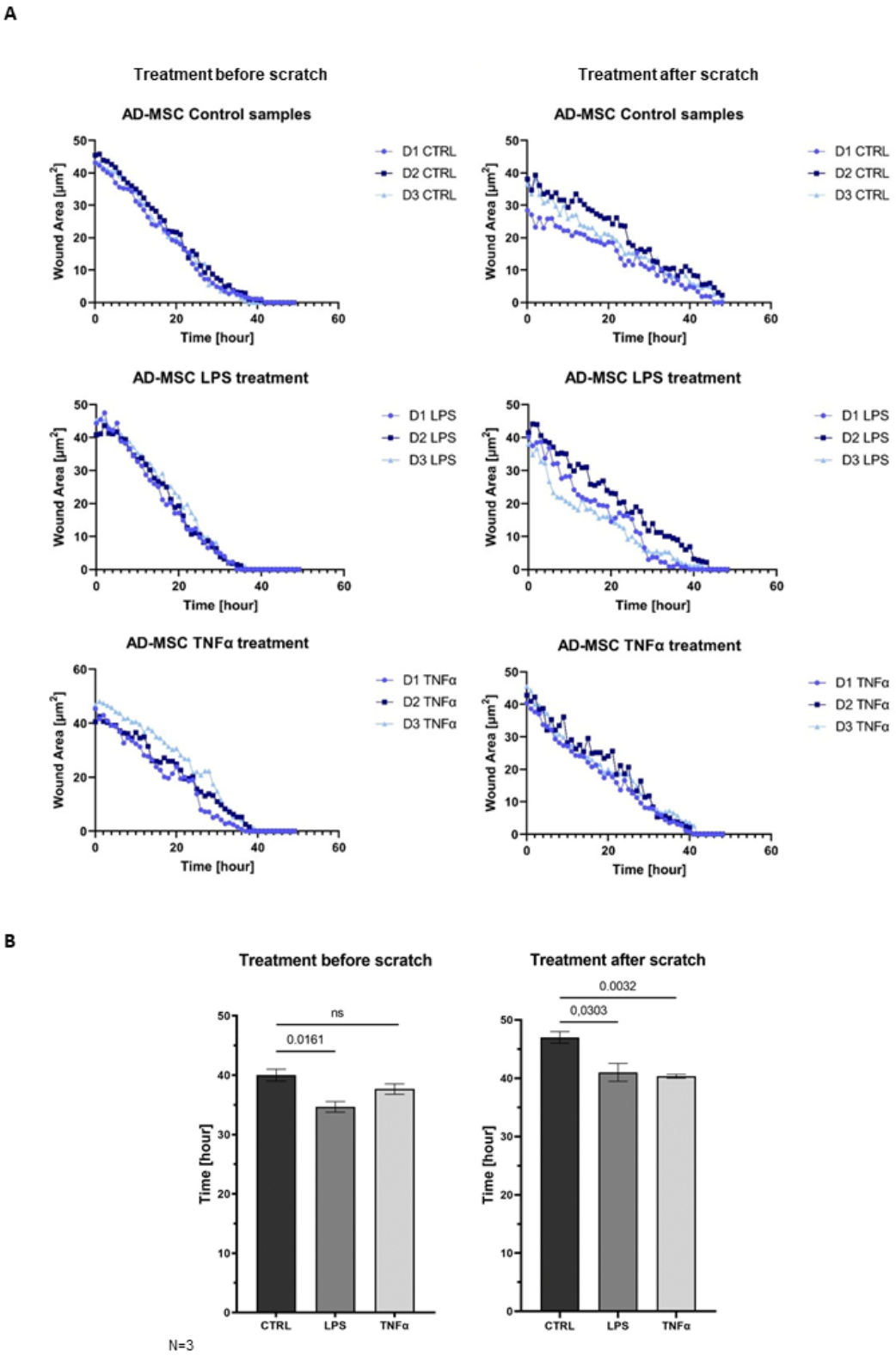


**Figure 6.** The wound healing test result displays the wound area as a function of time, monitored for 48 hours. Bar graphs compare wound closure length between conditions - treatment before and after scratching.

treatment. In scenarios where scratching occurred before the initiation of inflammation, control sample wounds closed around 47 hours.

In contrast, the treated samples exhibited faster closure and remodeling approximately 41 hours after LPS treatment and 40.33 hours after TNFα treatment. The graphical representation underscores significant alterations in wound closure rates between untreated controls and those subjected to inflammatory conditions. Notably, the closing speed was markedly higher when inflammation was induced after scratch formation. These findings signify that AD-MSCs are pivotal in accelerating wound healing under inflammatory conditions, responding to inflammatory factors to facilitate the reparative processes **(Figure 6B).**

### 4.2. Comprehensive Transcriptomic Profiling of Treated Cells

The Venn diagrams **(Figure 7A)** elucidate the profound influence of the administered treatments on gene expression, delineating concurrent upregulation and downregulation of numerous genes and highlighting significant intersections. Specifically, the treatments resulted in the downregulation of genes in the following manner: LPS (104 genes), TNF-α (87 genes), IL-1β (50 genes), IFN-γ (56 genes), and PolyI:C (83 genes), collectively impacting 25 shared genes. Conversely, the treatments elicited the upregulation of several genes: LPS (14 genes), TNF-α (34 genes), IL-1β (26 genes), IFN-γ (38 genes), and PolyI:C (14 genes), with a shared effect observed in 109 genes. These observations underscore the intricate and multifaceted nature of the treatments' impact on the transcriptomic profile, revealing shared and distinct regulatory responses across the various treated conditions. The Volcano plot **(Figure 7B)** visually encapsulates the extensive alterations in gene expression induced by the treatments, encompassing upregulation and downregulation of gene expression. Notably, most of the top 10 most significantly altered genes exhibit noteworthy changes.

### 4.3. ViSEAGO Analysis and Clustered Pathways

The heatmap generated through ViSEAGO analysis provides insights into the segregation of treatments into two primary clusters, with PolyI:C, TNF-α, and IFN-γ forming one cluster and IL-1β and LPS constituting the other **(Figure 8A)**. These clusters exhibit distinctions in defense and immune response, signal transduction, chemotaxis, cellular response to chemical stimulus, biological regulation, and T-cell activation while sharing common effects on organelle

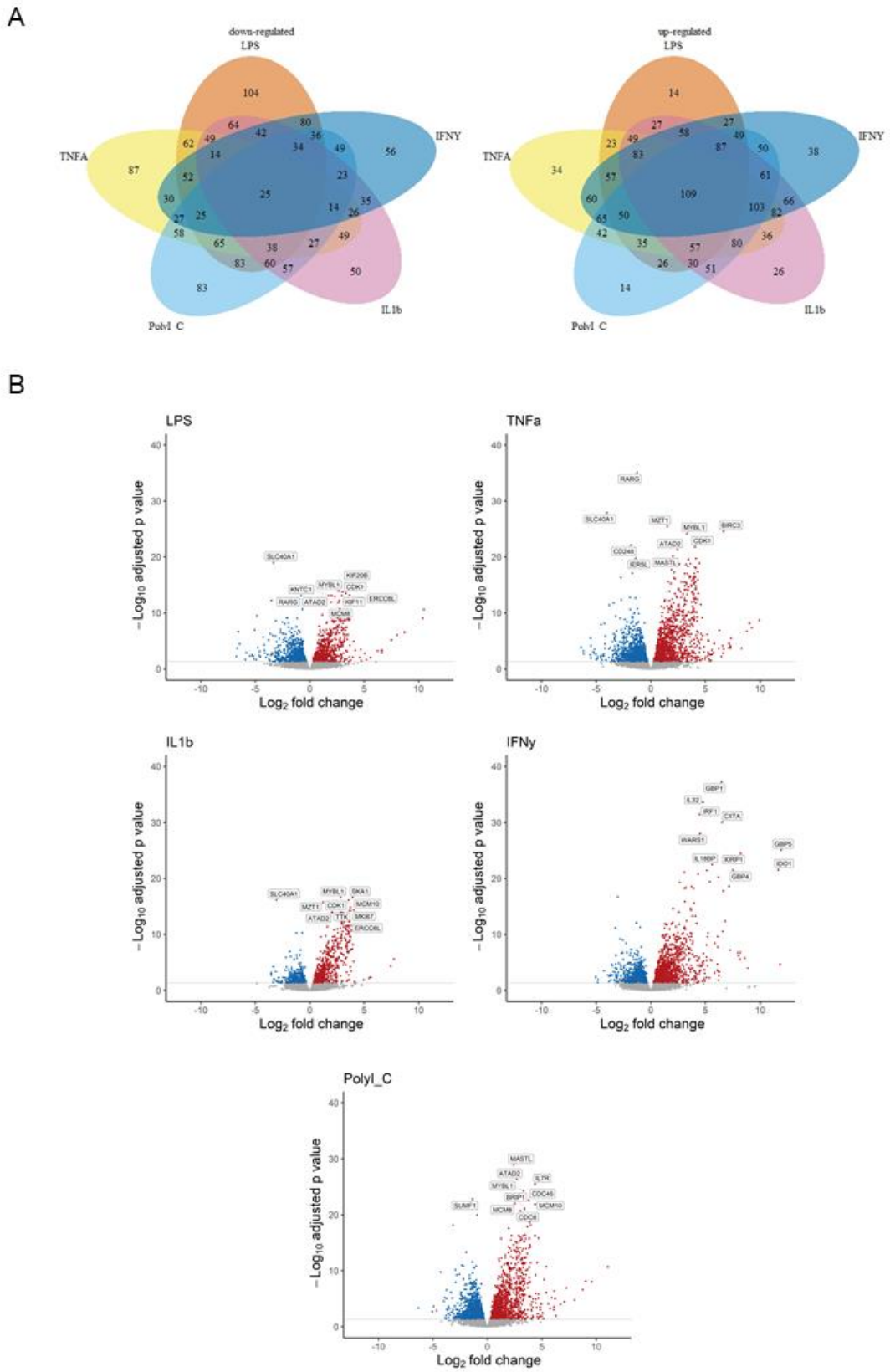


**Figure 7.** DEGs in Response to Pro-Inflammatory Treatment vs. Control. Panel (A) Venn diagrams show gene overlap, and (B) Volcano plots highlight significant gene alterations (p adjusted < 0.05).

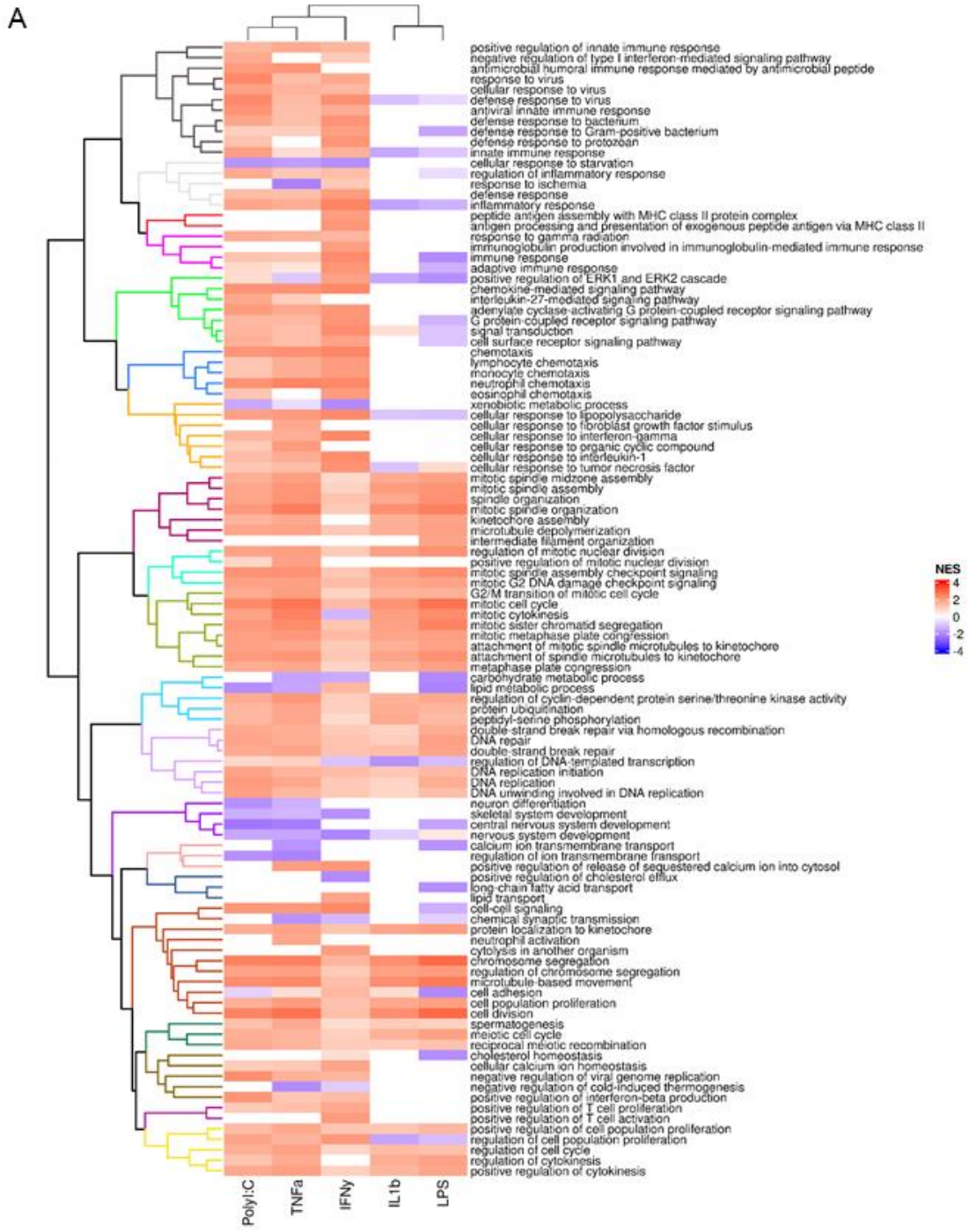


**Figure 8A.** Visualization of a clustered pathways heatmap generated by ViSEAGO. Different colors denote uniform groups comprising various pathways and biological processes.

organization, mitotic cell cycle, primary metabolic process, DNA repair, system development, ion transmembrane transport, lipid transport, cellular process, meiotic cell cycle, and cell cycle regulation.

Furthermore, the treatments exert unique effects on multiple pathways: LPS impacts 2 pathways, TNFα influences 8 pathways, IL-1β affects 1 pathway, IFN-γ modulates 3 pathways, and PolyI:C impacts 5 pathways **(Figure 8B)**. This variance in the influence on distinct molecular pathways underscores the intricate nature of the treatments' interactions with cellular processes. Shared alterations in multiple pathways are also observed, with LPS and TNFα affecting 4 common pathways, while IFNγ and PolyI:C induce changes in 3 overlapping pathways. LPS and IFN-γ, LPS and PolyI:C, and TNFα and PolyI:C, impact one common pathway each. Notably, the combined treatment of LPS, TNFα, and PolyI:C results in concurrent modifications in 3 pathways, whereas the combination of LPS, TNFα, and IL-1β influences one shared pathway. Furthermore, TNFα, IFNγ, and PolyI:C collectively impact one common pathway. Lastly, the joint influence of LPS, TNFα, IL-1β, and PolyI:C is reflected in alterations in 14 pathways, emphasizing the intricate interplay of these treatments in affecting cellular processes.

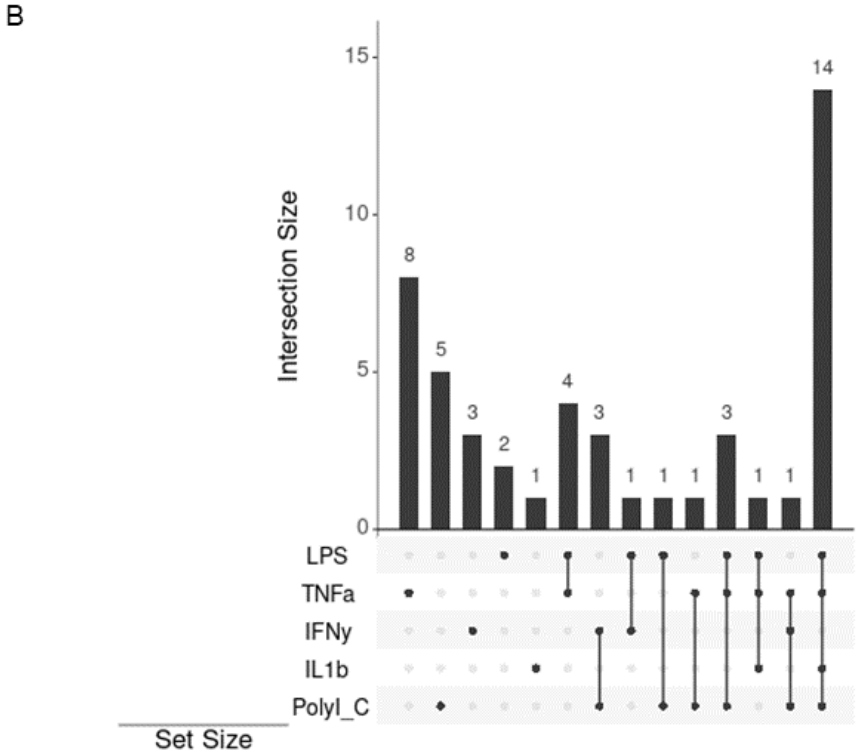


**Figure 8B.** UpSet plots visually represent gene intersections within different pathways in AD-MSCs after treatment with pro-inflammatory agents.

Our transcriptomic dataset has undergone visualization through a series of heatmaps stratified based on predefined pathways **(Figure 9)**. Throughout all heatmaps, discernible differences

emerge between the transcriptional patterns of treated and control samples while acknowledging notable inter-donor variabilities. This dataset illustrates the varied cellular responses elicited by treatments, each reflecting individual patients' distinctive molecular landscape. Particularly noteworthy is the tendency of genes modulated by TNF-α and IFN-γ in the angiogenesis pathway heatmap to cluster together. In cell cycle and cell division pathways, TNF-α, IL-1β, and PolyI:C demonstrate analogous effects, while IFN-γ delineates a distinct grouping. Concerning stem cell differentiation, the impact of LPS and IL-1β aligns closely with that of the control group. In contrast, TNF-α exhibits similarity with PolyI:C, and IFN-γ manifests as an independent cluster.

The heatmap depicting tissue regeneration reveals that LPS and IL-1β treatments display profiles comparable to the control group, whereas TNF-α delineates discrete gene clusters. LPS and IL-1β treatments in wound healing pathways deviate from the control group, while TNF-α, IFN-γ, and PolyI:C treatments segregate into distinct clusters. These observations underscore the nuanced and pathway-specific effects of the treatments on cellular responses, emphasizing the intricate nature of treatment outcomes across diverse biological contexts.

### 4.4. Cellular Characterization and Safety Evaluation of Treatment

Primary cell cultures were meticulously maintained and subjected to an assessment of their differentiation potential. Notably, these cells exhibited a tri-lineage differentiation capacity, successfully navigating the adipogenic, chondrogenic, and osteogenic lineages. This differentiation was thoroughly validated through microscopic examination of distinct cell type-specific features, reinforcing the appropriateness of these cultures as a valuable model for our study. Furthermore, FACS analysis was conducted to unveil critical cell characteristics, affirming their mesenchymal origin and solidifying their identity. These insights facilitate a more profound exploration of their unique traits and functions within the scope of our study.

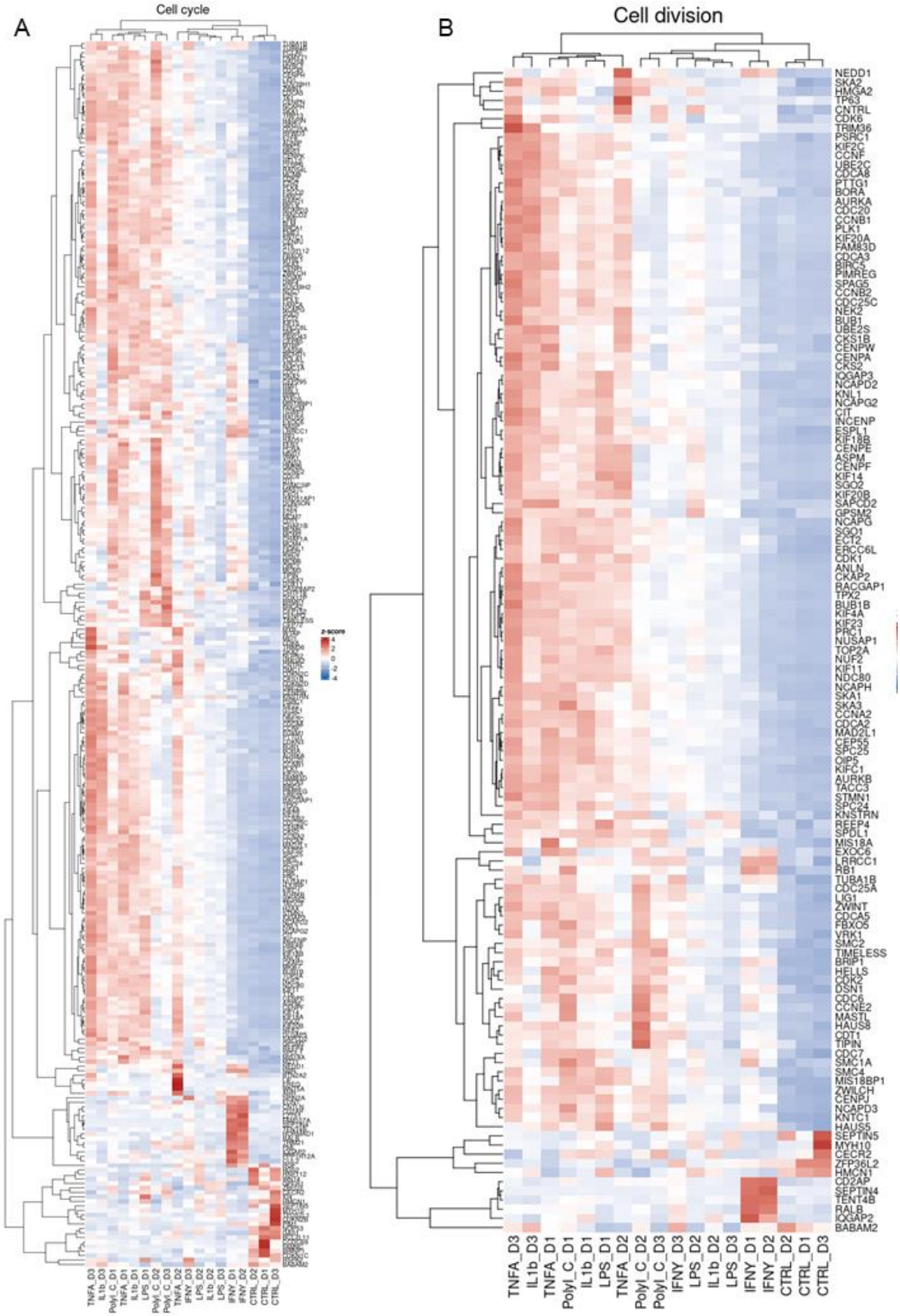


**Figure 9A-B.** Clustered heatmaps portraying various processes: (A) Cell cycle, (B) Cell division.

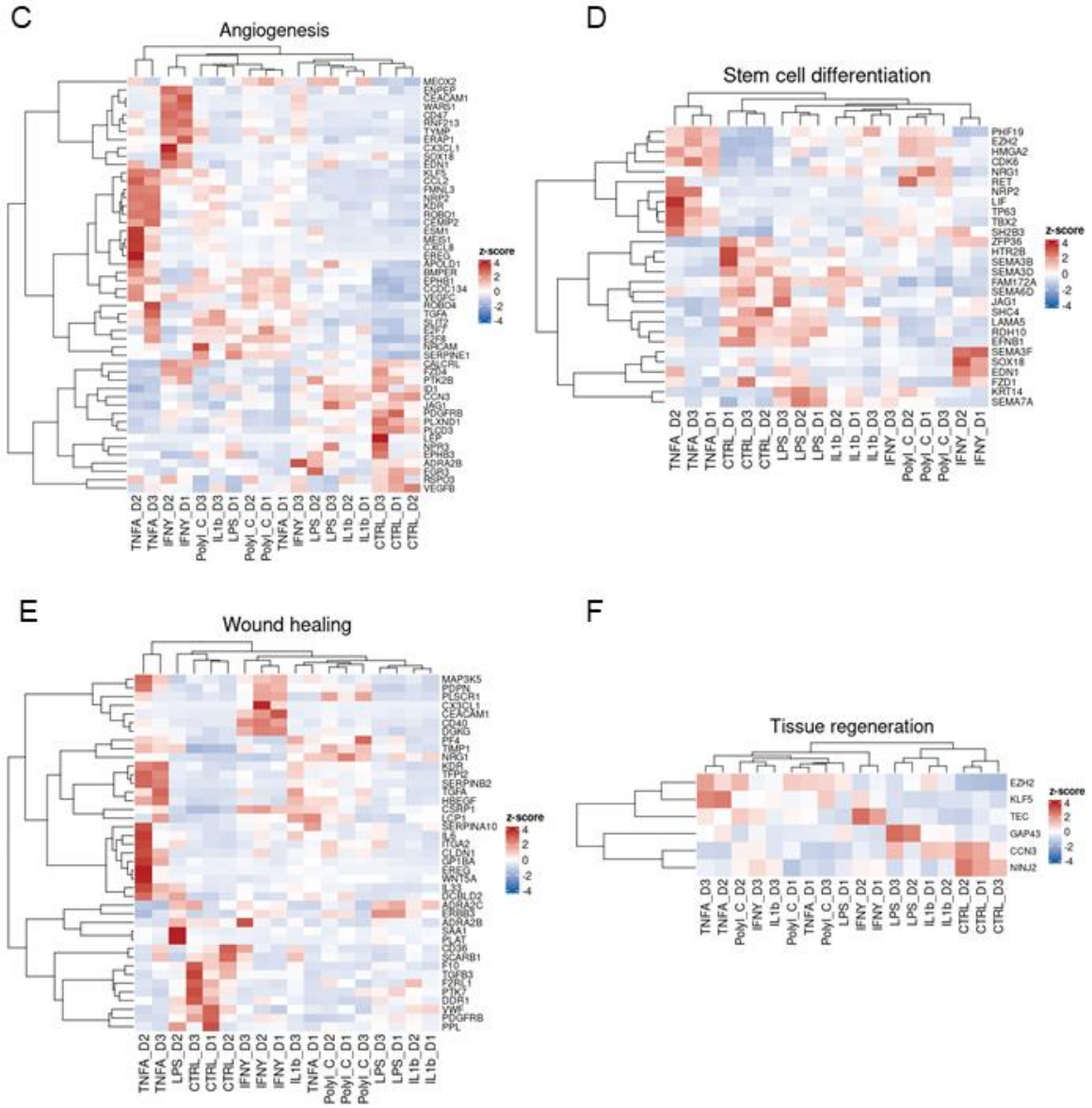


**Figure 9C-F.** Clustered heatmaps portraying various processes: (C) Angiogenesis, (D) Stem cell differentiation, (E) Wound healing, and (F) Tissue regeneration.

Cytotoxicity and viability tests were employed to ensure the cells did not encounter cytotoxic levels of inflammatory agents. The results demonstrated that cellular metabolism and viability were preserved during treatment, underscoring the administered agents' safety and potential therapeutic significance in maintaining cellular health and function **(Figure 10)**.

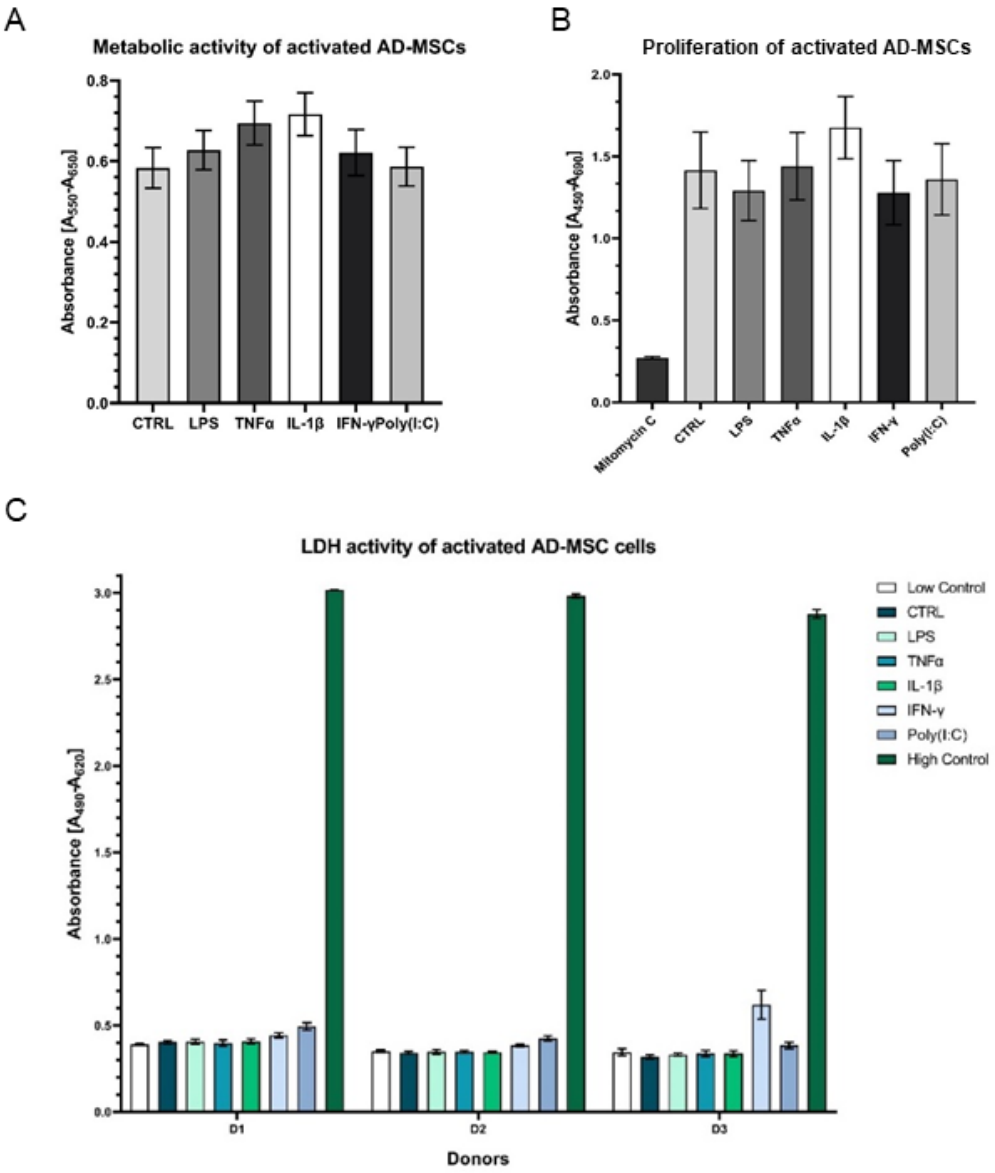


**Figure 10.** Assessment of Metabolic and Proliferation Activity in Treated AD-MSCs. (A) MTT assay reveals no significant change in metabolic activity compared to control. (B) BrdU incorporation indicates unaffected cell proliferation. (C) Treatment does not affect cell viability, ensuring accurate results.

### 4.5. Influence of treatments on cell proliferation and migration

The cell proliferation and migration assay utilized impedance measurements to assess the rate of cell migration during wound closure in treated samples relative to a control group after the injury. Two experimental conditions were examined: one where the wound was introduced before treatment **(Figure 11A)** and another where treatment preceded wound induction **(Figure 11B)**. In both cases, distinct variations in wound closure dynamics were evident between cells

subjected to IL-1β treatment and the control group. Specifically, when applied before wound initiation, IL-1β significantly hastened wound closure, whereas its post-wound application decelerated the process.

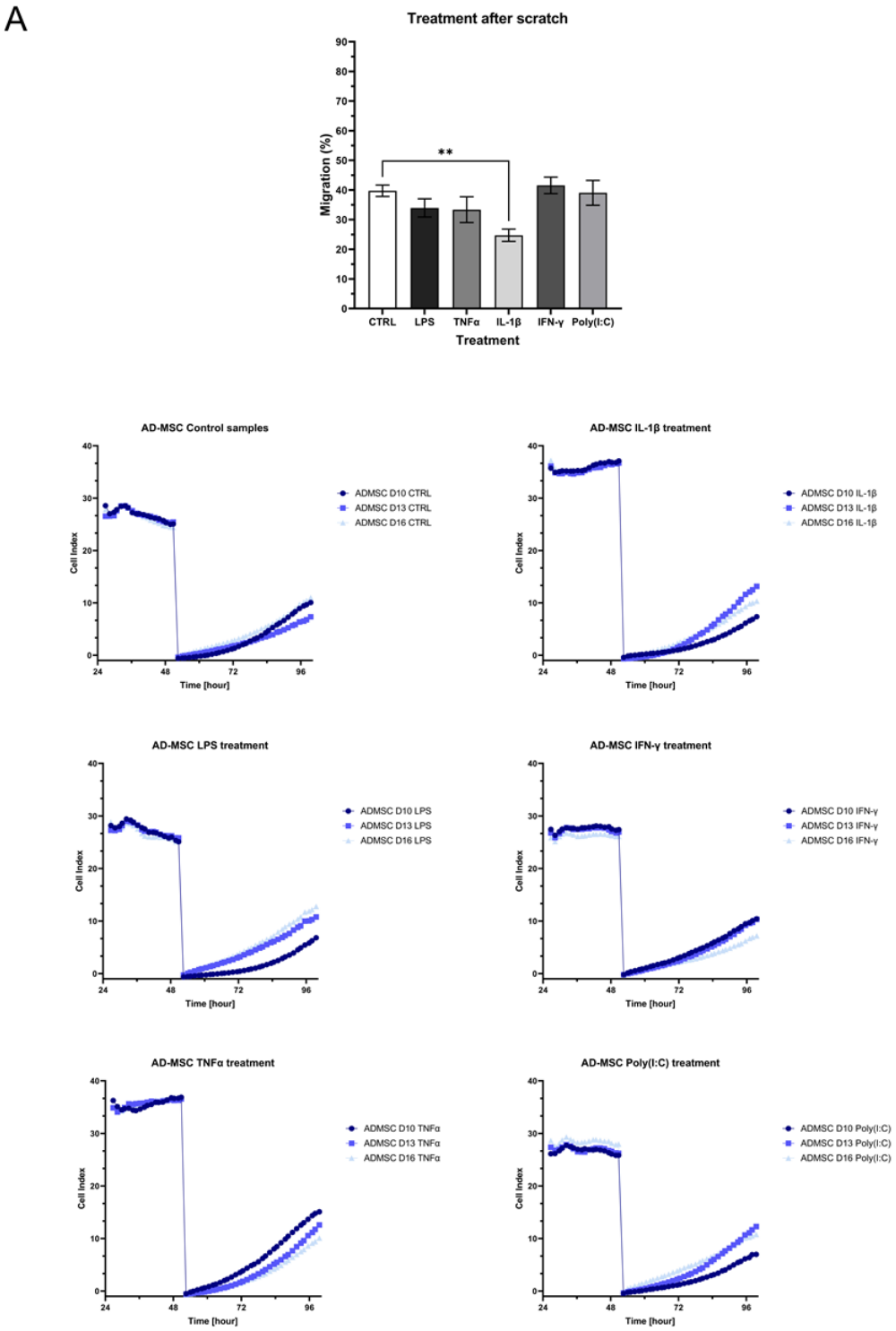


**Figure 11A**. The impedance-based method measures the re-population of the direct wound size in (A) "treatment before scratch," simulating an initially inflammatory environment.

B

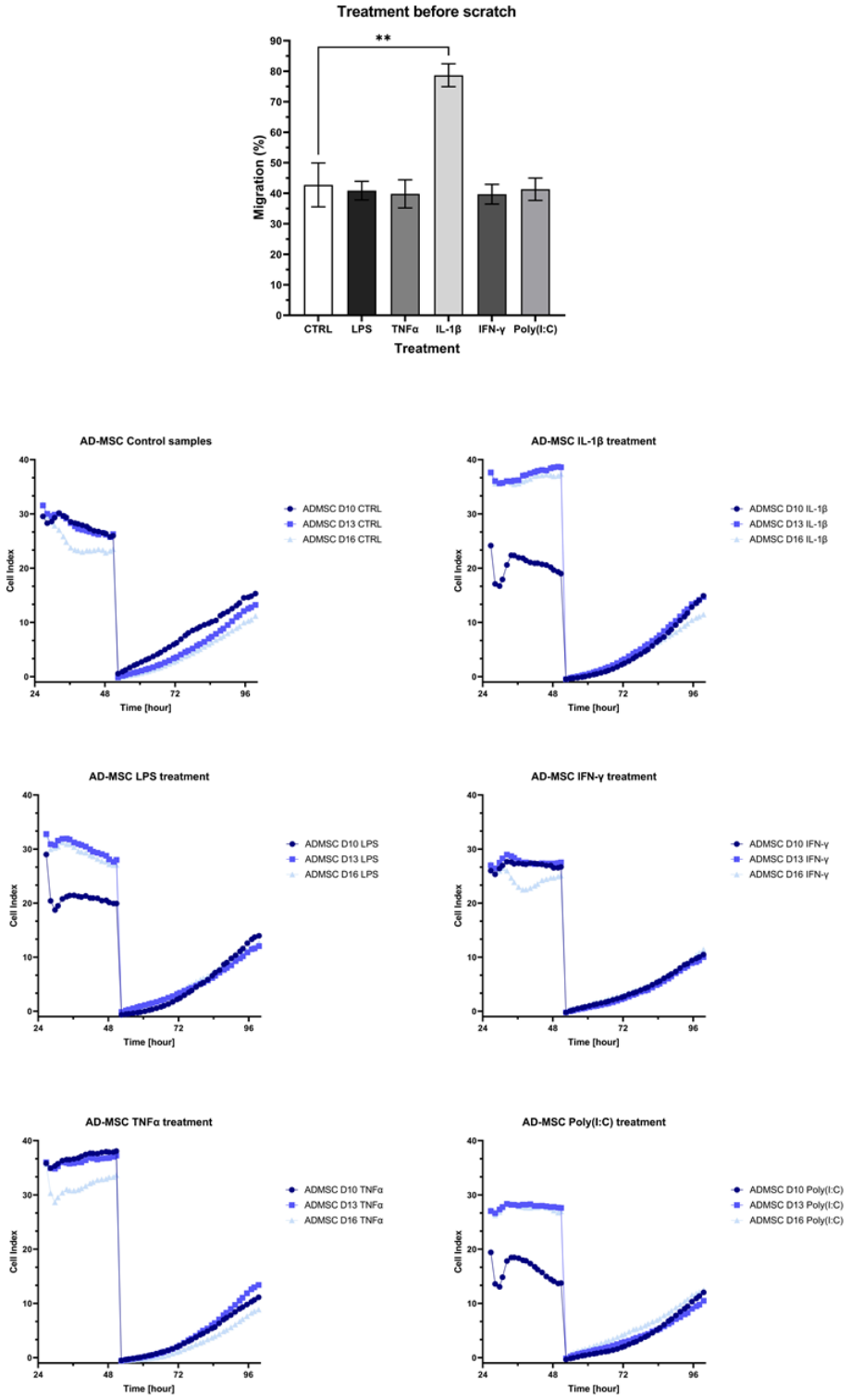


**Figure 11B.** The impedance-based method measures the re-population of the direct wound size in (B) "treatment after scratch," mimicking an infected wound.

### 4.6. Analysis of Gene and Protein Expression using qPCR and ELISA

The quantitative polymerase chain reaction (qPCR) analysis results unveiled distinct gene expression patterns in response to various treatments **(Figure 12)**. CXCL-8 exhibited robust upregulation in response to all treatments, particularly following exposure to LPS, TNFα, and IL-1β. Conversely, both NAGS and STAT6 consistently demonstrated downregulation across all treatment conditions. Interestingly, while TNFα treatment did not significantly affect IL-6 expression, the other administered treatments induced a notable reduction in IL-6 mRNA levels. Additionally, CXCL-10 displayed elevated expression following TNFα treatment and a modest increase following IFNγ exposure. Conversely, ASGR1 exhibited a notable decrease in expression levels following treatment with LPS, TNFα, and IFNγ, while it demonstrated an elevation in response to IL1β and PolyI:C. In the case of ICAM1, its expression slightly increased following TNFα treatment, but conversely, it decreased when subjected to all other treatments.

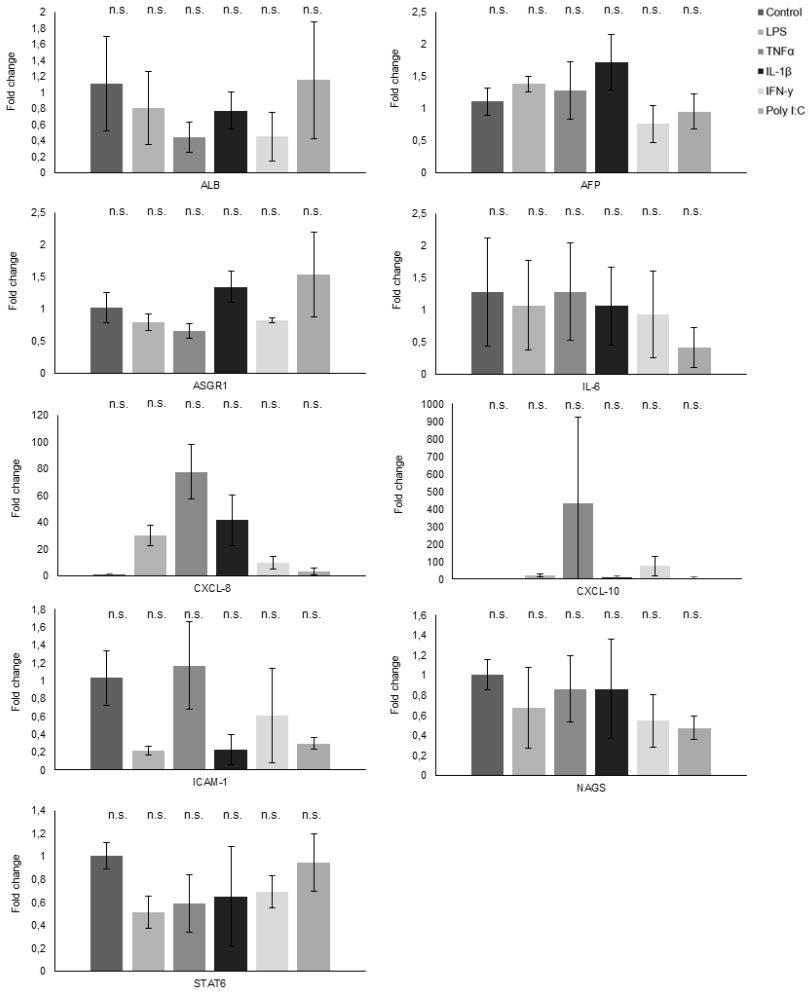


**Figure 12.** Gene expression analysis through qPCR reveals the fold change in various genes following treatments.

At the protein level, distinct differences emerged **(Figure 13A)**. Specifically, treatments with LPS, TNFα, and IL-1β resulted in a notable increase in IL-6 levels, whereas IFNγ and Poly I:C treatments led to a discernible reduction in IL-6 protein concentrations. CXCL-8 exhibited an augmentation in response to LPS and TNFα treatments, contrasting with a diminishment observed following the remaining treatment regimens. Interestingly, CXCL-10 demonstrated an elevation in protein levels across all administered treatments, with particularly significant peaks observed following TNFα and IFNγ treatments. The multiplex ELISA findings revealed notable changes in IFNγ, IL-5, IL-12p70, and IL-22 levels. Specifically, IL-5, IL-12p70, and IL-22 significantly increased following IL-1β treatment **(Figure 13B)**.

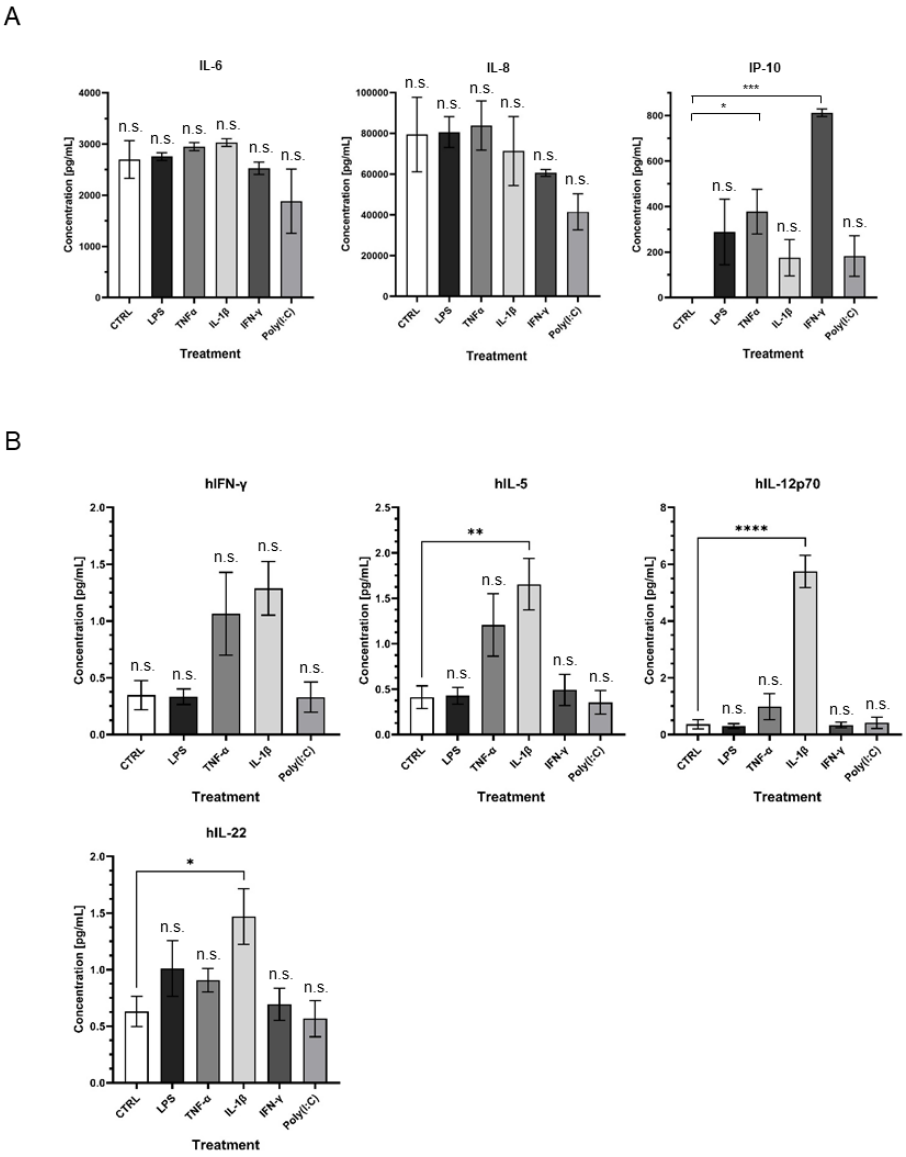


**Figure 13.** (A) Visual representation of ELISA results and (B) presentation of Quanterix findings.

## 5. DISCUSSION

The regenerative and immunomodulatory capabilities of mesenchymal stem cells (MSCs) are well-established; however, developing an efficacious therapeutic protocol remains a critical goal. Utilizing animal models and in vitro cell cultures, prior research has indicated that MSC licensing significantly enhances tissue regeneration, reduces inflammation, and expedites wound closure. (3,4,34,50,62,70–72) In our investigations, human adipose tissue-derived MSC (AD-MSC) primary cell cultures were subjected to treatment with lipopolysaccharide (LPS) and tumor necrosis factor-alpha (TNFα) to induce an inflammatory microenvironment. Subsequently, we conducted a comprehensive examination of gene and protein expression alterations. Both treatments led to substantial changes in the RNA-Seq profile compared to the control, manifesting increased expression of genes associated with cell proliferation, differentiation, wound healing, and migration in the LPS and TNFα environments. Notably, TNFα treatment significantly elevated the expression of interleukins, chemokines, chemokine ligands, and growth factors related to the immune response.

Additionally, certain interleukins exhibited heightened protein levels in response to LPS treatment. STRING analysis of secreted cytokines unveiled the involvement of proteins like MMP-9, VEGFA, ICAM-1, and ANGPT-2 in vascular remodeling, a pivotal aspect of wound healing. (40,42,43,73) Proteins such as HGF and FGF-19, along with chemokines LIF, CXCL-12, CCL7, and CCL5, implicated in MSC migration and local immunosuppression, were also activated by both treatments. (40,42,43,73) While the overall pattern and pathways were similar for LPS and TNFα treatments, TNFα induced a more pronounced activation of immune response pathways, particularly CD40L, indicative of a pro-inflammatory MSC phenotype. These findings suggest that MSC activation can enhance wound healing, endorsing the therapeutic potential of cell licensing. Notably, pathways identified through gene expression studies were corroborated using cytokine expression, albeit with the acknowledgment of the greater detail offered by gene expression data. Both treatments significantly accelerated wound closure in wound healing assays, supporting the hypothesis that MSC activation contributes to tissue regeneration and immunomodulation. Despite these promising outcomes, further studies are warranted to refine potential therapeutic procedures. By refining our experimental setup, a preclinical test may be devised to monitor gene expression changes in patients with chronic, non-healing wounds, ulcers, or burns in response to the inflammatory microenvironment,

allowing for personalized autologous therapy in the long term. Our results underscore the potential of AD-MSCs in treating persistent inflammatory conditions, emphasizing their clinical therapeutic efficacy in promoting tissue healing, extracellular matrix remodeling, and regeneration. The multifaceted attributes of AD-MSCs, including their regenerative, antiapoptotic, antifibrotic, antioxidant, and immunomodulating capabilities, enhance their clinical therapeutic potential.

Moreover, research indicates that the secretome of AD-MSCs, influenced by appropriate pretreatments, can positively impact disease progression. (4,33) Literature also suggests that specific pretreatments can augment the effectiveness of MSCs, often seeking to emulate the inflammatory milieu. Although ongoing research explores the biological processes and safe treatment modalities, outcomes thus far are promising, positioning licensed MSCs as a potential next-generation therapeutic approach for injuries associated with acute and sub-acute inflammation. (54,60,74–76)

Mesenchymal stem cells (MSCs) are crucial in various immunological processes. They actively regulate their microenvironment and influence the differentiation of different cells, including immune cells, by producing cytokines and growth factors. (75) In their basal state, MSCs exhibit antiangiogenic properties, and their immunomodulatory effectiveness depends on the nature and intensity of inflammatory signals, such as interferon-γ (IFN-γ), tumor necrosis factor-α (TNF-α), and Toll-like receptor (TLR)-mediated activation. Under specific inflammatory stimuli, MSCs gain an antiapoptotic, proangiogenic, and immunosuppressive feature. (51,75,77–79) They contribute to inflammation reduction by secreting factors like interleukin-6 (IL-6), indoleamine 2,3-dioxygenase (IDO), HLA G5 (human leukocyte antigen G5), interleukin-10 (IL-10), transforming growth factor beta-1 (TGFb1), hepatocyte growth factor (HGF), HOX-1, IL-1Ra (IL-1 receptor antagonist), prostaglandin E2 (PGE2), and through cell-cell contact. (75,77,80,81) The immunomodulatory potential of MSCs is contingent on their response to specific inflammatory cues. (82,83)

MSCs actively produce a diverse array of chemokines and adhesion molecules, including ligands for CXC chemokine receptor 3 (CXCR3), C-C chemokine receptor type 5 (CCR5), intercellular adhesion molecule 1 (ICAM-1/CD54), and vascular cell adhesion molecule 1 (VCAM-1). (79,84) The pronounced expression of CXCR3 in effector and memory T cells underscores the significance of MSC-generated chemokines, particularly CXCL9 (chemokine

ligand 9), CXCL10 (chemokine ligand 10), and CXCL11 (chemokine ligand 11), in orchestrating the recruitment of lymphocytes to the site of tissue damage for optimal immunosuppression. (75,85,86) The ability of MSCs to influence the immune system depends on variables such as tissue origin, the specific microenvironment, and interactions with other cellular partners.

Adipose-derived mesenchymal stem cells (AD-MSCs) hold considerable significance in wound healing, exhibiting regenerative, anti-apoptotic, antifibrotic, anti-oxidative, and immunomodulatory properties. (10,30,33–35,37,40,43,47,48,50–53,55–62,73,74,87–89) The secretome of AD-MSCs, representing the substances they release, has positively impacted various diseases. Priming or pre-conditioning AD-MSCs with pro-inflammatory cytokines like interferon-gamma (IFN-γ) and tumor necrosis factor-alpha (TNFα) enhances their immunomodulatory capabilities, influencing specific genes associated with signaling proteins, immune molecules, and cell surface markers. (30,33–35,72,75,76,90) However, achieving a precise balance between immunosuppressive and pro-inflammatory effects remains an area of ongoing exploration.

MSC therapy has grown substantially, with over 1000 trials conducted, but only a fraction has progressed to industry-sponsored phase III trials due to the field's relative novelty. Challenges persist in optimizing cell quantity and delivery methods and understanding the importance of MSC localization at the injury site. Licensing AD-MSCs with IFN-γ is suggested to enhance their immunomodulatory potential, showing promise in treating immune-related diseases. (30,33–35,72,75,76,90–93) Studies on immunoglobulin kappa chains in various cancer cell types highlight the significance of critical proteins like RAG1, RAG2, and AID in immunoglobulin production and rearrangement. (94) The functional consequences of immunoglobulin expression in cancer cell growth remain unclear, emphasizing the need for in-depth research in cancer biology and therapeutic strategies. (94,95) As we can see, MSC-secreted factors have a prominent role in tissue regeneration and immunomodulation. (87) Tailoring the secretome can be achieved through targeted pretreatments, augmenting its therapeutic versatility. Research exploring the paracrine impacts of AD-MSCs has produced compelling results. For example, priming AD-MSCs with tumor necrosis factor-alpha (TNFα) and administering their secretome to skin wounds in rats has significantly accelerated wound healing, as evidenced by increased proliferation, angiogenesis, epithelialization, and

recruitment of macrophages.(72,75) Significantly, inflammatory cytokines such as IL-6 and IL-8 have been acknowledged as facilitators of this hastened progression. (72,75) Likewise, AD-MSCs exposed to prior treatment with lipopolysaccharides (LPS) have showcased their capacity to enhance wound healing and angiogenesis. This is accompanied by an elevated secretion of growth factors linked to tissue regeneration and immune reactions. (71) In a mouse model of atopic dermatitis, AD-MSCs have demonstrated their ability to modulate the immune system, effectively inhibiting the proliferation and maturation of B-lymphocytes. (96) These encouraging discoveries emphasize the wide-ranging potential of AD-MSCs and their secretome in the field of regenerative medicine. The diverse functions of cytokines, the influence of factors like MMP-9 and MMP-8 on wound healing, and the identification of possible therapeutic targets collectively enhance the scope of AD-MSC therapy. The complex interaction of these components underscores their crucial importance in propelling forward regenerative medicine. (97) Croitoru-Lamoury and colleagues investigated the impact of proinflammatory cytokines TNF-α and IFN-γ on the gene expression of chemokines and their receptors in human mesenchymal stem cells (HuMSCs). HuMSCs were subjected to TNF-α, IFN-γ, or a combination of both for a duration of up to 72 hours, and gene expression was analyzed using RT-PCR at different time intervals. (98) The findings unveiled that TNF-α elevated the expression of the receptor CXCR4, while both TNF-α and IFN-γ boosted the gene transcription of multiple chemokines (CCL2/MCP-1, CCL3/MIP-1α, CCL4/MIP-1β, CCL5/RANTES, CXCL8/IL-8, CXCL10/IP-10) and cytokines (IL-1β and IL-6). IFN-γ specifically increased the gene expression of particular chemokines (CXCL9/MIG, CX3CL1/fractalkine) and IL-6. Remarkably, the simultaneous application of TNF-α and IFN-γ synergistically heightened the expression of several genes, including CCL3/MIP-1α, CCL4/MIP-1β, CCL5/RANTES, CXCL9/MIG, CXCL10/IP-10, CX3CL1/fractalkine, IL-1β, and IL-6. (98) IL-10 stands out as one of the most crucial anti-inflammatory cytokines. MSCs have the ability to induce IL-10 production in macrophages or dendritic cells, yet the question of whether MSCs themselves can secrete IL-10 remains a topic of debate. (99)

A thorough and detailed comparative study has shown that MSCs from different tissues secrete MCP-1, IL-8, VEGF, IL-6, IL-5, IFNy, and MIP-1β, with secretion patterns influenced by the age of the culture. (98) In these investigations, untreated MSCs from various tissues were examined, revealing that adipose-derived MSCs secrete the highest levels of IL-6. Additionally,

pro-inflammatory cytokines TNF-α, IL-2, IL-9, and IL-17 expressed in the supernatant were linked to myogenic differentiation. (98) The combined administration of IFN-γ and TNF-α markedly enhances MSCs' capacity to produce factor H, a critical molecule essential for inhibiting complement activation. (75,100) Comparable to our findings, IL-1b stimulation led to the secretion of TNF-α, IL-6, IL-8, IL-23A, CCL5, CCL20, CXCL10, and CXCL11 cytokines, accompanied by elevated expression of adhesion molecules (VCAM-1, ICAM-1, ICAM-4). (75) When MSCs underwent multi-cytokine priming, including TNF-α, IL-1β, and IFN-γ, the addition of IL-1β further enhanced the already established immunoregulatory activity initiated by TNF-α/IFN-γ. (101) Extended exposure to TNFα led to gene expression and cytokine secretion profiles (IL-4, IL-8, IL-6, and IL-10) similar to those observed in our study. (102,103) Nevertheless, the impact of these treatments on the innate wound healing capacity remained untested. TLR receptors represent one of the oldest defense mechanisms against pathogens and innate immunity components. Experiments involving LPS (TLR4) and PolyI:C (TLR3) revealed that MSCs upregulated their IL-6 and IL-8 expression (45,79,84,104,105), and TLR3 display a heightened immunosuppressive phenotype. (104,105) In conclusion, AD-MSCs have proven to be powerful allies in the quest for effective therapies for non-healing, chronic, and inflamed wounds, even in cases of prolonged inflammation. Although these varied treatments may trigger different pathways, their combined potential to enhance tissue healing, remodel the extracellular matrix, and facilitate regeneration in clinical settings is unquestionably remarkable.(3,31,45,70,92)

## 6. SUMMARY

While adipose-derived mesenchymal stem cells (AD-MSCs) have been increasingly harnessed in regenerative medicine, their behavior in clinical applications, particularly under inflammatory environments, remains crucial for therapy outcomes. Our investigation sought to unravel the pathways induced by an inflammatory microenvironment in these cells. High-throughput gene expression assays were conducted on AD-MSCs activated with lipopolysaccharide (LPS) and tumor necrosis factor-alpha (TNFα). RNA-Seq data analysis revealed distinct gene expression patterns in control, LPS-treated, and TNFα-treated samples. LPS treatment induced gene changes associated with cell division, DNA repair, the cell cycle, and various metabolic processes. TNFα treatment impacted genes related to cell division, the immune response, cell proliferation, and differentiation. Mapping these changes to biological pathways through Gene Ontology and KEGG databases provided insights into the affected processes. Protein-level examination of secreted cytokines and a functional wound healing assay demonstrated that activated AD-MSCs increased the secretion of IL-6, IL-8, and CXCL-10, along with accelerated wound closure. These findings underscore the potential clinical utility of AD-MSCs, especially in inflammation, and contribute valuable insights for advancing regenerative medicine applications.

Regenerative medicine has increasingly spotlighted the therapeutic potential of mesenchymal stem cells (MSCs) sourced from adipose tissue, particularly notable for their adeptness in tissue regeneration and modulation of the immune system. This is especially pertinent in addressing chronic inflammatory conditions such as ulcers and wounds. Our research delves into the transformative impact of pretreatment on these adipose-derived mesenchymal stem cells (AD-MSCs). A 24-hour exposure to six inflammatory factors resulted in noteworthy alterations in gene expression, proteome profiles, and accelerated wound closure rates, indicating a discernible shift in therapeutic effectiveness. Through RNA-Seq and bioinformatic analysis, we elucidated the biological pathways influenced by the in vitro inflammatory microenvironment. Cytokine secretion studies revealed that activated MSCs exhibited an increased release of IP-10, IL-5, IL12p70, and IL-22, underscoring their potential to expedite wound closure. These findings portend a promising clinical application of MSCs in treating chronic ulcers, contributing to a deeper understanding of MSC immunological dynamics and paving the way for transformative interventions in regenerative medicine.

## 7 FUNDING

This work was supported by the National Research, Development, and Innovation Office (NKFI PD 132570 to Z.V.) and GINOP_PLUSZ-2.1.1-21-2022-00043 project (co-financed by the European Union and the European Regional Development Fund) Z.V. was supported by the Bolyai János Postdoctoral Fellowship (BO/00190/20/5). Project no. TKP2021-EGA-28 has been implemented with support from the Ministry of Innovation and Technology of Hungary from the National Research, Development and Innovation Fund, financed under the TKP2021-EGA funding scheme. L.K. has received funding from the EU's Horizon 2020 research and innovation program under grant agreement No. 739593. The Translational Biomedicine Competence Centre and the Biobank ACF of the Life Sciences Cluster of the Centre of Excellence for Interdisciplinary Research, Development, and Innovation of the University of Szeged supported the research. The author is a member of the Regenerative Medicine research group. The study was conducted in the Personalised Medicine Research Infrastructure, a member of the TOP50 Excellent Research Infrastructure in Hungary, awarded by the National Research, Development and Innovation Office.

## 8. ACKNOWLEDGMENTS

I wish to extend my sincere gratitude to Prof. Dr. Lajos Kemény and Prof. Dr. Rolland Gyulai for granting me the opportunity to participate in their Ph.D. program and conduct my research in the laboratory of the Department of Dermatology and Allergology at the University of Szeged.

I am profoundly grateful to my supervisor, Dr. Zoltán Veréb, for his precious guidance and insightful advice throughout my doctoral studies.

I'm deeply thankful to Tamás Monostori for his collaborative spirit and significant contributions to experiments and statistical analysis in this project. Thanks for his uplifting chats and playful banter, which brought brightness to my day.

I am also thankful to Vanda Miklós for her contributions to sequencing data analysis and statistical support, which greatly enhanced the credibility of my research findings.

I express my heartfelt thanks to Katalin Boldog for her administrative and technical assistance during the research, as well as for her many positive and humorous thoughts that brightened up the everyday routine.

My appreciation extends to Dr. Szilárd Póliska for his expertise in performing RNA-sequencing, a pivotal aspect of our study.

Furthermore, I am grateful to Dr. Balázs Bende and Dr. Erika Kis for their involvement in procuring adipose tissue samples from patients.

I deeply appreciate the support and assistance provided by all members of the Department of Dermatology and Allergology throughout my Ph.D. journey.

Finally, and most importantly, I wish to convey my genuine appreciation, deep gratitude, and admiration to my love, family, and friends. Their unwavering love has provided me with stability during challenging times and celebrated alongside me in moments of joy.

## 9. REFERENCES


1. Baron JM, Glatz M, Proksch E. Optimal Support of Wound Healing: New Insights. Dermatol Basel Switz. 2020;236(6):593–600.

2. Guillamat-Prats R. The Role of MSC in Wound Healing, Scarring and Regeneration. Cells. 2021. július 8.;10(7):1729.

3. Mazini L, Rochette L, Admou B, Amal S, Malka G. Hopes and Limits of Adipose-Derived Stem Cells (ADSCs) and Mesenchymal Stem Cells (MSCs) in Wound Healing. Int J Mol Sci. 2020. február;21(4).

4. Gimble JM, Katz AJ, Bunnell BA. Adipose-Derived Stem Cells for Regenerative Medicine. Circ Res. 2007. május 11.;100(9):1249–60.

5. Konno M, Hamabe A, Hasegawa S, Ogawa H, Fukusumi T, Nishikawa S, és mtsai. Adipose-derived mesenchymal stem cells and regenerative medicine. Dev Growth Differ. 2013. április;55(3):309–18.

6. Brembilla NC, Vuagnat H, Boehncke WH, Krause KH, Preynat-Seauve O. Adipose-Derived Stromal Cells for Chronic Wounds: Scientific Evidence and Roadmap Toward Clinical Practice. Stem Cells Transl Med. 2023. 0;12(1):17–25.

7. Clinical application of mesenchymal stem cell in regenerative medicine: a narrative review - PubMed [Internet]. [idézi 2024. március 22.]. Elérhető: https://pubmed.ncbi.nlm.nih.gov/35902958/

8. Wilkinson HN, Hardman MJ. Wound healing: cellular mechanisms and pathological outcomes. Open Biol. 2020. szeptember;10(9):200223.

9. Hassanshahi A, Hassanshahi M, Khabbazi S, Hosseini-Khah Z, Peymanfar Y, Ghalamkari S, és mtsai. Adipose-derived stem cells for wound healing. J Cell Physiol. 2019. június;234(6):7903–14.

10. Huerta CT, Voza FA, Ortiz YY, Liu ZJ, Velazquez OC. Mesenchymal stem cell-based therapy for non-healing wounds due to chronic limb-threatening ischemia: A review of preclinical and clinical studies. Front Cardiovasc Med. 2023;10:1113982.

11. Krawczenko A, Klimczak A. Adipose Tissue-Derived Mesenchymal Stem/Stromal Cells and Their Contribution to Angiogenic Processes in Tissue Regeneration. Int J Mol Sci. 2022. március;23(5).

12. Bowers S, Franco E. Chronic Wounds: Evaluation and Management. Am Fam Physician. 2020. február 1.;101(3):159–66.

13. Atkin L. Chronic wounds: the challenges of appropriate management. Br J Community Nurs. 2019. szeptember 1.;24(Sup9):S26–32.

14. Azevedo M, Lisboa C, Rodrigues A. Chronic wounds and novel therapeutic approaches. Br J Community Nurs. 2020;25(Sup12):S26–32.

15. Kathawala MH, Ng WL, Liu D, Naing MW, Yeong WY, Spiller KL, és mtsai. Healing of Chronic Wounds: An Update of Recent Developments and Future Possibilities. Tissue Eng Part B Rev. 2019. október;25(5):429–44.

16. Williams M. Wound infections: an overview. Br J Community Nurs. 2021. június 1.;26(Sup6):S22–5.

17. Vasanthan J, Gurusamy N, Rajasingh S, Sigamani V, Kirankumar S, Thomas EL, és mtsai. Role of Human Mesenchymal Stem Cells in Regenerative Therapy. Cells. 2020;10(1):54.

18. Wang Y, Fang J, Liu B, Shao C, Shi Y. Reciprocal regulation of mesenchymal stem cells and immune responses. Cell Stem Cell. 2022;29(11):1515–30.

19. Huang JN, Cao H, Liang KY, Cui LP, Li Y. Combination therapy of hydrogel and stem cells for diabetic wound healing. World J Diabetes. 2022;13(11):949–61.

20. Huang JN, Cao H, Liang KY, Cui LP, Li Y. Combination therapy of hydrogel and stem cells for diabetic wound healing. World J Diabetes. 2022;13(11):949–61.

21. Liu J, Gao J, Liang Z, Gao C, Niu Q, Wu F, és mtsai. Mesenchymal stem cells and their microenvironment. Stem Cell Res Ther. 2022;13(1):429.

22. Ullah M, Liu DD, Thakor AS. Mesenchymal Stromal Cell Homing: Mechanisms and Strategies for Improvement. iScience. 2019. május 31.;15:421–38.

23. Miceli V. Use of priming strategies to advance the clinical application of mesenchymal stromal/stem cell-based therapy. World J Stem Cells. 2024;16(1):7–18.

24. Ding DC, Shyu WC, Lin SZ. Mesenchymal stem cells. Cell Transplant. 2011;20(1):5–14.

25. Galipeau J, Sensébé L. Mesenchymal Stromal Cells: Clinical Challenges and Therapeutic Opportunities. Cell Stem Cell. 2018. június 1.;22(6):824–33.

26. Han Y, Li X, Zhang Y, Han Y, Chang F, Ding J. Mesenchymal Stem Cells for Regenerative Medicine. Cells. 2019;8(8):886.

27. Naji A, Eitoku M, Favier B, Deschaseaux F, Rouas-Freiss N, Suganuma N. Biological functions of mesenchymal stem cells and clinical implications. Cell Mol Life Sci. 2019. szeptember;76(17):3323–48.

28. Brown C, McKee C, Bakshi S, Walker K, Hakman E, Halassy S, és mtsai. Mesenchymal stem cells: Cell therapy and regeneration potential. J Tissue Eng Regen Med. 2019. szeptember;13(9):1738–55.

29. Mishra VK, Shih HH, Parveen F, Lenzen D, Ito E, Chan TF, és mtsai. Identifying the Therapeutic Significance of Mesenchymal Stem Cells. Cells. 2020. május 6.;9(5):1145.

30. Bunnell BA. Adipose Tissue-Derived Mesenchymal Stem Cells. Cells. 2021. 0;10(12).

31. Pittenger MF, Discher DE, Peault BM, Phinney DG, Hare JM, Caplan AI. Mesenchymal stem cell perspective: cell biology to clinical progress. NPJ Regen Med. 2019;4:22.

32. Mazini L, Rochette L, Admou B, Amal S, Malka G. Hopes and Limits of Adipose-Derived Stem Cells (ADSCs) and Mesenchymal Stem Cells (MSCs) in Wound Healing. Int J Mol Sci. 2020. február;21(4).

33. Al-Ghadban S, Bunnell BA. Adipose Tissue-Derived Stem Cells: Immunomodulatory Effects and Therapeutic Potential. Physiol Bethesda. 2020. március 1.;35(2):125–33.

34. Konno M, Hamabe A, Hasegawa S, Ogawa H, Fukusumi T, Nishikawa S, és mtsai. Adipose-derived mesenchymal stem cells and regenerative medicine. Dev Growth Differ. 2013. április;55(3):309–18.

35. Cao W, Cao K, Cao J, Wang Y, Shi Y. Mesenchymal stem cells and adaptive immune responses. Immunol Lett. 2015. 0;168(2):147–53.

36. Li N, Hua JL. Interactions between mesenchymal stem cells and the immune system. Cell Mol Life Sci. 2017. július;74(13):2345–60.

37. Mushahary D, Spittler A, Kasper C, Weber V, Charwat V. Isolation, cultivation, and characterization of human mesenchymal stem cells. Cytometry A. 2018. 0;93A(1):19–31.

38. Qi K, Li N, Zhang Z, Melino G. Tissue regeneration: The crosstalk between mesenchymal stem cells and immune response. Cell Immunol. 2018. április;326:86–93.

39. Song N, Scholtemeijer M, Shah K. Mesenchymal Stem Cell Immunomodulation: Mechanisms and Therapeutic Potential. Trends Pharmacol Sci. 2020. szeptember;41(9):653–64.

40. Krawczenko A, Klimczak A. Adipose Tissue-Derived Mesenchymal Stem/Stromal Cells and Their Contribution to Angiogenic Processes in Tissue Regeneration. Int J Mol Sci. 2022. március;23(5).

41. Carelli S, Colli M, Vinci V, Caviggioli F, Klinger M, Gorio A. Mechanical Activation of Adipose Tissue and Derived Mesenchymal Stem Cells: Novel Anti-Inflammatory Properties. Int J Mol Sci. 2018. 0;19(1).

42. Anton K, Banerjee D, Glod J. Macrophage-Associated Mesenchymal Stem Cells Assume an Activated, Migratory, Pro-Inflammatory Phenotype with Increased IL-6 and CXCL10 Secretion. Plos One. 2012. április 4.;7(4).

43. Ridiandries A, Tan JTM, Bursill CA. The Role of Chemokines in Wound Healing. Int J Mol Sci. 2018. október;19(10).

44. Zwick RK, Guerrero-Juarez CF, Horsley V, Plikus MV. Anatomical, Physiological, and Functional Diversity of Adipose Tissue. Cell Metab. 2018. 0;27(1):68–83.

45. Szucs D, Miklós V, Monostori T, Guba M, Kun-Varga A, Póliska S, és mtsai. Effect of Inflammatory Microenvironment on the Regenerative Capacity of Adipose-Derived Mesenchymal Stem Cells. Cells. 2023. 0;12(15).

46. Brembilla NC, Vuagnat H, Boehncke WH, Krause KH, Preynat-Seauve O. Adipose-Derived Stromal Cells for Chronic Wounds: Scientific Evidence and Roadmap Toward Clinical Practice. Stem Cells Transl Med. 2023. 0;12(1):17–25.

47. Cheng HY, Anggelia MR, Lin CH, Wei FC. Toward transplantation tolerance with adipose tissue-derived therapeutics. Front Immunol. 2023;14:1111813.

48. Carelli S, Colli M, Vinci V, Caviggioli F, Klinger M, Gorio A. Mechanical Activation of Adipose Tissue and Derived Mesenchymal Stem Cells: Novel Anti-Inflammatory Properties. Int J Mol Sci. 2018. 0;19(1).

49. Guasti L, New SE, Hadjidemetriou I, Palmiero M, Ferretti P. Plasticity of human adipose-derived stem cells - relevance to tissue repair. Int J Dev Biol. 2018;62(6-7–8):431–9.

50. Munir S, Basu A, Maity P, Krug L, Haas P, Jiang DS, és mtsai. TLR4-dependent shaping of the wound site by MSCs accelerates wound healing. Embo Rep. 2020. május 6.;21(5).

51. Krampera M, Le Blanc K. Mesenchymal stromal cells: Putative microenvironmental modulators become cell therapy. Cell Stem Cell. 2021. október 7.;28(10):1708–25.

52. Fu X, Han B, Cai S, Lei Y, Sun T, Sheng Z. Migration of bone marrow-derived mesenchymal stem cells induced by tumor necrosis factor-alpha and its possible role in wound healing. Wound Repair Regen. 2009. április;17(2):185–91.

53. DelaRosa O, Lombardo E. Modulation of adult mesenchymal stem cells activity by toll-like receptors: implications on therapeutic potential. Mediat Inflamm. 2010;2010:865601.

54. François M, Romieu-Mourez R, Li MY, Galipeau J. Human MSC Suppression Correlates With Cytokine Induction of Indoleamine 2,3-Dioxygenase and Bystander M2 Macrophage Differentiation. Mol Ther. 2012. 0;20(1):187–95.

55. Shohara R, Yamamoto A, Takikawa S, Iwase A, Hibi H, Kikkawa F, és mtsai. Mesenchymal stromal cells of human umbilical cord Wharton's jelly accelerate wound healing by paracrine mechanisms. Cytotherapy. 2012;14(10):1171–81.

56. Furuta T, Miyaki S, Ishitobi H, Ogura T, Kato Y, Kamei N, és mtsai. Mesenchymal Stem Cell-Derived Exosomes Promote Fracture Healing in a Mouse Model. Stem Cells Transl Med. 2016. 0;5(12):1620–30.

57. Feldbrin Z, Omelchenko E, Lipkin A, Shargorodsky M. Osteopontin levels in plasma, muscles, and bone in patient with non-healing diabetic foot ulcers: A new player in wound healing process? J Diabetes Complications. 2018. 0;32(8):795–8.

58. Sahu A, Foulsham W, Amouzegar A, Mittal SK, Chauhan SK. The therapeutic application of mesenchymal stem cells at the ocular surface. Ocul Surf. 2019. április;17(2):198–207.

59. Kuca-Warnawin E, Janicka I, Szczesny P, Olesinska M, Bonek K, Gluszko P, és mtsai. Modulation of T-Cell Activation Markers Expression by the Adipose Tissue-Derived Mesenchymal Stem Cells of Patients with Rheumatic Diseases. Cell Transpl. 2020. 0;29:963689720945682.

60. Kurte M, Vega-Letter AM, Luz-Crawford P, Djouad F, Noël D, Khoury M, és mtsai. Time-dependent LPS exposure commands MSC immunoplasticity through TLR4 activation leading to opposite therapeutic outcome in EAE. Stem Cell Res Ther. 2020. szeptember 25.;11(1).

61. Xiao K, He W, Guan W, Hou F, Yan P, Xu J, és mtsai. Mesenchymal stem cells reverse EMT process through blocking the activation of NF-kappaB and Hedgehog pathways in LPS-induced acute lung injury. Cell Death Dis. 2020. október 15.;11(10):863.

62. Nieto-Nicolau N, Martinez-Conesa EM, Fuentes-Julian S, Arnalich-Montiel F, Garcia-Tunon I, De Miguel MP, és mtsai. Priming human adipose-derived mesenchymal stem cells for corneal surface regeneration. J Cell Mol Med. 2021. június;25(11):5124–37.

63. Love MI, Huber W, Anders S. Moderated estimation of fold change and dispersion for RNA-seq data with DESeq2. Genome Biol. 2014;15(12):550.

64. Gu Z, Eils R, Schlesner M. Complex heatmaps reveal patterns and correlations in multidimensional genomic data. Bioinformatics. 2016. szeptember 15.;32(18):2847–9.

65. Brionne A, Juanchich A, Hennequet-Antier C. ViSEAGO: a Bioconductor package for clustering biological functions using Gene Ontology and semantic similarity. BioData Min. 2019;12:16.

66. Gennady Korotkevich, Vladimir Sukhov, Nikolay Budin, Boris Shpak, Maxim N. Artyomov, Alexey Sergushichev. Fast gene set enrichment analysis. bioRxiv. 2021;060012.

67. Yu G, Li F, Qin Y, Bo X, Wu Y, Wang S. GOSemSim: an R package for measuring semantic similarity among GO terms and gene products. Bioinformatics. 2010. április 1.;26(7):976–8.

68. Saadh MJ, Ramírez-Coronel AA, Saini RS, Arias-Gonzáles JL, Amin AH, Gavilán JCO, és mtsai. Advances in mesenchymal stem/stromal cell-based therapy and their extracellular vesicles for skin wound healing. Hum Cell. 2023. július;36(4):1253–64.

69. Fu X, Liu G, Halim A, Ju Y, Luo Q, Song G. Mesenchymal Stem Cell Migration and Tissue Repair. Cells. 2019. augusztus;8(8):784.

70. Naji A, Eitoku M, Favier B, Deschaseaux F, Rouas-Freiss N, Suganuma N. Biological functions of mesenchymal stem cells and clinical implications. Cell Mol Life Sci. 2019. szeptember;76(17):3323–48.

71. Wang KX, Chen ZY, Jin L, Zhao LL, Meng LB, Kong FT, és mtsai. LPS-pretreatment adipose-derived mesenchymal stromal cells promote wound healing in diabetic rats by improving angiogenesis. Inj-Int J Care Inj. 2022. 0;53(12):3920–9.

72. Heo SC, Jeon ES, Lee IH, Kim HS, Kim MB, Kim JH. Tumor necrosis factor-alpha-activated human adipose tissue-derived mesenchymal stem cells accelerate cutaneous wound healing through paracrine mechanisms. J Invest Dermatol. 2011. július;131(7):1559–67.

73. Neuss S, Becher E, Wöltje M, Tietze L, Jahnen-Dechent W. Functional expression of HGF and HGF receptor/c-met in adult human mesenchymal stem cells suggests a role in cell mobilization, tissue repair, and wound healing. Stem Cells. 2004;22(3):405–14.

74. Skibber MA, Olson SD, Prabhakara KS, Gill BS, Cox CS. Enhancing Mesenchymal Stromal Cell Potency: Inflammatory Licensing Mechanotransduction. Front Immunol. 2022. július 6.;13.

75. Saparov A, Ogay V, Nurgozhin T, Jumabay M, Chen WC. Preconditioning of Human Mesenchymal Stem Cells to Enhance Their Regulation of the Immune Response. Stem Cells Int. 2016;2016:3924858.

76. Chinnadurai R, Rajan D, Ng S, McCullough K, Arafat D, Waller EK, és mtsai. Immune dysfunctionality of replicative senescent mesenchymal stromal cells is corrected by IFNγ priming. Blood Adv. 2017. április 25.;1(11):628–43.

77. Meisel R, Zibert A, Laryea M, Gobel U, Daubener W, Dilloo D. Human bone marrow stromal cells inhibit allogeneic T-cell responses by indoleamine 2,3-dioxygenase-mediated tryptophan degradation. Blood. 2004. június 15.;103(12):4619–21.

78. Ghannam S, Bouffi C, Djouad F, Jorgensen C, Noel D. Immunosuppression by mesenchymal stem cells: mechanisms and clinical applications. Stem Cell Res Ther. 2010;1(1):2.

79. Vereb Z, Mazlo A, Szabo A, Poliska S, Kiss A, Litauszky K, és mtsai. Vessel Wall-Derived Mesenchymal Stromal Cells Share Similar Differentiation Potential and Immunomodulatory Properties with Bone Marrow-Derived Stromal Cells. Stem Cells Int. 2020;2020:8847038.

80. Bartholomew A, Sturgeon C, Siatskas M, Ferrer K, McIntosh K, Patil S, és mtsai. Mesenchymal stem cells suppress lymphocyte proliferation in vitro and prolong skin graft survival in vivo. Exp Hematol. 2002. 0;30(1):42–8.

81. Aggarwal SP. Human mesenchymal stem cells modulate allogeneic immune cell responses. Blood. 2005. február 15.;105(4):1815–22.

82. Renner P, Eggenhofer E, Rosenauer A, Popp FC, Steinmann JF, Slowik P, és mtsai. Mesenchymal stem cells require a sufficient, ongoing immune response to exert their immunosuppressive function. Transpl Proc. 2009. 0;41(6):2607–11.

83. Li W, Ren G, Huang Y, Su J, Han Y, Li J, és mtsai. Mesenchymal stem cells: a double-edged sword in regulating immune responses. Cell Death Differ. 2012. szeptember;19(9):1505–13.

84. Vereb Z, Poliska S, Albert R, Olstad OK, Boratko A, Csortos C, és mtsai. Role of Human Corneal Stroma-Derived Mesenchymal-Like Stem Cells in Corneal Immunity and Wound Healing. Sci Rep. 2016. május 19.;6:26227.

85. Crop MJB. Inflammatory conditions affect gene expression and function of human adipose tissue-derived mesenchymal stem cells. Clin Exp Immunol. 2010. 0;162(3):474–86.

86. Wang Y, Chen X, Cao W, Shi Y. Plasticity of mesenchymal stem cells in immunomodulation: pathological and therapeutic implications. Nat Immunol. 2014. 0;15(11):1009–16.

87. Trayhurn P, Drevon CA, Eckel J. Secreted proteins from adipose tissue and skeletal muscle - adipokines, myokines and adipose/muscle cross-talk. Arch Physiol Biochem. 2011. május;117(2):47–56.

88. Ti D, Hao H, Tong C, Liu J, Dong L, Zheng J, és mtsai. LPS-preconditioned mesenchymal stromal cells modify macrophage polarization for resolution of chronic inflammation via exosome-shuttled let-7b. J Transl Med. 2015. szeptember 19.;13:308.

89. Wiese DM, Wood CA, Ford BN, Braid LR. Cytokine Activation Reveals Tissue-Imprinted Gene Profiles of Mesenchymal Stromal Cells. Front Immunol. 2022;13:917790.

90. Carvalho AES, Sousa MRR, Alencar-Silva T, Carvalho JL, Saldanha-Araujo F. Mesenchymal stem cells immunomodulation: The road to IFN-gamma licensing and the path ahead. Cytokine Growth Factor Rev. 2019. június;47:32–42.

91. Waterman RS, Tomchuck SL, Henkle SL, Betancourt AM. A new mesenchymal stem cell (MSC) paradigm: polarization into a pro-inflammatory MSC1 or an Immunosuppressive MSC2 phenotype. PLoS One. 2010. április 26.;5(4):e10088.

92. Hu C, Li L. Preconditioning influences mesenchymal stem cell properties in vitro and in vivo. J Cell Mol Med. 2018. március;22(3):1428–42.

93. Lu S, Qiao X. Single-cell profiles of human bone marrow-derived mesenchymal stromal cells after IFN-gamma and TNF-alpha licensing. Gene. 2021. március 1.;771:145347.

94. Zhao J, Peng H, Gao J, Nong A, Hua HM, Yang SL, és mtsai. Current insights into the expression and functions of tumor-derived immunoglobulins. Cell Death Discov. 2021. június 28.;7(1).

95. Chen Z, Qiu X, Gu J. Immunoglobulin expression in non-lymphoid lineage and neoplastic cells. Am J Pathol. 2009. április;174(4):1139–48.

96. Shin TH, Lee BC, Choi SW, Shin JH, Kang I, Lee JY, és mtsai. Human adipose tissue-derived mesenchymal stem cells alleviate atopic dermatitis via regulation of B lymphocyte maturation. Oncotarget. 2017. 0;8(1):512–22.

97. Chang M, Nguyen TT. Strategy for Treatment of Infected Diabetic Foot Ulcers. Acc Chem Res. 2021. március 2.;54(5):1080–93.

98. Croitoru-Lamoury J, Lamoury FM, Zaunders JJ, Veas LA, Brew BJ. Human mesenchymal stem cells constitutively express chemokines and chemokine receptors that can be upregulated by cytokines, IFN-beta, and Copaxone. J Interferon Cytokine Res. 2007. 0;27(1):53–64.

99. Yagi H, Soto-Gutierrez A, Kitagawa Y, Tilles AW, Tompkins RG, Yarmush ML. Bone marrow mesenchymal stromal cells attenuate organ injury induced by LPS and burn. Cell Transpl. 2010;19(6):823–30.

100. Tu Z, Li Q, Bu H, Lin F. Mesenchymal stem cells inhibit complement activation by secreting factor H. Stem Cells Dev. 2010. 0;19(11):1803–9.

101. Hackel A, Aksamit A, Bruderek K, Lang S, Brandau S. TNF-alpha and IL-1beta sensitize human MSC for IFN-gamma signaling and enhance neutrophil recruitment. Eur J Immunol. 2021. február;51(2):319–30.

102. Lee MJ, Kim J, Kim MY, Bae YS, Ryu SH, Lee TG, és mtsai. Proteomic analysis of tumor necrosis factor-alpha-induced secretome of human adipose tissue-derived mesenchymal stem cells. J Proteome Res. 2010. április 5.;9(4):1754–62.

103. Ting HK, Chen CL, Meng E, Cherng JH, Chang SJ, Kao CC, és mtsai. Inflammatory Regulation by TNF-alpha-Activated Adipose-Derived Stem Cells in the Human Bladder Cancer Microenvironment. Int J Mol Sci. 2021. április 13.;22(8).

104. Fuenzalida P, Kurte M, Fernandez-O'ryan C, Ibanez C, Gauthier-Abeliuk M, Vega-Letter AM, és mtsai. Toll-like receptor 3 pre-conditioning increases the therapeutic efficacy of umbilical cord mesenchymal stromal cells in a dextran sulfate sodium-induced colitis model. Cytotherapy. 2016. május;18(5):630–41.

105. Park KS, Kim SH, Das A, Yang SN, Jung KH, Kim MK, és mtsai. TLR3-/4-Priming Differentially Promotes Ca(2+) Signaling and Cytokine Expression and Ca(2+)-Dependently Augments Cytokine Release in hMSCs. Sci Rep. 2016. március 16.;6:23103.

*cells*

MDPI

*Article*

# Effect of Inflammatory Microenvironment on the Regenerative Capacity of Adipose-Derived Mesenchymal Stem Cells

**Diána Szűcs [1,2,3], Vanda Miklós [4], Tamás Monostori [1,3], Melinda Guba [1,3], Anikó Kun-Varga [1], Szilárd Póliska [5], Erika Kis [6], Balázs Bende [6], Lajos Kemény [1,3,7] and Zoltán Veréb [1,3,*]**

1 Regenerative Medicine and Cellular Pharmacology Laboratory, Department of Dermatology and Allergology, University of Szeged, 6720 Szeged, Hungary; szucs.diana@med.u-szeged.hu (D.S.); monostori.tamas.bence@med.u-szeged.hu (T.M.); guba.melinda@med.u-szeged.hu (M.G.); kun-varga.aniko@med.u-szeged.hu (A.K.-V.); kemeny.lajos@med.u-szeged.hu (L.K.)
2 Doctoral School of Clinical Medicine, University of Szeged, 6720 Szeged, Hungary
3 Centre of Excellence for Interdisciplinary Research, Development and Innovation, University of Szeged, 6720 Szeged, Hungary
4 Biobank, University of Szeged, 6720 Szeged, Hungary; miklos.vanda@szte.hu
5 Genomic Medicine and Bioinformatics Core Facility, Department of Biochemistry and Molecular Biology, Faculty of Medicine, University of Debrecen, H-4032 Debrecen, Hungary; poliska@med.unideb.hu
6 Dermatosurgery and Plastic Surgery, Department of Dermatology and Allergology, University of Szeged, 6720 Szeged, Hungary; kis.erika.gabriella@med.u-szeged.hu (E.K.); bende.balazs@med.u-szeged.hu (B.B.)
7 Hungarian Centre of Excellence for Molecular Medicine-USz Skin Research Group, University of Szeged, 6720 Szeged, Hungary
* Correspondence: vereb.zoltan@med.u-szeged.hu

**Abstract:** Adipose-derived mesenchymal stem cells are increasingly being used in regenerative medicine as cell therapy targets, including in the treatment of burns and ulcers. The regenerative potential of AD-MSCs and some of their immunological properties are known from in vitro studies; however, in clinical applications, cells are used in non-ideal conditions and can behave differently in inflammatory environments, affecting the efficacy and outcome of therapy. Our aim was to investigate and map the pathways that the inflammatory microenvironment can induce in these cells. High-throughput gene expression assays were performed on AD-MSCs activated with LPS and TNFα. Analysis of RNA-Seq data showed that control, LPS-treated and TNFα-treated samples exhibited distinct gene expression patterns. LPS treatment increased the expression of 926 genes and decreased the expression of 770 genes involved in cell division, DNA repair, the cell cycle, and several metabolic processes. TNFα treatment increased the expression of 174 genes and decreased the expression of 383 genes, which are related to cell division, the immune response, cell proliferation, and differentiation. We also map the biological pathways by further investigating the most altered genes using the Gene Ontology and KEGG databases. Secreted cytokines, which are important in the immunological response, were also examined at the protein level, and a functional assay was performed to assess wound healing. Activated AD-MSC increased the secretion of IL-6, IL-8 and CXCL-10, and also the closure of wounds. AD-MSCs presented accelerated wound healing under inflammation conditions, suggesting that we could use this cell in clinical application.

**Keywords:** adipose-derived mesenchymal stem cells; lipopolysaccharide; tumor necrosis factor α; inflammation; regenerative medicine



**Citation:** Szűcs, D.; Miklós, V.; Monostori, T.; Guba, M.; Kun-Varga, A.; Póliska, S.; Kis, E.; Bende, B.; Kemény, L.; Veréb, Z. Effect of Inflammatory Microenvironment on the Regenerative Capacity of Adipose-Derived Mesenchymal Stem Cells. *Cells* **2023**, *12*, 1966. https://doi.org/10.3390/cells12151966

Received: 26 May 2023
Revised: 12 July 2023
Accepted: 22 July 2023
Published: 29 July 2023



## 1. Introduction

Adipose tissue can be found in several locations in the human body, such as subcutaneous and visceral sites, intra-articular, intramuscular, intra-hepatic depots, and in bone marrow. Adipose tissue is not only an energy reservoir but also an endocrine organ since it produces mediators of metabolism and cell function. Adipocytes and nonadipocytes secrete adipokines (leptin, adiponectin, omentin, and resistin), pro- and anti-inflammatory

cytokines (IL-6, TNF-a, IL-1b, IL-8, MCP-1, IL-1Ra, IL-6, IL-7, IL-8 and IL-11), growth factors (VEGF, HGF, FGF, IGF-1 and BDNF), pro-apoptotic factors, pro-angiogenic factors and microvesicles filled with proteins and nucleic acids. Three types of adipose tissue can be distinguished: (I) white adipose tissue, which has a role in energy storage but also produces adipokines; (II) brown adipose tissue, which plays a role in thermogenesis regulation but can also store energy; and (III) beige adipose tissue, which is also included in thermogenesis and energy storage [1–4].

Adipose-tissue-derived mesenchymal stem cells (AD-MSCs) are located in adipose tissue, mainly in the stromal vascular fraction (SVF), which can be isolated via less invasive methods. AD-MSCs are multipotent cells with self-renewal capacity, and they have a multilineage ability to differentiate into cells of mesodermal lineages, such as adipocytes, chondrocytes, and osteoblasts. They have high proliferation and immunosuppressive properties; thus, they and even their secretome can be applied in regenerative medicine in diseases related to immune diseases. These cells have the potential to regulate the immune response since they can interact with several immune cells through direct cell–cell interactions or indirectly with their secretome. AD-MSCs have the ability to interact with T cells, B cells, macrophages, natural killer cells (NKs), dendritic cells (DCs), neutrophils, and mast cells [1–9].

AD-MSCs have an immunomodulatory effect through T-cell interactions via cell adhesion molecules and change the level of secreted mediators (IDO, TGFβ, IL-10, and PGE2). Furthermore, T cells can influence AD-MSCs by producing chemokines. Several studies showed, in the presence of a high amount of pro-inflammatory cytokines, that AD-MSCs activate Treg generation and inhibit T cell proliferation, activation, and differentiation, thus suppressing the immune response. On the other hand, in the presence of a low amount of pro-inflammatory cytokines, AD-MSCs inhibit Treg generation and activate T-cell proliferation, activation, and differentiation. AD-MSCs have an effect on B cells by suppressing and promoting their proliferation, activation, and differentiation and activating chemotaxis and Breg induction. They can inhibit NK cell proliferation, activation, and migration and induce NK cell progenitor proliferation and NK activation. Furthermore, AD-MSCs suppress DC differentiation, endocytosis, maturation, activation, and migration and inhibit mast cell degranulation, inflammatory cytokine expression, and chemotaxis. AD-MSCs can mediate macrophage polarization by suppressing the M1 and promoting the M2 phenotype, and they can influence neutrophils as well by inhibiting the activation, recruitment, formation of extracellular neutrophil traps, and protease secretion and promoting survival and recruitment [1–12].

Since AD-MSCs have immunomodulatory effects and angiogenic and differentiation potential, they provide the opportunity to replace, repair, and regenerate damaged tissues; thus, they can be applied in support of many diseases associated with tissue damage. AD-MSCs can be used on a wide scale for many different purposes, such as wound healing and skin regeneration (diabetic and non-diabetic ulcers and nonhealing wounds, extensive burns, and physicochemical skin injuries), autoimmune disorders, hematological disorders and graft-versus-host disease, bone and cartilage repair, cardiovascular and muscular diseases, neurodegenerative diseases, and radiation injuries. These cells provide an opportunity to recover the function of damaged tissues with high efficacy and safety. For therapeutic uses of AD-MSCs, their purity and potency must be identified prior to administration to ensure safe and successful application free from adverse events. The focus of our study is the wound healing and skin regeneration ability of AD-MSCs. In these diseases, AD-MSCs must regenerate tissues in a highly inflamed environment, which affects their expression profile. These experiments reflect the changes in gene and protein expression of AD-MSCs after exposure to inflammation agents [1–20].

The clinical treatment of chronic wounds and ulcers is a great challenge since the cells injected into the patient should regenerate the tissue in a non-physiological environment. Non-healing wounds are highly inflamed and often associated with bacterial infection, especially in diabetic patients. Thus, stem cells must survive and proliferate in an inflammatory microenvironment [6,7,13,21–26]. However, as stem cell therapies have become increasingly popular in recent years, the results of new therapies can be contradictory,

and the injected cells are not pretreated, which can reduce the effectiveness. According to the literature, pretreatment of stem cells can increase their regenerative capacity and promote faster wound closure, so we believe that pretreatment of stem cells may be the key to developing a more effective therapy [16,27–35]. The aim of our study is to investigate the response of mesenchymal stem cells from adipose tissue to the inflammatory factors TNFα and LPS at the molecular and cellular levels. Our results may contribute to the development of a new therapy in which cell licensing plays a decisive role in increasing efficiency. Our experimental arrangement may also be suitable for examining the response of patient cells to inflammatory factors. In this way, we were able to test whether the licensing given is suitable for the given patient, thus helping to develop personalized therapy.

## 2. Materials and Methods

### 2.1. Isolation of SVF Fraction

The collection of adipose tissue was in accordance with the guidelines of the Declaration of Helsinki and was approved by the National Public Health and Medical Officer Service (NPHMOS) and the National Medical Research Council (16821-6/2017/EÜIG, STEM-01/2017), which follows the Directive 2004/23/CE of the EU Member States on the practice of presumed written consent for tissue collection. Abdominal adipose tissues were removed from the patients (Sex:2/3 F/M, Age: 50.2 ± 11.7 years), and the isolation was performed within 1 h after plastic surgery. Adipose tissue was homogenized and washed with $Ca^{2+}$ and $Mg^{2+}$ free PBS (Biosera, Nuaille, France), and then the sample was centrifuged at 600 rpm for 8 min at RT. The SVF fraction was located in the upper fraction, and it contains mesenchymal stem cells. After two steps of washing, tissue digestion was performed with (0.25 mg/mL) Collagenase Type IA (Merck KGaA, Darmstadt, Germany) for 1 h at 37 °C on a tube rotator. The collected cells were washed, and then the upper layer was removed to preserve only the SVF fraction at the bottom of the tube. The cell pellet was suspended in $Ca^{2+}$ and $Mg^{2+}$ free PBS (Biosera, Nuaille, France), and it was filtered using a 100 µm Corning® cell strainer. After the washing step was repeated, the yellowish upper layer was kept and suspended in 1 ml of medium. Cells were counted using the EVE automatic cell counter, NanoEntek (NanoEntek, Seoul, Korea), then they were seeded in a T25 $cm^2$ flask. For maintenance, DMEM-HG medium (Biosera, Nuaille, France) was applied supplemented with 10% FBS (Biosera, Nuaille, France), 1% L-glutamine (Biosera, Nuaille, France) and 1% Antibiotic–Antimycotic Solution (Biosera, Nuaille, France) for further experiments.

### 2.2. Differentiation of Adipose-Tissue-Derived Mesenchymal Stem Cells

The differentiation capacity of adipose-tissue-derived mesenchymal stem cells was validated by differentiation into adipocyte, chondrocyte and osteocyte lines. They were seeded in a 24-well plate, $5 \times 10^4$ cells/well, and after 24 h, the medium was replaced with a differentiation medium. For this purpose, commercially available Gibco's StemPro® Adipogenesis, Osteogenesis and cholndrogenesis differentiation kits were applied according to the manufacturer's guidelines (Gibco, Thermo Fisher Scientific, Waltham, MA, USA). After 21 days of upkeep, cells were fixed with 4% methanol-free formaldehyde (Molar Chemicals, Hungary) for 20 min at RT. The differentiation statuses of AD-MSCs were validated using different staining. For visualization of lipid-laden particles, Nile red staining (Sigma-Aldrich, Merck KGaA, Darmstadt, Germany) was applied, Alizarin red staining (Sigma-Aldrich, Merck KGaA, Darmstadt, Germany) was utilized to show mineral deposits during osteogenesis, and Toluidine blue staining (Sigma-Aldrich, Merck KGaA, Darmstadt, Germany) was used to label the chondrogenic mass.

### 2.3. Flow Cytometry

Characterization of the surface antigen expression pattern was implemented using three-color flow cytometry using fluorochrome-conjugated antibodies with isotype-matching controls. For fluorochrome signal measurement, the BD FACSAria TM Fusion II flow cytometer (BD Biosciences Immunocytometry Systems, Franklin Lakes, NJ, USA) was

applied, and the data were analyzed using Flowing Software (Cell Imaging Core, Turku Centre for Biotechnology, Finland).

### 2.4. Treatment with LPS and TNFα Treatment for RNA Isolation

The AD-MSC cells utilized were derived from abdominal adipose tissue from three different donors. In a T25 $cm^2$ flask, 2.8 × $10^5$ cells were seeded, using the cell culture medium described above, and the cells were maintained for 24 h. After that, the cell culture medium was replaced for treatment, and the cells were treated with (A) LPS [100 ng/mL] (ultrapure, Invivogen, San Diego, CA, USA) or (B) TNFα [100 ng/mL] (Peprotech, London, UK), and cells were incubated for 24 h under standard conditions (37 °C, 5% $CO_2$, untreated cells left as control). Upon 24 h treatment, cells were collected and used for RNA isolation.

### 2.5. RNA Isolation for RNA Sequencing

Cells were collected, and the pellet was suspended in 1 mL TRI Reagent® (Genbiotech Argentina, Bueno Aries, Argentina) and stored at −80 °C for 24 h. Upon thawing, 200 µL chloroform was measured in the samples, and after rigorous mixing, they were incubated at RT for 10 min. The samples were centrifuged at 13,400× *g* at 4 °C for 20 min for phase separation. The aqueous phase was transferred to clean tubes, and 500 µL 2-propanol was added and thoroughly mixed. The incubation and phase separation steps were then repeated. The supernatants were discarded, and the pellets were washed with 750 µL 75% EtOH-DEPC. The samples were centrifuged at 7500× *g* at 4 °C for 5 min, then the supernatants were removed, and the samples were dried at 45 °C for 20 min. The pellets were dissolved in RNase-free water and incubated at 55 °C for 10 min. The concentration was determined using an IMPLEN N50 UV/Vis nanophotometer (Implen GmbH, Munich, Germany) and the RNA samples were stored at −80 °C until use.

### 2.6. RNA-Sequencing

To obtain global transcriptome data, high-throughput mRNA sequencing analysis was performed on the Illumina sequencing platform. Total RNA sample quality was checked on Agilent BioAnalyzer using the eukaryotic Total RNA Nano Kit according to the manufacturer's protocol. Samples with an RNA integrity number (RIN) value >7 were accepted for the library preparation process. RNA-Seq libraries were prepared from total RNA using the Ultra II RNA Sample Prep kit (New England BioLabs) according to the manufacturer's protocol. Briefly, poly-A RNAs were captured by oligo-dT conjugated magnetic beads, and then the mRNAs were eluted and fragmented at a degree of 94 Celsius. First-strand cDNA was generated via random priming reverse transcription, and after the second-strand synthesis step, double-stranded cDNA was generated. After repairing ends, A-tailing and adapter ligation steps adapter ligated fragments were amplified in enrichment PCR, and finally, sequencing libraries were generated. The sequence runs were executed on the Illumina NextSeq 500 instrument using single-end 75-cycles sequencing.

### 2.7. Data Analysis

Gene expression analysis was performed in R (version 4.2.0). As a prefiltering step, we removed genes with low expression values (rows that only have 10 counts across all samples were removed) from further analysis. Principal component analysis (PCA) was used to visualize sample-to-sample distances. The PCA plot was created with the R package PCAtools, and it has not shown any significant batch effects. Differential expression analysis was performed using DESeq2 [36]. Significantly differentially expressed genes (DEG) were defined based on adjusted $p$ values < 0.05 and log2-fold change threshold = 0.

The visualization of the DEG heat map was performed using the R package ComplexHeatmap [37], where Pearson correlation was used in rows and columns, and the z scores were calculated from normalized count data (normalization was performed using DESeq2 counts (dds, normalized = T). Volcano plots were created using the EnhancedVolcano package. In gene set enrichment (GSEA), DEGs were ordered by their log2-fold changes

and used as input for gene set enrichment analysis. The R package ClusterProfiler was used with pvalueCutoff = 0.05 for both GO and KEGG GSEA. GO terms were further clustered using rrvgo with default settings. Heat maps of the different pathways were created based on preselected gene sets. DEGs that were part of each gene set were visualized with the same method as the heat map visualization of all the genes (for further details, see Supplementary Materials). The DEGs were selected and ordered according to log2-fold changes, and this ordered list was used as input for the gene set enrichment analysis (GSEA). They were aligned with the Gene Ontology and KEGG databases.

### 2.8. Protein Array

Three AD-MSC donors were treated with LPS and TNFα, as described above. Supernatants were collected and stored at −80 °C until use. After thawing the samples, the supernatants were pooled by type of treatment and applied to the Human XL cytokine array Kit Proteome Profiler (R&D Systems, Biotechne, McKinley Place NE, Minneapolis, MN, USA) to determine secreted factors. The array was carried out according to the manufacturer. The images were quantified using Fiji (Image J 1.53S) with an embedded Protein Array Analyzer (Version:1.1.c) macro.

### 2.9. Wound Healing Assay

Three primary cell lines derived from abdominal adipose tissue were applied from three different donors. Cells were collected and counted using the EVE automatic cell counter (NanoEntek, Hwaseong, Republic of Korea). For the wound healing assay, $5 \times 10^4$ cells were seeded per well of 24-well plates seeded in the upkeep medium. After seeding, cells were cultured for 24 h under standard conditions (37 °C, 5% $CO_2$), and then the protocol was divided into two different lines. (I) After 24 h of incubation, the scratch was made, and the medium was immediately changed to a medium containing inflammatory agents, and it was followed by 48 h of time-lapse microscopy. (II.) After 24 h of incubation, the medium was changed to media containing inflammatory agents, and cells were incubated for 24 h under standard conditions, and then the scratch was made and the medium was changed immediately to agents-free maintaining media, and it was accompanied by 48 h of time-lapse microscopy. During treatment, six conditions were applied in both cases: (A) control (B) TNFα [100 ng/mL] and (C) LPS [100 ng/mL]. Scratches were generated using the AutoScratch Wound Making Tool (Agilent/BioTek, Santa Clara, CA, USA). Microscopic images were taken with Olympus Fluorescent Microscopy (Shinjuku, Tokyo, Japan) and analyzed by Fiji/ImageJ.

### 2.10. RNA Isolation for qPCR

Upon LPS and TNFα treatment (described above), the Macherey–Nagel NucleoSpin RNA Mini kit (Dueren, Germany) was applied according to the manufacturer's instructions. Hereinafter, all work with RNA and cDNA samples was performed in a BioSan UVT-B-AR DNA/RNA UV-Cleaner box (Riga, Latvia).

### 2.11. Real-Time PCR

After extracting RNA and checking their quality and quantity with IMPLEN N50 UV/Vis nanophotometer, cDNA synthesis was carried out using High-Capacity cDNA Reverse Transcription Kit (Applied Biosystems™, Thermo Fisher Scientific, Waltham, MA, USA) according to the manufacturer's guidelines. For reverse transcription, Analytik Jena qTOWER$^3$ G Touch Real-Time Thermal Cycler (Jena, Germany) was applied.

### 2.12. qPCR

The Xceed 2x Mix No-ROX kit (Institute of Applied Biotechnologies, Prague, Czech Republic) and TaqMan probes (250 rxns, FAM-MGB, Thermo Fisher Scientific, Waltham, MA, USA) were applied for quantitative PCR. Three technical and three biological replicates were used in all cases, and data were analyzed using the $2^{-\Delta\Delta Ct}$ method. The protocol

was performed according to the manufacturer's instructions, and the following probes were selected for the experiment: Hs00427620, Hs99999903, Hs00153133, Hs00361185, Hs 00194611, Hs00747615, Hs00174103, Hs00164932, Hs01001602, Hs 00171042, Hs00598625, Hs00265033, Hs00985639, Hs00165814, Hs01003372.

### 2.13. Cellular Impedance Measurement

Label-free cellular impedance measurements were performed with an Agilent xCELLingence Real-Time Cell Analysis (RTCA) DP (dual-purpose) instrument (Agilent/BioTek, Santa Clara, CA, USA). In total, $1 \times 10^4$ AD-MSCs were seeded per well of E-Plate 16. Cells were incubated overnight under standard conditions (37 °C, 5% $CO_2$) for attachment. The cells were then treated with LPS and TNFα (described above), and the cellular impedance was measured for 24 h (37 °C, 5% $CO_2$).

## 3. Results

The isolated AD-MSC primary cell lines were characterized via trilineage differentiation and FACS analysis to validate their specific cell type properties (Supplementary Figure S1).

To dissect the expressional changes and associated pathways that accompany the preconditioning of AD-MSC with LPS and TNFα preconditioning of AD-MSCs, we performed a differential gene expression analysis of the RNA sequence data. Furthermore, we employed distinct strategies in investigating signaling pathways: a hypothesis-driven gene set investigation of preselected terms and a hypothesis-free gene set enrichment analysis (GSEA) using GO and KEGG databases. RNA was collected after conditioning AD-MSCs with inflammatory factors for 24 h.

Both treatments had an effect on global gene expression (Supplementary Figure S2A); we identified 2752 DEG in TNFα and 1613 DEG in cells treated with LPS. Normalized expression values of these genes were clustered according to Pearson's correlation in the control and treated samples and are shown on a heatmap (Figure 1A). To further dissect the differences between the two treatments, we investigated the number of genes overlapping up- and down-regulated (Figure 1B). There is a notable overlap in the effects of treatments, with 607 genes showing elevated expression and 449 genes showing decreased expression. The LPS treatment affected a similar number of genes up- and down-regulated, while TNFα slightly distorted the number of genes up-regulated (Figure 1C).

AD-MSCs have been shown to express cytokines, chemokines, and growth factors with wound-microenvironment-modulating capabilities, consequently promoting wound healing processes [38]. Interestingly, as an effect of preconditioning, we found several DEGs connected to these processes.

Among immunomodulatory factors released by AD-MSCs, IL1B, IL1RN, IL11, IL6, and IL15 showed elevated expression, while IL16 and TGFB3 showed decreased expression in a TNFα environment. LPS had less effect on immunomodulatory gene expression; it decreased the expression of IL1RN and TGFB3.

In addition, we observed changes in the expression of IDO and KYNU, which are associated with the apoptosis of T cells [2]. They were up-regulated in TNFα, while they were not significantly altered in LPS-treated stem cells. ICAM and VCAM play a role in lymphocyte recruitment to the injured site, both of which we found to be up-regulated in TNFα conditioning [2].

This shows that both treatments elicited immunomodulatory responses from AD-MSCs, potentially changing the behavior of these cells at the damaged tissue site to facilitate the healing process.

In addition to these molecules, chemokines that play a role in cell migration and immune regulation were also affected [39]. The expression of chemokines from members of the CXCL family (CXCL2, CXCL3, CXCL6, CXCL8, CXCL9, CXCL10, CXCL11) and the CCL chemokine ligand family (CCL1, CCL2, CCL5, CCL7, CCL20, CCL28) was strongly altered as a result of TNFα treatment, while LPS had very little effect on them.

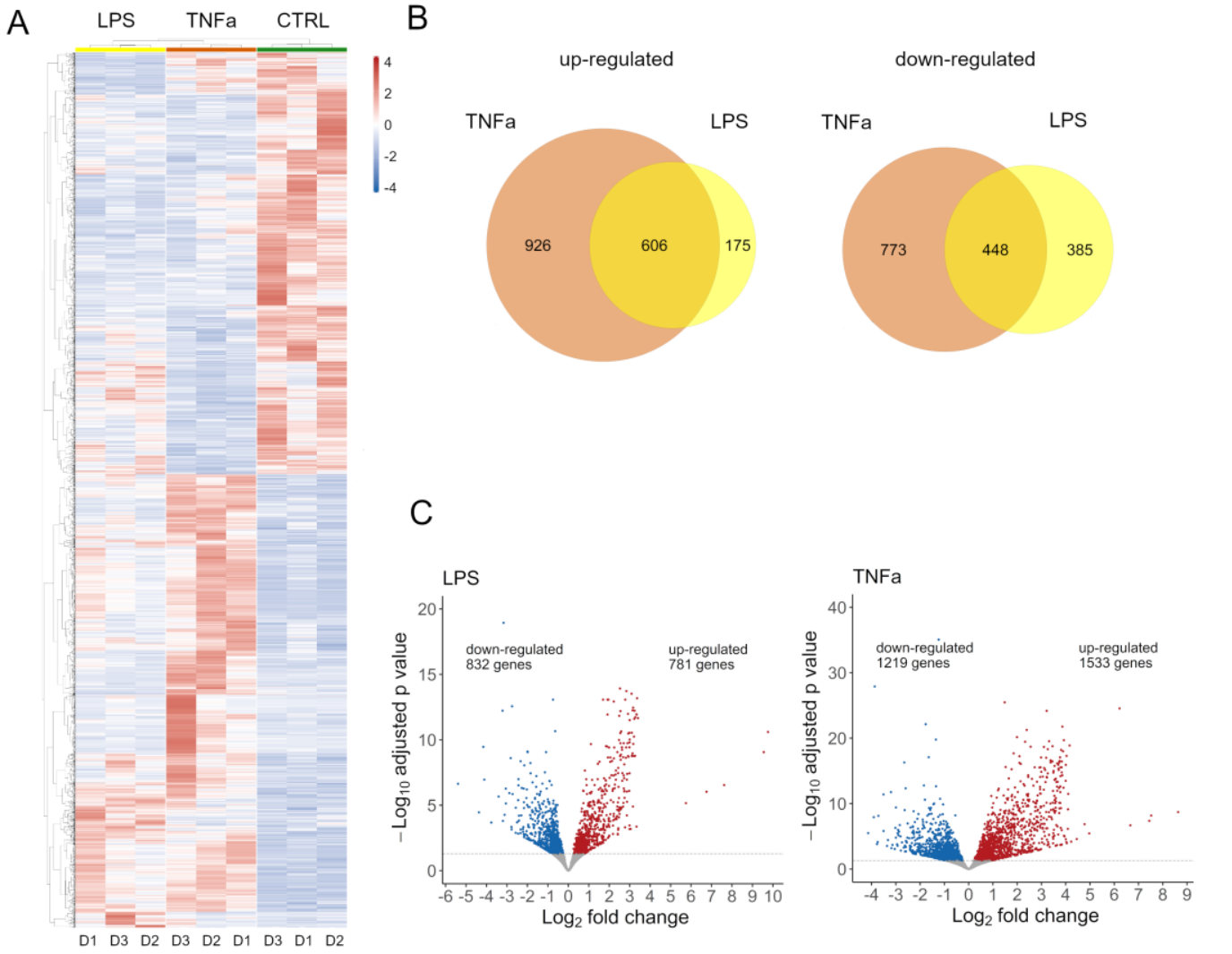


**Figure 1.** (**A**) The result of the RNA sequencing evaluation can be seen on the heat map. Gene expression changes of three human AD-MSC donors can be observed under treated conditions with control (green), LPS (yellow), and TNFα (red) treated conditions. The three conditions can be well separated, but there are some similarities between them. (**B**) Venn diagram (left) represents the number of genes with increased expression by TNFα (brown) and LPS (yellow), and the fitted cross-section shows genes that were affected by the two treatments. The Venn diagram (right) represent the number of genes with reduced expression due to TNFα (brown) and LPS (yellow) treatment; the adjusted cross-section shows genes affected by the two treatments. (**C**) Volcano plots show the genes with significantly increased or decreased gene expression that changed the most as a result of treatments. Genes with the highest reduced expression (blue) and those with increased expression (red) are shown.

**Figure 1.** (**A**) The result of the RNA sequencing evaluation can be seen on the heat map. Gene expression changes of three human AD-MSC donors can be observed under treated conditions with control (green), LPS (yellow), and TNFα (red) treated conditions. The three conditions can be well separated, but there are some similarities between them. (**B**) Venn diagram (left) represents the number of genes with increased expression by TNFα (brown) and LPS (yellow), and the fitted cross-section shows genes that were affected by the two treatments. The Venn diagram (right) represent the number of genes with reduced expression due to TNFα (brown) and LPS (yellow) treatment; the adjusted cross-section shows genes affected by the two treatments. (**C**) Volcano plots show the genes with significantly increased or decreased gene expression that changed the most as a result of treatments. Genes with the highest reduced expression (blue) and those with increased expression (red) are shown.

AD-MSCs have been shown to express cytokines, chemokines, and growth factors with wound-microenvironment-modulating capabilities, consequently promoting wound healing processes [38]. Interestingly, as an effect of preconditioning, we found several DEGs connected to these processes.

Among immunomodulatory factors released by AD-MSCs, IL1B, IL1RN, IL11, IL6, and IL15 showed elevated expression, while IL16 and TGFB3 showed decreased expression in a TNFα environment. LPS had less effect on immunomodulatory gene expression; it decreased the expression of IL1RN and TGFB3.

In addition to immunomodulatory molecules, growth factors also play a crucial role in wound healing, especially in cell migration, proliferation, differentiation, and extracellular matrix synthesis [40]. Both treatments decreased VEGFB and TGFB3 and up-regulated VEGFC and FGF2. Additionally, TNFα up-regulated TGFA. These changes indicate that LPS and TNFα have an effect on MSC homing and tissue regeneration.

The repair of tissue damage by AD-MSCs requires the interplay of processes such as inflammation, proliferation, cell migration, and re-epithelization. These mechanisms often involve the same genes. Based on previously collected gene sets related to stem cell behavior in the wound-healing process, we investigated the response of treatments to AD-MSCs and the overlap of these responding genes.

We selected genes from the gene sets that were differentially expressed in at least one of the treatments; wherever we found identical genes, we made a connecting line between the sets represented by dots (Figure 2A). The widths of the lines represent the number of identical genes, while the size of each dot represents the fraction of DEGs in the entire gene set. In general, we can see that each set of genes is connected to at least five other sets and "wound healing migration", "cellular senescence", "cytokines growth factors", "immune response", and "stem cell EMT TEM" are connected to every other set, displaying dense interconnectedness.



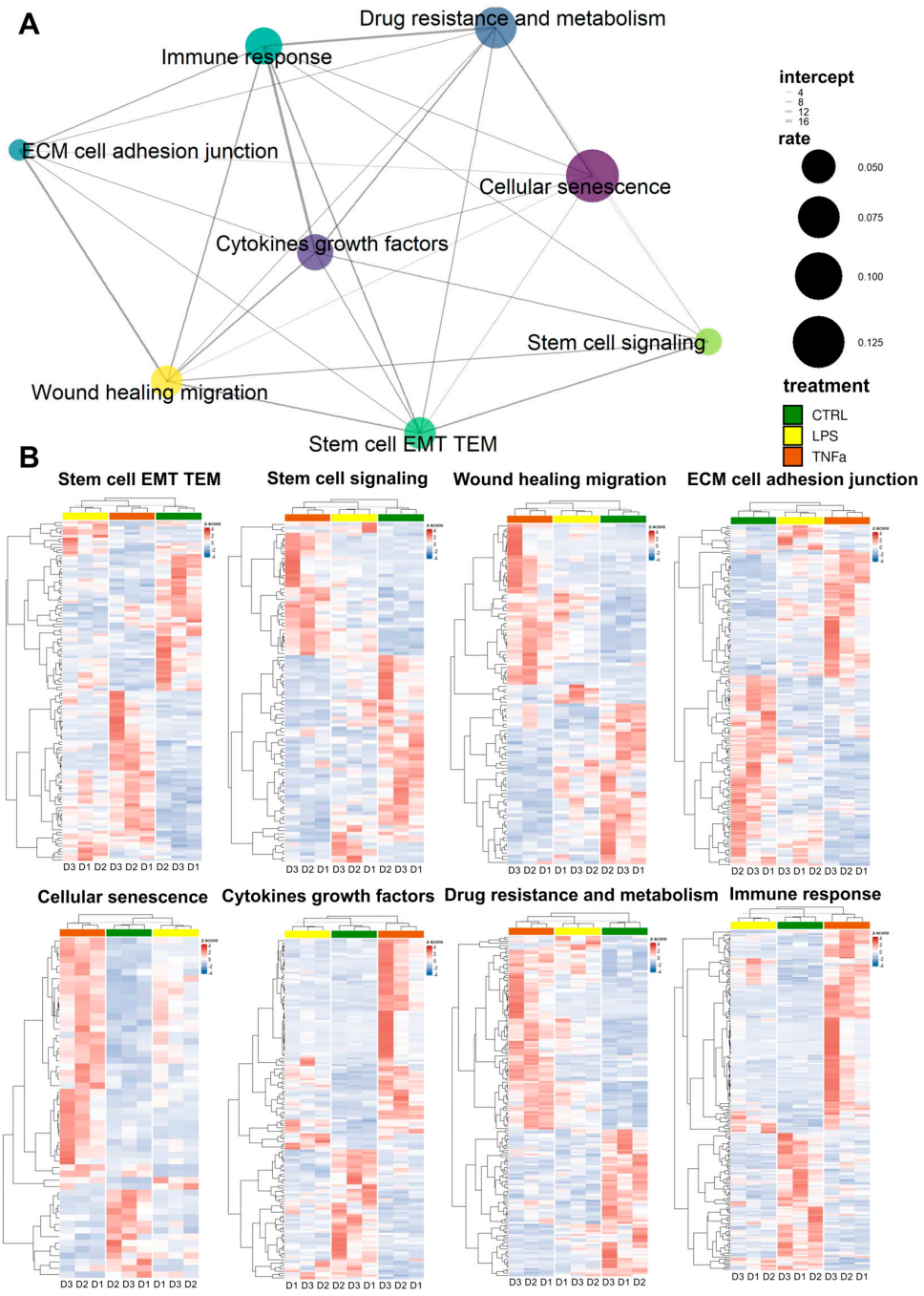


**Figure 2.** (**A**) The enrichment analysis of the gene set shows the percentage of genes in the wound healing-related pathway that changed as a result of the treatments. The size of the circles is directly proportional to the proportion of changed genes, and the thickness of the lines between them is directly proportional to the overlap of the genes. (**B**) The changes in gene expression of the pathways shown in Figure 2A can be seen in detail in the heat maps. Control (green), LPS (yellow), TNF$\alpha$ (red).

To further investigate global gene expression changes, we conducted gene set enrichment analysis (GSEA) using two databases: Gene Ontology (GO) and Kyoto Encyclopedia

Based on DEGs in most gene sets, LPS and TNF$\alpha$ treatment show comparable effects; consequently, as a result of hierarchical clustering, the two treatments form a distinct cluster from the control samples (Figure 2B). However, in three gene sets—"cellular senescence", "immune response" and "cytokine growth factors"—clustering showed that LPS-treated AD-MSCs produced an expression pattern that is more similar to the control samples. Consequently, genes related to these terms showed greater expressional changes due to TNF$\alpha$ treatment, and results could thus be observed.

To further investigate global gene expression changes, we conducted gene set enrichment analysis (GSEA) using two databases: Gene Ontology (GO) and Kyoto Encyclopedia of Genes and Genomes (KEGG). Similar results could be observed among the results of each database. The GSEA using GO terms resulted in redundant pathway terms due to the hierarchical structure of the database; therefore, we further clustered them based on semantic similarity (Supplementary Figure S3). The parent terms within a group were chosen according to the adjusted p-values.

LPS and TNF$\alpha$ treatments had analogous effects in cell division, differentiation, cytoskeleton organization, and cell cycle-related processes (Figure 3, Supplementary Tables S1 and S2). Consequently, they gained an enhanced ability to increase cell proliferation, differentiation, and migration, which can be advantageous in wound healing.

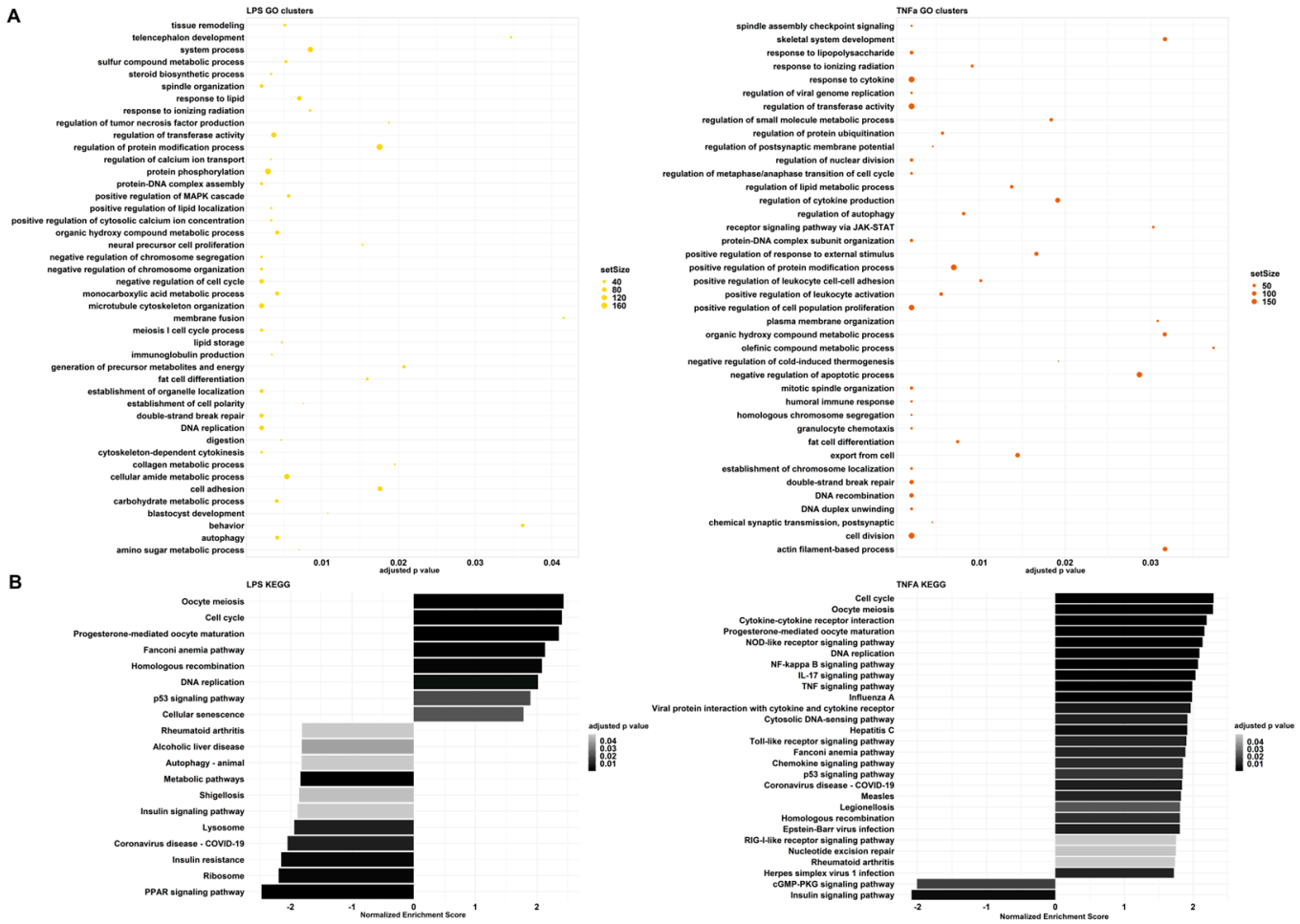


**Figure 3.** (**A**) Parent terms of the results of the gene set enrichment analysis based on GO terms in the LPS and TNF$\alpha$ treatments. The x-axis represents adjusted *p*-values, the size of the dots shows the size of each GO term's gene set. (**B**) Results of the gene set enrichment analysis based on KEGG in LPS and TNF$\alpha$ treatments. The pathways are ordered according to their normalized enrichment score, and the color intensity of the columns depends on the adjusted *p*-value.

**Figure 3.** (**A**) Parent terms of the results of the gene set enrichment analysis based on GO terms in the LPS and TNF$\alpha$ treatments. The x-axis represents adjusted *p*-values, the size of the dots shows the size of each GO term's gene set. (**B**) Results of the gene set enrichment analysis based on KEGG in LPS and TNF$\alpha$ treatments. The pathways are ordered according to their normalized enrichment score, and the color intensity of the columns depends on the adjusted *p*-value.

Although the processes mentioned above change in the same direction, immune-related pathways seem to greatly differ in the two treatment-resulting changes. Among the

Although the processes mentioned above change in the same direction, immune-related pathways seem to greatly differ in the two treatment-resulting changes. Among the GO clusters, LPS demonstrates regulation of tumor necrosis factor (TNF) production (Figure 3A). The first cluster contains: tumor necrosis factor production, tumor necrosis factor superfamily cytokine production, and relative regulation terms (Supplementary Table S3). GSEA resulted in negative normalized enrichment scores (NESs) for these pathways, therefore, indicating that the production of cytokines from the TNF and TNF superfamily is down-regulated. On the contrary, TNFα preconditioning affected several GO groups that are related to immune system processes: response to LPS, response to cytokines, regulation of cytokine production, receptor signaling through JAK-STAT, positive regulation of response to external stimulus, positive regulation of leukocyte cell–cell adhesion, positive regulation of leukocyte activation, negative regulation of cold-induced thermogenesis, humoral immune response, and granulocyte chemotaxis. All of these responses are up-regulated, showing an enhanced immune response.

These observations are also highlighted among the KEGG results (Figure 3B). In the case of TNFα, we can see signaling pathways, such as NOD-like receptor, NF-kappa B, IL-17, TNF, Toll-like receptor, Chemokine, and RIG-I-like receptor signaling pathways. These are all part of an immune response and have positive NESs. Furthermore, disease pathways such as influenza A, Hepatitis C, COVID-19, Measles, Legionellosis, Epstein–Barr virus infection and Herpes simplex virus 1 infection-including Toll-like receptor, RIG-I-like receptor, TNF, Jak-STAT, or NF-kappa B signaling pathways were also significant with positive NESs. In contrast, LPS treatment caused a different change and down-regulated COVID-19 and Shigellosis, while the immune pathways that were activated after TNFα treatment did not change significantly. Analysis with the QIAGEN IPA platform yielded similar results. For both treatments, the inflammatory environment manifested itself mainly in the regulation of the cell cycle, with effects on cell division and migration. The other biological functions were related to this, forming patterns that are most characteristic of tumor cells. We believe that this may be because the steps of tumor formation and metastasis are almost identical to those during wound healing, with similar stages observed (Supplementary Figure S2B).

The expression of certain genes was validated using quantitative real-time PCR, and the results show changes in the response of both treatments. As a result of the treatments, there were expression changes of genes that can be divided into different groups: STAT6, which is important in the initiation of signaling cascades; various cytokines: IL-6, CXCL-8, CXCL-10; factors involved in regeneration: TDO2, PTGS2, ICAM-1 and VCAM.1; and the expression of CCR4, which plays a role in migration, also changed. Both agents caused an elevation in the levels of CXCL8, IL-6, and PTGS2 proteins and a decay in STAT6 levels. Inflammatory factors altered the production of some proteins in the opposite direction, KRT14 (data not shown) was elevated and CCR4, TDO2, and VCAM-1 decreased with the use of LPS, while CXCL10 was increased upon TNFα treatment (Supplementary Figure S4). The cellular impedance measurement showed that cell viability was not altered by the addition of inflammatory agents, and the seeded cells showed the same cell index before (12 h) and after (24 h, 36 h) treatment (Figure 4A). To underline the data for the analysis of gene expression, protein production was measured in AD-MSC supernatants after treatments with LPS and TNFα treatments. The protein array showed that Angiopoietin-2, CD40 ligand, Dkk1, FGF-19, HGF, ICAM-1, IGFBP-3, IL-17A, IL-22, IL-23, IL-24, LIF, MCP-3, MMP-9, RANTES, SDF-1α, Thrombospondin-1, uPAR, VEGF, Cystatin C, IL-6, IL-8, MIF, Osteopontin, and Pentraxin 3 protein expression increased with both treatments compared to the control. However, treatments have opposite effects on the production of a few proteins, such as LPS treatment decreasing DDPIV and GDF-15 expression, while TNFα decreases Apoliporotein A1, IL-4 and angiogenin synthesis (Figure 4B–D, Supplementary Figure S5).

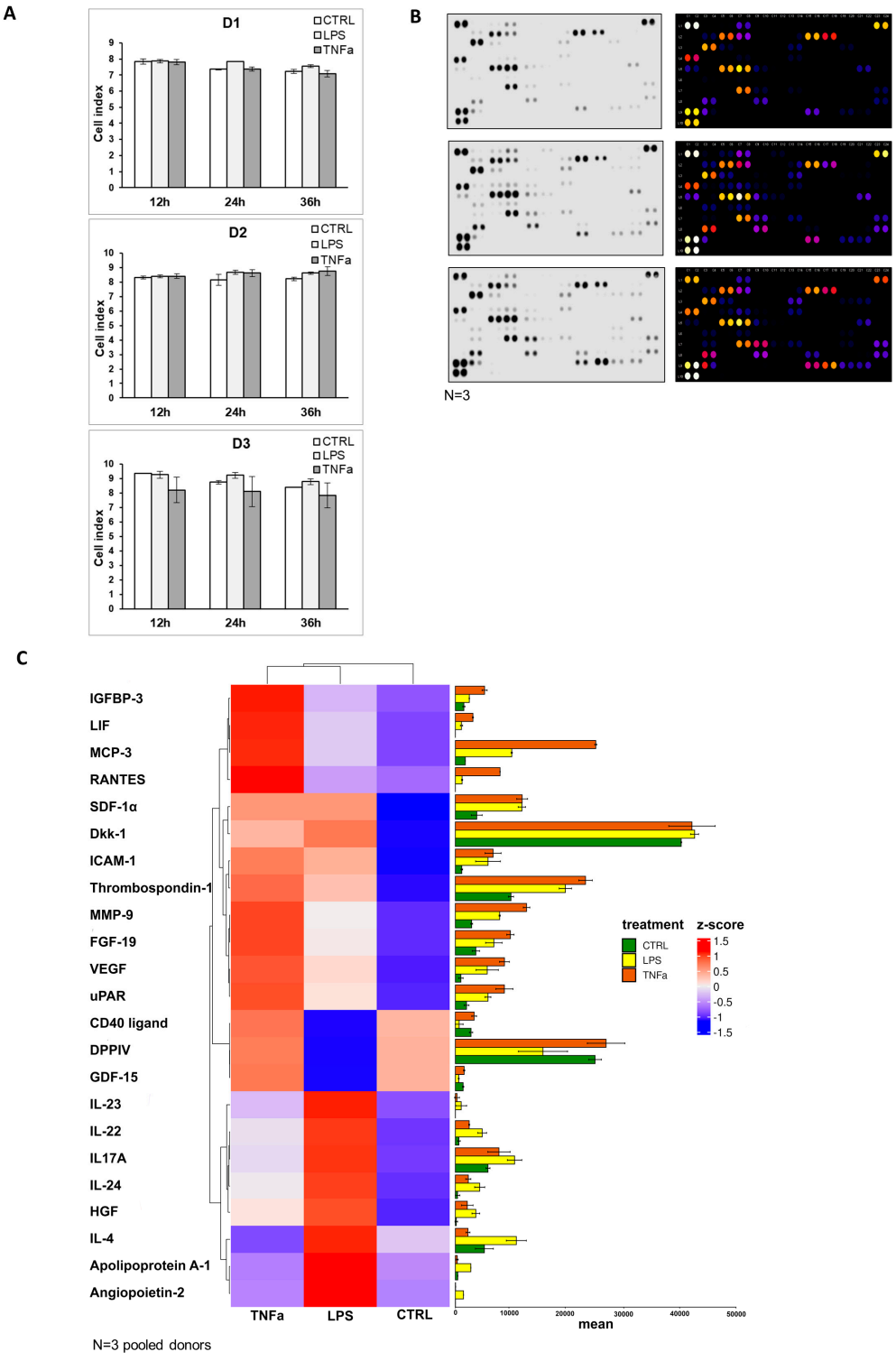


**Figure 4.** *Cont.*

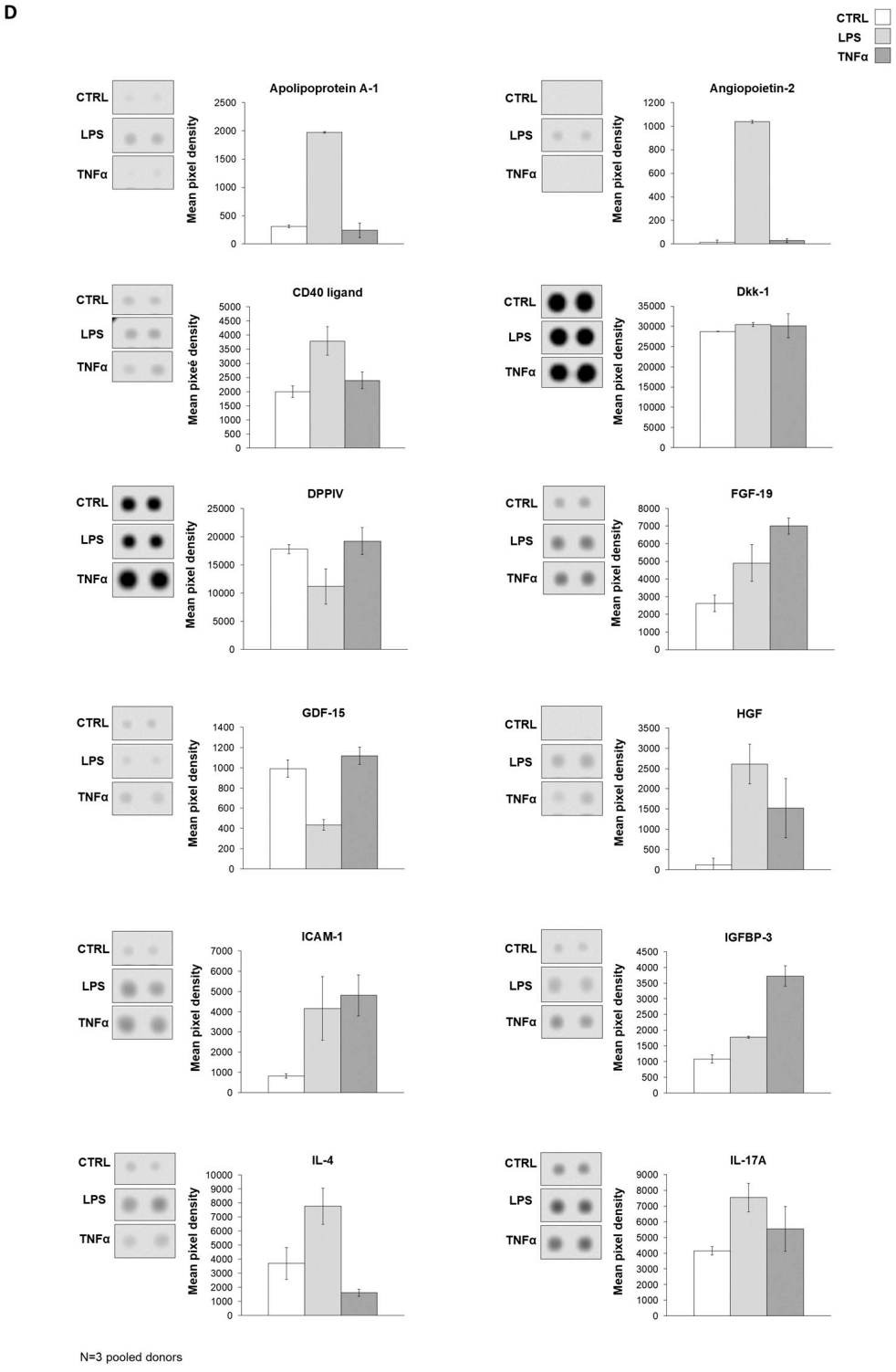


**Figure 4.** *Cont.*

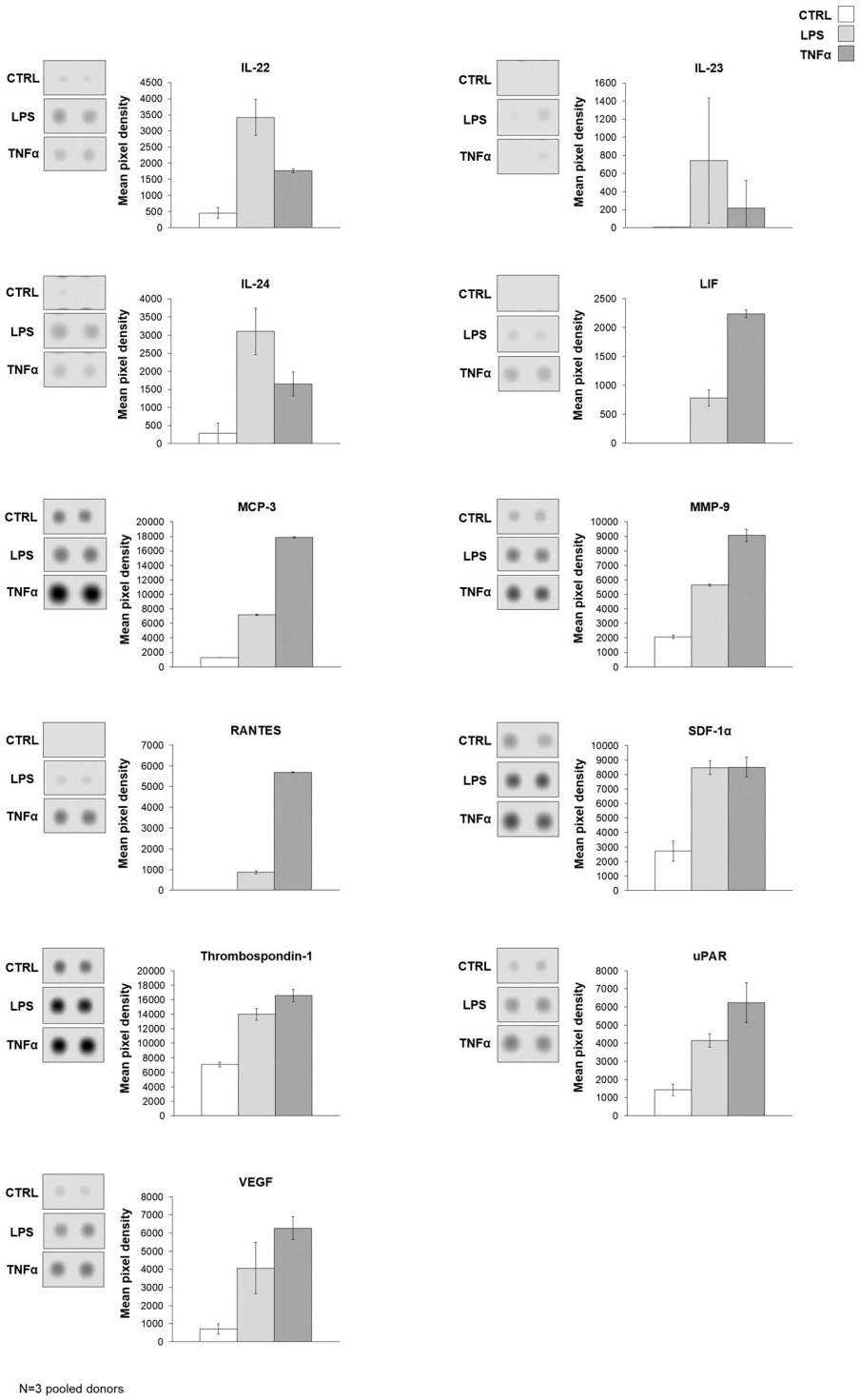


**Figure 4.** (**A**) As a result of impedance measurement, it can be seen that the cell index did not change significantly during treatment (24 h, 36 h) compared to the untreated state of the cells (12 h). From this result, it can be concluded that the viability of the cells remained unchanged during the treatment. Control (white), LPS treatment (light gray), and TNFα treatment (dark gray). (**B**) The result of the protein array is the original image of the membrane, followed by the Fiji diagram created to determine the pixel density. (**C**) The visual representation of the protein level changes from the protein array results can be seen on the heat map, as well as on the protein bar chart showing the greatest changes after treatment, control (green), LPS treated (yellow), and TNFα treated (red). (**D**) Detailed representation of the protein array results with the attachment of the original membrane photo. Bar graphs show individual changes per protein, control (white), LPS-treated (light gray), TNFα-treated (dark gray).

AD-MSCs are involved in all three parts of wound healing: the inflammation phase, proliferation phase, and remodeling phase. The wound healing assay demonstrated that MSCs promote faster wound closure after LPS and TNFα treatment compared to the control (Figure 5A). In that case, when treatment took place before woundmaking, the wounds of the control sample were closed around 40 h and the treated samples presented wound healing around 34.67 h after LPS and 37.67 h upon TNFα treatment. In the condition where scratching occurred before inflammation was triggered, the wounds of control samples closed around 47 h, and the treated samples closed faster, and they were remodeled around 41 h after LPS and 40.33 h after TNFα treatment. Graphs show significant changes in wound-closure speed between controls and in the presence of inflammation. It appeared that the closing speed was significantly higher in the case where inflammation induced after scratch formation was formed. AD-MSCs presented accelerated wound healing under inflammation conditions, and AD-MSCs were triggered by inflammatory factors to facilitate wound healing (Figure 5B).

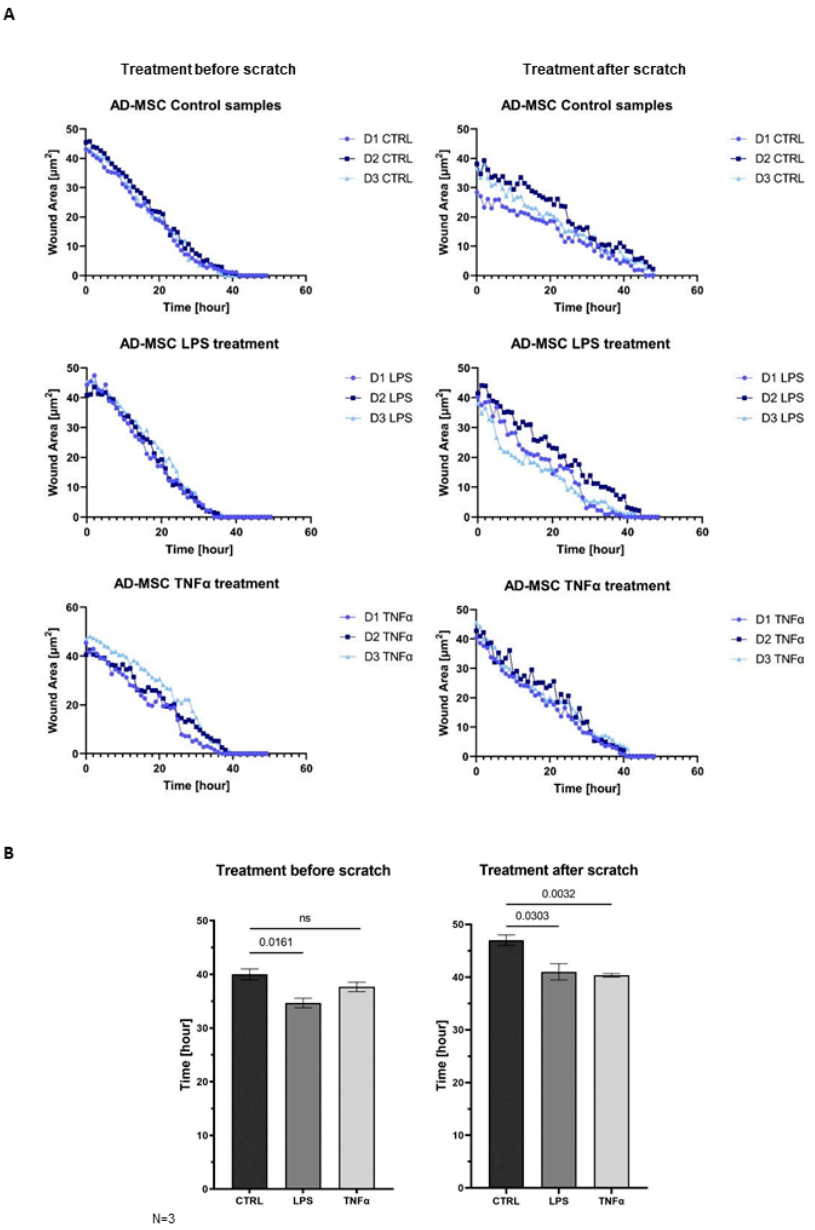


**Figure 5.** (**A**) The result of the wound healing test shows the area of the wound as a function of time. The wound closure process was monitored for 48 hours. Each donor is marked with a different color: D1 (medium blue), D2 (dark blue), and D3 (light blue). (**B**) Bar graphs show comparison of wound closure length between conditions - treatment before and after scratching.

## 4. Discussion

The regenerating and immunomodulatory ability of mesenchymal stem cells is already known, but the development of an effective therapeutic procedure is still pending. Applying animal models and in vitro cell cultures showed that MSC licensing can significantly improve tissue regeneration efficiency, reduce the degree of inflammation, and promote faster wound closure [6,9,13,30,31,35,41,42]. During our experiments, we treated human AD-MSC primary cell cultures with LPS and TNFα in order to induce an inflammatory microenvironment. Then, we examine the expression alterations at the gene and protein levels. We observed that both treatments resulted in significant changes in the RNA-Seq profile compared to the control. In the LPS and TNFα environment, the expression of genes related to cell proliferation, differentiation, wound healing, and migration increased. Furthermore, the TNFα treatment significantly elevated the expression of interleukins, chemokines, chemokine ligands and growth factors involved in the immune response. Furthermore, some interleukins showed an increased level in response to LPS treatment at the protein level. STRING analysis of secreted cytokines shows that LPS treatment induces the participation of the proteins MMP-9, VEGFA, ICAM-1, and ANGPT-2 in vascular remodelling, which is a major player in the overall wound healing process (Supplementary Figure S6) [12,39,43,44]. HGF and FGF-19 proteins are involved in differentiation and, together with the LIF, CXCL-12, CCL7, and CCL5 chemokines, in the migration of MSC and local immunosuppression [12,39,43,44]. A similar pattern and pathways were activated by TNFα treatment, but here the activation of the immune response was more pronounced, with CD40L activation being more characteristic of pro-inflammatory MSC. Taken together, these data suggest that MSC activation can result in stronger wound healing. This confirms the hypothesis that licensing (preactivation) of cells may have therapeutic benefits. Pathways identified via gene expression studies were also confirmed using cytokine expression. Here, we have to take into account the limitation that much more information and pathways are available when examining gene expression data than when identifying 105 cytokines. Therefore, pathways based on gene expression data are more detailed and take into account the link to the cell cycle.

In the wound healing assay, both treatments significantly accelerated wound closure in the 'treatment after scratch' condition, and LPS also triggered faster wound closure in the 'treatment before scratch' condition, supporting our previous hypothesis. In general, both treatments were beneficial in terms of tissue regeneration, wound healing, and immunomodulation. It is promising, but more studies are needed to develop a possible therapeutic procedure. According to another approach, by developing our experimental setup, we can prepare a preclinical test. This may be suitable for tracking gene expression profile changes caused by the inflammatory microenvironment in the cells of patients with nonhealing wounds, ulcers, or burns. With our improved system, long-term personalized autogen therapy can be achieved.

Our results confirm that AD-MSCs can be used to treat chronic, inflamed, nonhealing wounds, even if the inflammation persists for a long time. While it is true that in the latter case, there is a difference in the processes induced by LPS and those in the presence of TNFα, from a clinical point of view, all treatments activate pathways that can promote tissue healing, ECM remodeling, and regeneration.

AD-MSCs have great clinical therapeutic potential due to their regenerative, antiapoptotic, antifibrotic, antioxidant, and immunomodulating capabilities. The delivery of not only AD-MSCs but also their secretome can have a positive effect on the course of the disease. Research also reveals that the secretion profile of AD-MSCs changes during appropriate pretreatments, making them even more suitable for therapy [21,42]. There is evidence in the literature that certain treatments can improve the effectiveness of MSCs. Most of these strategies seek to mimic the inflammatory medium. The effect of pro-inflammatory cytokines, hypoxia, has, in some cases, been shown to enhance MSC-mediated anti-inflammatory processes [45–49]. However, in these cases, classical pro-inflammatory signals were also detected during the induced response, making it unclear whether immunosuppressive

or pro-inflammatory MSCs are formed and responsible for the possible therapeutic effect [45,50,51]. These indications have not yet been fully developed, as neither the type of agents nor their therapeutic concentrations are known or standardized. Suboptimally, a pro-inflammatory phenotype may be present more frequently, while high concentrations affect cell viability [50,52]. Pretreatments in GMP manufacturing of cell therapy products may also raise licensing issues. However, it should be noted that licensed MSCs are often considered the next generation of MSC therapies for the treatment of injuries associated with acute and sub-acute inflammation [50,52,53]. Research into the background of biological processes and safe treatments is still ongoing, but the results so far are extremely promising [21,42].

**Supplementary Materials:** The following supporting information can be downloaded at: https://www.mdpi.com/article/10.3390/cells12151966/s1, Supplementary methods, Figure S1A: The DEG analysis shows the genes changed as a result of LPS treatment on a heat map. Figure S1B: The PC plot analysis shows that the different donors are similar for all conditions and that the conditions can be clearly separated from each other. Figure S2A: The heat map illustrates the change in the levels of all proteins examined with the protein array; Figure S2B: Detailed visualization of the results of the protein array with the attachment of the original membrane photo. The bar graphs show the changes per protein, control (white), LPS-treated (light gray), and TNFα-treated (dark gray). Figure S3: Heatmap of the similarity matrix calculated by the rrvgo package from the GSEA results of the GO terms in LPS (A) and TNFα (B). Rows and columns are both clustered, thus similar terms are arranged together. Clusters were named according to the parent term, calculating the parent term was based on the p values of the terms within a cluster; Figure S4: The quantitative real-time PCR results represent the altered genes, but only CXCL8 showed significant fold change as a result of the treatments. Control (white), LPS treatment (light gray), TNFα treatment (dark gray); Figure S5A: The heat map illustrates the change in the levels of all proteins examined with the protein array; Figure S5B: Detailed visualization of the protein array results with the attachment of the original membrane photo. The bar graphs show the changes per protein, control (white), LPS-treated (light gray), TNFα -treated (dark gray); Figure S6: STRING analysis of secreted cytokines by LPS and TNFα-activated AD-MSCs. Proteins are shown as nodes, and the color of each link defines the type of evidence available for the interaction between two proteins; Table S1: Gene set enrichment results based on GO; Table S2: Gene set enrichment results based on KEGG; Table S3: Clustered GO terms based on semantic similarity.

**Author Contributions:** Conceptualization, D.S. and Z.V.; methodology, D.S., T.M., M.G., A.K.-V. and S.P.; software, V.M., D.S., T.M. and Z.V.; validation, Z.V.; writing, original draft preparation, D.S., T.M. and V.M.; writing, review and editing, Z.V., B.B., E.K. and L.K.; visualization, D.S., T.M. and V.M.; supervision, Z.V. Funding acquisition, Z.V. and L.K. All authors have read and agreed to the published version of the manuscript.

**Funding:** This work was supported by the National Research, Development and Innovation Office (NKFI PD 132570 to Z.V.) and the GINOP PLUSZ-2.1.1-21 project (co-financed by the European Union and the European Regional Development Fund) Z.V. was supported by the Bolyai János Postdoctoral Fellowship (BO/00190/20/5) and the NKP-22-5 Bolyai + Fellowship (NKP-NKP-22-5-SZTE-319) financed by the New National Excellence Program of the Hungarian Ministry of Innovation and Technology from the source of the National Research Development and Innovation Fund. Project no. TKP2021-EGA-28 and TKP2021-EGA-32 have been implemented with the support provided by the Ministry of Innovation and Technology of Hungary from the National Research, Development and Innovation Fund, financed under the TKP2021-EGA funding scheme. LK was supported by the New National Excellence Program of the Hungarian Ministry of Innovation and Technology from the source of the National Research Development and Innovation Fund. K.L-HCEMM: H2020-EU.4.a. The research was supported by the Biobank Competence Center of the Life Sciences Cluster of the Centre of Excellence for Interdisciplinary Research, Development, and Innovation of the University of Szeged. Vanda Miklós is a member of the Biobank research group.

**Institutional Review Board Statement:** The collection of adipose tissue complied with the guidelines of the Declaration of Helsinki and was approved by the National Public Health and Medical Officer Service (NPHMOS) and the National Medical Research Council (16821-6/2017/EÜIG, STEM-01/2017, 6 September 2017) which follows the EU Member States' Directive 2004/23/EC on the practice of presumed written consent for tissue collection.

**Informed Consent Statement:** Informed consent was obtained from all subjects involved in the study.

**Data Availability Statement:** All data generated and analyzed during this study are included in this manuscript (and its Supplementary Information files).

**Acknowledgments:** We express our very great appreciation to Katalin Boldog for administrative and technical support during our research work.

**Conflicts of Interest:** The authors declare that they have no conflict of interest.

## References

1. Bunnell, B.A. Adipose Tissue-Derived Mesenchymal Stem Cells. *Cells* **2021**, *10*, 3433. [CrossRef]
2. Li, N.; Hua, J.L. Interactions between mesenchymal stem cells and the immune system. *Cell Mol. Life Sci.* **2017**, *74*, 2345–2360. [CrossRef] [PubMed]
3. Mushahary, D.; Spittler, A.; Kasper, C.; Weber, V.; Charwat, V. Isolation, cultivation, and characterization of human mesenchymal stem cells. *Cytom. Part A* **2018**, *93*, 19–31. [CrossRef] [PubMed]
4. Trayhurn, P.; Drevon, C.A.; Eckel, J. Secreted proteins from adipose tissue and skeletal muscle - adipokines, myokines and adipose/muscle cross-talk. *Arch. Physiol. Biochem.* **2011**, *117*, 47–56. [CrossRef]
5. Zwick, R.K.; Guerrero-Juarez, C.F.; Horsley, V.; Plikus, M.V. Anatomical, Physiological, and Functional Diversity of Adipose Tissue. *Cell Metab.* **2018**, *27*, 68–83. [CrossRef]
6. Konno, M.; Hamabe, A.; Hasegawa, S.; Ogawa, H.; Fukusumi, T.; Nishikawa, S.; Ohta, K.; Kano, Y.; Ozaki, M.; Noguchi, Y.; et al. Adipose-derived mesenchymal stem cells and regenerative medicine. *Dev. Growth Differ.* **2013**, *55*, 309–318. [CrossRef]
7. Guasti, L.; New, S.E.; Hadjidemetriou, I.; Palmiero, M.; Ferretti, P. Plasticity of human adipose-derived stem cells - relevance to tissue repair. *Int. J. Dev. Biol.* **2018**, *62*, 431–439. [CrossRef] [PubMed]
8. Carelli, S.; Colli, M.; Vinci, V.; Caviggioli, F.; Klinger, M.; Gorio, A. Mechanical Activation of Adipose Tissue and Derived Mesenchymal Stem Cells: Novel Anti-Inflammatory Properties. *Int. J. Mol. Sci.* **2018**, *19*, 267. [CrossRef]
9. Naji, A.; Eitoku, M.; Favier, B.; Deschaseaux, F.; Rouas-Freiss, N.; Suganuma, N. Biological functions of mesenchymal stem cells and clinical implications. *Cell. Mol. Life Sci.* **2019**, *76*, 3323–3348. [CrossRef]
10. Al-Ghadban, S.; Bunnell, B.A. Adipose Tissue-Derived Stem Cells: Immunomodulatory Effects and Therapeutic Potential. *Physiology* **2020**, *35*, 125–133. [CrossRef]
11. DelaRosa, O.; Lombardo, E. Modulation of adult mesenchymal stem cells activity by toll-like receptors: Implications on therapeutic potential. *Mediat. Inflamm.* **2010**, *2010*, 865601. [CrossRef]
12. Krawczenko, A.; Klimczak, A. Adipose Tissue-Derived Mesenchymal Stem/Stromal Cells and Their Contribution to Angiogenic Processes in Tissue Regeneration. *Int. J. Mol. Sci.* **2022**, *23*, 2425. [CrossRef]
13. Mazini, L.; Rochette, L.; Admou, B.; Amal, S.; Malka, G. Hopes and Limits of Adipose-Derived Stem Cells (ADSCs) and Mesenchymal Stem Cells (MSCs) in Wound Healing. *Int. J. Mol. Sci.* **2020**, *21*, 1306. [CrossRef] [PubMed]
14. Wu, L.; Cai, X.; Zhang, S.; Karperien, M.; Lin, Y. Regeneration of articular cartilage by adipose tissue derived mesenchymal stem cells: Perspectives from stem cell biology and molecular medicine. *J. Cell. Physiol.* **2013**, *228*, 938–944. [CrossRef]
15. Cao, W.; Cao, K.; Cao, J.; Wang, Y.; Shi, Y. Mesenchymal stem cells and adaptive immune responses. *Immunol. Lett.* **2015**, *168*, 147–153. [CrossRef] [PubMed]
16. Ti, D.; Hao, H.; Tong, C.; Liu, J.; Dong, L.; Zheng, J.; Zhao, Y.; Liu, H.; Fu, X.; Han, W. LPS-preconditioned mesenchymal stromal cells modify macrophage polarization for resolution of chronic inflammation via exosome-shuttled let-7b. *J. Transl. Med.* **2015**, *13*, 308. [CrossRef]
17. Kuca-Warnawin, E.; Janicka, I.; Szczesny, P.; Olesinska, M.; Bonek, K.; Gluszko, P.; Kontny, E. Modulation of T-Cell Activation Markers Expression by the Adipose Tissue-Derived Mesenchymal Stem Cells of Patients with Rheumatic Diseases. *Cell Transplant.* **2020**, *29*, 963689720945682. [CrossRef]
18. Xiao, K.; He, W.; Guan, W.; Hou, F.; Yan, P.; Xu, J.; Zhou, T.; Liu, Y.; Xie, L. Mesenchymal stem cells reverse EMT process through blocking the activation of NF-kappaB and Hedgehog pathways in LPS-induced acute lung injury. *Cell Death Dis.* **2020**, *11*, 863. [CrossRef] [PubMed]
19. Fu, X.; Han, B.; Cai, S.; Lei, Y.; Sun, T.; Sheng, Z. Migration of bone marrow-derived mesenchymal stem cells induced by tumor necrosis factor-alpha and its possible role in wound healing. *Wound Repair Regen. Off. Publ. Wound Heal. Soc. Eur. Tissue Repair Soc.* **2009**, *17*, 185–191. [CrossRef]
20. Cheng, H.Y.; Anggelia, M.R.; Lin, C.H.; Wei, F.C. Toward transplantation tolerance with adipose tissue-derived therapeutics. *Front. Immunol.* **2023**, *14*, 1111813. [CrossRef]

21. Al-Ghadban, S.; Artiles, M.; Bunnell, B.A. Adipose Stem Cells in Regenerative Medicine: Looking Forward. *Front. Bioeng. Biotechnol.* **2021**, *9*, 837464. [CrossRef]
22. Chang, M.; Nguyen, T.T. Strategy for Treatment of Infected Diabetic Foot Ulcers. *Acc. Chem. Res.* **2021**, *54*, 1080–1093. [CrossRef]
23. Feldbrin, Z.; Omelchenko, E.; Lipkin, A.; Shargorodsky, M. Osteopontin levels in plasma, muscles, and bone in patient with non-healing diabetic foot ulcers: A new player in wound healing process? *J. Diabetes Its Complicat.* **2018**, *32*, 795–798. [CrossRef]
24. Furuta, T.; Miyaki, S.; Ishitobi, H.; Ogura, T.; Kato, Y.; Kamei, N.; Miyado, K.; Higashi, Y.; Ochi, M. Mesenchymal Stem Cell-Derived Exosomes Promote Fracture Healing in a Mouse Model. *Stem Cells Transl. Med.* **2016**, *5*, 1620–1630. [CrossRef] [PubMed]
25. Shohara, R.; Yamamoto, A.; Takikawa, S.; Iwase, A.; Hibi, H.; Kikkawa, F.; Ueda, M. Mesenchymal stromal cells of human umbilical cord Wharton's jelly accelerate wound healing by paracrine mechanisms. *Cytotherapy* **2012**, *14*, 1171–1181. [CrossRef]
26. Brembilla, N.C.; Vuagnat, H.; Boehncke, W.H.; Krause, K.H.; Preynat-Seauve, O. Adipose-Derived Stromal Cells for Chronic Wounds: Scientific Evidence and Roadmap Toward Clinical Practice. *Stem Cells Transl. Med.* **2023**, *12*, 17–25. [CrossRef]
27. Chen, H.; Min, X.H.; Wang, Q.Y.; Leung, F.W.; Shi, L.; Zhou, Y.; Yu, T.; Wang, C.M.; An, G.; Sha, W.H.; et al. Pre-activation of mesenchymal stem cells with TNF-alpha, IL-1beta and nitric oxide enhances its paracrine effects on radiation-induced intestinal injury. *Sci. Rep.* **2015**, *5*, 8718. [CrossRef] [PubMed]
28. Lee, S.C.; Jeong, H.J.; Lee, S.K.; Kim, S.J. Lipopolysaccharide preconditioning of adipose-derived stem cells improves liver-regenerating activity of the secretome. *Stem Cell Res. Ther.* **2015**, *6*, 75. [CrossRef] [PubMed]
29. Liu, C.; Xu, Y.; Lu, Y.; Du, P.; Li, X.; Wang, C.; Guo, P.; Diao, L.; Lu, G. Mesenchymal stromal cells pretreated with proinflammatory cytokines enhance skin wound healing via IL-6-dependent M2 polarization. *Stem Cell Res. Ther.* **2022**, *13*, 414. [CrossRef]
30. Wang, K.; Chen, Z.; Jin, L.; Zhao, L.; Meng, L.; Kong, F.; He, C.; Kong, F.; Zheng, L.; Liang, F. LPS-pretreatment adipose-derived mesenchymal stromal cells promote wound healing in diabetic rats by improving angiogenesis. *Injury* **2022**, *53*, 3920–3929. [CrossRef]
31. Munir, S.; Basu, A.; Maity, P.; Krug, L.; Haas, P.; Jiang, D.; Strauss, G.; Wlaschek, M.; Geiger, H.; Singh, K.; et al. TLR4-dependent shaping of the wound site by MSCs accelerates wound healing. *EMBO Rep.* **2020**, *21*, e48777. [CrossRef]
32. Kerstan, A.; Dieter, K.; Niebergall-Roth, E.; Klingele, S.; Junger, M.; Hasslacher, C.; Daeschlein, G.; Stemler, L.; Meyer-Pannwitt, U.; Schubert, K.; et al. Translational development of ABCB5(+) dermal mesenchymal stem cells for therapeutic induction of angiogenesis in non-healing diabetic foot ulcers. *Stem Cell Res. Ther.* **2022**, *13*, 455. [CrossRef]
33. Silva-Carvalho, A.E.; Sousa, M.R.R.; Alencar-Silva, T.; Carvalho, J.L.; Saldanha-Araujo, F. Mesenchymal stem cells immunomodulation: The road to IFN-gamma licensing and the path ahead. *Cytokine Growth Factor Rev.* **2019**, *47*, 32–42. [CrossRef] [PubMed]
34. Serejo, T.R.T.; Silva-Carvalho, A.E.; Braga, L.D.D.F.; Neves, F.D.R.; Pereira, R.W.; de Carvalho, J.L.; Saldanha-Araujo, F. Assessment of the Immunosuppressive Potential of INF-gamma Licensed Adipose Mesenchymal Stem Cells, Their Secretome and Extracellular Vesicles. *Cells* **2019**, *8*, 22. [CrossRef] [PubMed]
35. Nieto-Nicolau, N.; Martinez-Conesa, E.M.; Fuentes-Julian, S.; Arnalich-Montiel, F.; Garcia-Tunon, I.; De Miguel, M.P.; Casaroli-Marano, R.P. Priming human adipose-derived mesenchymal stem cells for corneal surface regeneration. *J. Cell Mol. Med.* **2021**, *25*, 5124–5137. [CrossRef] [PubMed]
36. Love, M.I.; Huber, W.; Anders, S. Moderated estimation of fold change and dispersion for RNA-seq data with DESeq2. *Genome Biol.* **2014**, *15*, 550. [CrossRef]
37. Gu, Z.; Eils, R.; Schlesner, M. Complex heatmaps reveal patterns and correlations in multidimensional genomic data. *Bioinformatics* **2016**, *32*, 2847–2849. [CrossRef]
38. Saadh, M.J.; Ramirez-Coronel, A.A.; Saini, R.S.; Arias-Gonzales, J.L.; Amin, A.H.; Gavilan, J.C.O.; Sarbu, I. Advances in mesenchymal stem/stromal cell-based therapy and their extracellular vesicles for skin wound healing. *Human Cell* **2023**, *36*, 1253–1264. [CrossRef]
39. Ridiandries, A.; Tan, J.T.M.; Bursill, C.A. The Role of Chemokines in Wound Healing. *Int. J. Mol. Sci.* **2018**, *19*, 3217. [CrossRef]
40. Fu, X.R.; Liu, G.; Halim, A.; Ju, Y.; Luo, Q.; Song, G.B. Mesenchymal Stem Cell Migration and Tissue Repair. *Cells* **2019**, *8*, 784. [CrossRef]
41. Heo, S.C.; Jeon, E.S.; Lee, I.H.; Kim, H.S.; Kim, M.B.; Kim, J.H. Tumor necrosis factor-alpha-activated human adipose tissue-derived mesenchymal stem cells accelerate cutaneous wound healing through paracrine mechanisms. *J. Investig. Dermatol.* **2011**, *131*, 1559–1567. [CrossRef]
42. Gimble, J.M.; Katz, A.J.; Bunnell, B.A. Adipose-derived stem cells for regenerative medicine. *Circ. Res.* **2007**, *100*, 1249–1260. [CrossRef] [PubMed]
43. Anton, K.; Banerjee, D.; Glod, J. Macrophage-associated mesenchymal stem cells assume an activated, migratory, pro-inflammatory phenotype with increased IL-6 and CXCL10 secretion. *PLoS ONE* **2012**, *7*, e35036. [CrossRef]
44. Neuss, S.; Becher, E.; Woltje, M.; Tietze, L.; Jahnen-Dechent, W. Functional expression of HGF and HGF receptor/c-met in adult human mesenchymal stem cells suggests a role in cell mobilization, tissue repair, and wound healing. *Stem Cells* **2004**, *22*, 405–414. [CrossRef]
45. Skibber, M.A.; Olson, S.D.; Prabhakara, K.S.; Gill, B.S.; Cox, C.S., Jr. Enhancing Mesenchymal Stromal Cell Potency: Inflammatory Licensing via Mechanotransduction. *Front. Immunol.* **2022**, *13*, 874698. [CrossRef] [PubMed]
46. Saparov, A.; Ogay, V.; Nurgozhin, T.; Jumabay, M.; Chen, W.C. Preconditioning of Human Mesenchymal Stem Cells to Enhance Their Regulation of the Immune Response. *Stem Cells Int.* **2016**, *2016*, 3924858. [CrossRef] [PubMed]

47. Kurte, M.; Vega-Letter, A.M.; Luz-Crawford, P.; Djouad, F.; Noel, D.; Khoury, M.; Carrion, F. Time-dependent LPS exposure commands MSC immunoplasticity through TLR4 activation leading to opposite therapeutic outcome in EAE. *Stem Cell Res. Ther.* **2020**, *11*, 416. [CrossRef]
48. Chinnadurai, R.; Rajan, D.; Ng, S.; McCullough, K.; Arafat, D.; Waller, E.K.; Anderson, L.J.; Gibson, G.; Galipeau, J. Immune dysfunctionality of replicative senescent mesenchymal stromal cells is corrected by IFNgamma priming. *Blood Adv.* **2017**, *1*, 628–643. [CrossRef] [PubMed]
49. Francois, M.; Romieu-Mourez, R.; Li, M.; Galipeau, J. Human MSC suppression correlates with cytokine induction of indoleamine 2,3-dioxygenase and bystander M2 macrophage differentiation. *Mol. Ther. J. Am. Soc. Gene Ther.* **2012**, *20*, 187–195. [CrossRef]
50. Hu, C.; Li, L. Preconditioning influences mesenchymal stem cell properties in vitro and in vivo. *J. Cell Mol. Med.* **2018**, *22*, 1428–1442. [CrossRef]
51. Waterman, R.S.; Tomchuck, S.L.; Henkle, S.L.; Betancourt, A.M. A new mesenchymal stem cell (MSC) paradigm: Polarization into a pro-inflammatory MSC1 or an Immunosuppressive MSC2 phenotype. *PLoS ONE* **2010**, *5*, e10088. [CrossRef] [PubMed]
52. Krampera, M.; Le Blanc, K. Mesenchymal stromal cells: Putative microenvironmental modulators become cell therapy. *Cell Stem Cell* **2021**, *28*, 1708–1725. [CrossRef] [PubMed]
53. Li, M.; Jiang, Y.; Hou, Q.; Zhao, Y.; Zhong, L.; Fu, X. Potential pre-activation strategies for improving therapeutic efficacy of mesenchymal stem cells: Current status and future prospects. *Stem Cell Res. Ther.* **2022**, *13*, 146. [CrossRef] [PubMed]

frontiers | Frontiers in Cell and Developmental Biology

TYPE Original Research
PUBLISHED 28 March 2024
DOI 10.3389/fcell.2024.1367242



OPEN ACCESS

EDITED BY
Tokiko Nagamura-Inoue,
The University of Tokyo, Japan

REVIEWED BY
Yuyao Tian,
Massachusetts General Hospital and Harvard Medical School, United States
Xiaolei Li,
University of Pennsylvania, United States

*CORRESPONDENCE
Zoltán Veréb,
vereb.zoltan@med.u-szeged.hu

†These authors have contributed equally to this work and share first authorship

RECEIVED 08 January 2024
ACCEPTED 15 March 2024
PUBLISHED 28 March 2024

CITATION
Szűcs D, Monostori T, Miklós V, Páhi ZG, Póliska S, Kemény L and Veréb Z (2024), Licensing effects of inflammatory factors and TLR ligands on the regenerative capacity of adipose-derived mesenchymal stem cells. *Front. Cell Dev. Biol.* 12:1367242. doi: 10.3389/fcell.2024.1367242



# Licensing effects of inflammatory factors and TLR ligands on the regenerative capacity of adipose-derived mesenchymal stem cells

Diána Szűcs[1,2,3†], Tamás Monostori[1,2,3†], Vanda Miklós[4†], Zoltán G. Páhi[5,6], Szilárd Póliska[7], Lajos Kemény[1,3,8] and Zoltán Veréb[1,3,4*]

[1]Regenerative Medicine and Cellular Pharmacology Laboratory, Department of Dermatology and Allergology, University of Szeged, Szeged, Hungary, [2]Doctoral School of Clinical Medicine, University of Szeged, Szeged, Hungary, [3]Centre of Excellence for Interdisciplinary Research, Development and Innovation, University of Szeged, Szeged, Hungary, [4]Biobank, University of Szeged, Szeged, Hungary, [5]Genome Integrity and DNA Repair Core Group, Hungarian Centre of Excellence for Molecular Medicine (HCEMM), University of Szeged, Szeged, Hungary, [6]Department of Pathology, Albert Szent-Györgyi Medical School, University of Szeged, Szeged, Hungary, [7]Genomic Medicine and Bioinformatics Core Facility, Department of Biochemistry and Molecular Biology, Faculty of Medicine, University of Debrecen, Debrecen, Hungary, [8]Hungarian Centre of Excellence for Molecular Medicine-USz Skin Research Group, University of Szeged, Szeged, Hungary

**Introduction:** Adipose tissue-derived mesenchymal stem cells are promising contributors to regenerative medicine, exhibiting the ability to regenerate tissues and modulate the immune system, which is particularly beneficial for addressing chronic inflammatory ulcers and wounds. Despite their inherent capabilities, research suggests that pretreatment amplifies therapeutic effectiveness.

**Methods:** Our experimental design exposed adipose-derived mesenchymal stem cells to six inflammatory factors for 24 h. We subsequently evaluated gene expression and proteome profile alterations and observed the wound closure rate post-treatment.

**Results:** Specific pretreatments, such as IL-1β, notably demonstrated an accelerated wound-healing process. Analysis of gene and protein expression profiles revealed alterations in pathways associated with tissue regeneration.

**Discussion:** This suggests that licensed cells exhibit potentially higher therapeutic efficiency than untreated cells, shedding light on optimizing regenerative strategies using adipose tissue-derived stem cells.

KEYWORDS

**adipose-derived mesenchymal stem cells, regenerative medicine, licensing, inflammation, immune system**

## 1 Introduction

Adipose tissue is distributed throughout various anatomical sites in the human body, including subcutaneous and visceral locations, intra-articular spaces, intramuscular regions, intra-hepatic depots, and the bone marrow. Beyond an energy reservoir, adipose tissue functions as an endocrine organ, producing many bioactive molecules that modulate

metabolic and cellular processes. Among these molecules are adipokines (e.g., leptin, adiponectin, omentin, and resistin), pro- and anti-inflammatory cytokines (e.g., IL-6, TNF-α, IL-1β, IL-8, MCP-1, IL-1Ra, IL-6, IL-7, IL-8, and IL-11), growth factors (e.g., VEGF, HGF, FGF, IGF-1, and BDNF), pro-apoptotic and pro-angiogenic factors, as well as microvesicles enriched with proteins and nucleic acids. Adipose tissue can be categorized into three main types: white adipose tissue, primarily involved in energy storage but also secreting adipokines; brown adipose tissue, responsible for thermogenesis regulation while retaining some energy storage capacity; and beige adipose tissue, which contributes to thermogenesis and energy storage (Konno et al., 2013; Cao et al., 2015; Li and Hua, 2017; Mushahary et al., 2018; Qi et al., 2018; Pittenger et al., 2019; Mazini et al., 2020; Song et al., 2020; Bunnell BA, 2021).

Adipose tissue-derived mesenchymal stem cells (AD-MSCs) reside within adipose tissue, primarily within the stromal vascular fraction (SVF) accessible through minimally invasive procedures. AD-MSCs are multipotent cells characterized by self-renewal potential and the ability to differentiate into mesodermal lineage cells such as adipocytes, chondrocytes, and osteoblasts. They exhibit high proliferation rates and possess immunosuppressive properties, rendering them and their secretome valuable assets in regenerative medicine applications for diseases associated with immune-related disorders. AD-MSCs play a pivotal role in immune response regulation by engaging in direct cell–cell interactions or through the secretion of bioactive factors. These cells interact with various immune cell types, including T cells, B cells, macrophages, natural killer cells (NKs), dendritic cells (DCs), neutrophils, and mast cells (Anton et al., 2012; Konno et al., 2013; Cao et al., 2015; Li and Hua, 2017; Mushahary et al., 2018; Qi et al., 2018; Ridiandries et al., 2018; Zwick et al., 2018; Pittenger et al., 2019; Al-Ghadban and Bunnell, 2020; Mazini et al., 2020; Song et al., 2020; Bunnell BA, 2021; Szucs et al., 2023).

AD-MSCs exert their immunomodulatory influence by interacting with T cells through cell adhesion molecules and modifying the secretion of mediators such as IDO, TGFβ, IL-10, and PGE2. Additionally, T cells reciprocally affect AD-MSCs through chemokine production. Studies have demonstrated that AD-MSCs, in the presence of high pro-inflammatory cytokine levels, promote regulatory T cell (Treg) generation while inhibiting T cell proliferation, activation, and differentiation, thus suppressing immune responses. Conversely, under low pro-inflammatory cytokine exposure conditions, AD-MSCs suppress Treg generation and activate T cell proliferation, activation, and differentiation. AD-MSCs exhibit dual effects on B cells, inhibiting and promoting their proliferation, activation, and differentiation while also inducing chemotaxis and Breg induction. These cells can impede NK cell proliferation, activation, and migration while stimulating NK cell progenitor proliferation and activation.

Furthermore, AD-MSCs hinder DC differentiation, endocytosis, maturation, activation, and migration, inhibiting mast cell degranulation, inflammatory cytokine expression, and chemotaxis. Macrophage polarization is influenced by AD-MSCs, favoring the M2 phenotype and inhibiting the M1 phenotype. At the same time, AD-MSCs modulate neutrophils by inhibiting activation, recruitment, extracellular neutrophil trap formation, and protease secretion while promoting neutrophil survival and recruitment (Anton et al., 2012; Konno et al., 2013; Cao et al., 2015; Li and Hua, 2017; Carelli et al., 2018; Guasti et al., 2018; Mushahary et al., 2018; Qi et al., 2018; Ridiandries et al., 2018; Zwick et al., 2018; Pittenger et al., 2019; Al-Ghadban and Bunnell, 2020; Mazini et al., 2020; Munir et al., 2020; Song et al., 2020; Bunnell BA, 2021; Krampera and Le Blanc, 2021; Szucs et al., 2023).

Due to their immunomodulatory properties, angiogenic potential, and differentiation capacity, AD-MSCs offer a promising avenue for tissue repair (Szucs et al., 2023), regeneration, and replacement in a broad spectrum of conditions characterized by tissue damage. AD-MSCs hold significant therapeutic potential for applications such as wound healing and skin regeneration in various contexts, including diabetic and non-diabetic ulcers, non-healing wounds, extensive burns, and physicochemical skin injuries. Moreover, AD-MSCs find relevance in autoimmune disorders, hematological conditions, graft-versus-host disease, bone and cartilage repair, cardiovascular and muscular diseases, neurodegenerative disorders, and radiation-induced injuries. These versatile cells offer a means to restore tissue function effectively and safely. To ensure secure and successful application in AD-MSC-based therapies, the purity and potency of these cells must be rigorously assessed before administration (Fu et al., 2009; DelaRosa and Lombardo, 2010; Anton et al., 2012; François et al., 2012; Shohara et al., 2012; Konno et al., 2013; Cao et al., 2015; Furuta et al., 2016; Li and Hua, 2017; Carelli et al., 2018; Feldbrin et al., 2018; Guasti et al., 2018; Mushahary et al., 2018; Qi et al., 2018; Ridiandries et al., 2018; Zwick et al., 2018; Pittenger et al., 2019; Sahu et al., 2019; Al-Ghadban and Bunnell, 2020; Kuca-Warnawin et al., 2020; Kurte et al., 2020; Mazini et al., 2020; Munir et al., 2020; Song et al., 2020; Xiao et al., 2020; Bunnell BA, 2021; Krampera and Le Blanc, 2021; Nieto-Nicolau et al., 2021; Krawczenko and Klimczak, 2022; Cheng et al., 2023; Huerta et al., 2023; Szucs et al., 2023).

Adipose tissue-derived mesenchymal stem cells (AD-MSCs) hold significant clinical therapeutic promise attributed to their multifaceted attributes encompassing regenerative, anti-apoptotic, antifibrotic, antioxidant, and immunomodulatory capacities. Beyond the application of AD-MSCs themselves, harnessing their secretome has emerged as an avenue with the potential to influence disease progression positively. Emerging research underscores the dynamic nature of AD-MSC secretion profiles, which can be further tailored through strategic pretreatments, enhancing their suitability for therapeutic applications (Anton et al., 2012; François et al., 2012; Konno et al., 2013; Wu et al., 2013; Cao et al., 2015; Li and Hua, 2017; Guasti et al., 2018; Qi et al., 2018; Zwick et al., 2018; Pittenger et al., 2019; Al-Ghadban and Bunnell, 2020; Mazini et al., 2020; Song et al., 2020; Bunnell BA, 2021; Chang and Nguyen, 2021; Brembilla et al., 2023; Szucs et al., 2023).

Existing literature highlights strategies to augment the effectiveness of MSC-based therapies, focusing on mimicking inflammatory microenvironments. Pro-inflammatory cytokines and hypoxic conditions have been explored as factors capable of potentiating MSC-mediated anti-inflammatory responses. Nevertheless, in these instances, the concomitant detection of classical pro-inflammatory signals has raised questions regarding whether immunosuppressive or pro-inflammatory MSC phenotypes are primarily responsible for

the observed therapeutic effects. The complete elucidation of these indications remains a work in progress, with the precise nature of agents and their therapeutically effective concentrations yet to be definitively determined or standardized. Notably, suboptimal conditions may promote the prevalence of a pro-inflammatory MSC phenotype, while excessive concentrations can impact cell viability. In the context of Good Manufacturing Practice (GMP) for cell therapy product manufacturing, pretreatment strategies may also raise regulatory and licensing considerations. However, it is worth highlighting that licensed MSCs often represent the next Frontier in MSC-based therapies, particularly for addressing injuries associated with acute and sub-acute inflammation. Ongoing research continues to delve into the underlying biological processes and the development of safe and efficacious pretreatment approaches. Thus far, the findings have been exceedingly promising, offering significant prospects for advancing the field of regenerative medicine (Anton et al., 2012; François et al., 2012; Konno et al., 2013; Wu et al., 2013; Cao et al., 2015; Li and Hua, 2017; Guasti et al., 2018; Hu and Li, 2018; Qi et al., 2018; Zwick et al., 2018; Pittenger et al., 2019; Al-Ghadban and Bunnell, 2020; Mazini et al., 2020; Song et al., 2020; Bunnell BA, 2021; Chang and Nguyen, 2021; Brembilla et al., 2023; Szucs et al., 2023).

Our study evaluates the wound healing and skin regeneration capabilities of AD-MSCs, particularly in the context of highly inflamed environments, which can influence their expression profile. We hypothesize that the pretreatment of AD-MSCs may be vital to enhancing therapeutic efficacy. Our investigation aims to shed light on the molecular and cellular responses of AD-MSCs to inflammatory factors, specifically LPS, TNFα, IL1β, IFNγ, and PolyI:C. Our findings may contribute to developing more effective therapies where cell preconditioning is pivotal in augmenting therapeutic outcomes. Moreover, our experimental framework has the potential to assess patient-specific responses to inflammatory factors, aiding in the development of personalized therapeutic approaches.

# 2 Materials and methods

## 2.1 AD-MSC isolation

The collection of adipose tissue complied with the guidelines of the Helsinki Declaration, and it was approved by the National Public Health and Medical Officer Service (NPHMOS) and the National Medical Research Council (16821-6/2017/EÜIG, STEM-01/2017), which follows the EU Member States' Directive 2004/23/EC on presumed written consent practice for tissue collection. Abdominal adipose tissues were removed from patients (Sex:2/3 F/M, Age: 50.2 ± 11.7 years), and the isolation was performed within 1 h after plastic surgery. A detailed description of the AD-MSC isolation protocol can be found in our previous article (Szucs et al., 2023).

## 2.2 Differentiation of adipose-tissue-derived mesenchymal stem cells

The differentiation potential of adipose-tissue-derived mesenchymal stem cells was verified by differentiating into adipocyte, chondrocyte, and osteocyte lines. They were cultured in a 24-well plate, $5 \times 10^4$ cells/well; after 24 h of incubation, the differentiation medium was added. The commercially available Gibco's StemPro® Adipogenesis (A1007001), Osteogenesis (A1007201), and Chondrogenesis (A1007101) Differentiation Kits were applied according to the manufacturer's guidelines (Gibco, Thermo Fisher Scientific, Waltham, MA United States). After 21 days of maintenance, the cells were fixed with 4% methanol-free formaldehyde (37,308, Molar Chemicals, Hungary) for 20 min at RT. Differentiation stages of AD-MSCs were validated using different dyes. For visualization of lipid-laden particles, Nile red staining (19,123, Sigma-Aldrich, Merck KGaA, Darmstadt, Germany) was utilized, and Alizarin red staining (A5533, Sigma-Aldrich, Merck KGaA, Darmstadt, Germany) was applied to show the mineral deposits during osteogenesis. Toluidine blue staining (89640-5G, Sigma-Aldrich, Merck KGaA, Darmstadt, Germany) was wielded to label the chondrogenic mass.

## 2.3 Flow cytometry

The surface antigen expression pattern was characterized by three-color flow cytometry using fluorochrome-conjugated antibodies with isotype-matching controls. For the measurement of the fluorochrome signal, the BD FACSAriaTM Fusion II flow cytometer (BD Biosciences Immunocytometry Systems, Franklin Lakes, NJ, United States) was applied, and data were processed by Flowing Software (Cell Imaging Core, Turku Centre for Biotechnology, Finland).

## 2.4 Treatment of AD-MSC

The applied AD-MSC cells were derived from the abdominal adipose tissue of three different donors. In a T25 $cm^2$ flask, $2.8 \times 10^5$ cells were seeded using the upkeeping cell culture media described above, and the cells were incubated for 24 h. Next, the cell culture media was changed for treatment; cells were treated with (A) LPS [100 ng/mL] (tlrl-peklps, ultrapure, Invivogen, San Diego, CA, United States), (B) TNFα [100 ng/mL] (300-01A, Peprotech, London, United Kingdom), (C) IL-1β [10 ng/mL] (200-01B, Peprotech, London, United Kingdom), (D) IFNγ [10 ng/mL] (300-02, Peprotech, London, United Kingdom) or (E) PolyI:C [25 ng/mL] (tlrl-pic, Invivogen, San Diego, CA, United States). After adding inflammatory agents, the cells were maintained for 24 h under standard conditions (37°C, 5% $CO_2$, untreated cells left as control). Upon 24-h treatment, the cells were collected and processed for RNA isolation.

## 2.5 RNA isolation for RNA-Sequencing

In the context of RNS sequencing, three biological replicates were employed, consistent with the methodology employed in our preceding investigations. The cells were collected, and the pellet was dissolved in 1 mL TRI Reagent® (TR118/200, Genbiotech Argentina, Bueno Aries, Argentina) and kept at −80°C for 24 h. After thawing, 200 µL chloroform (83,627.320, VWR, Radnor, PA, United States) was added to samples, and they were incubated at RT for 10 min

after rigorous mixing. For phase separation, the samples were centrifuged at 13,400 g at 4°C for 20 min. The aqueous phase was measured into clean tubes, and 500 µL 2-propanol (SO-9352-B025, Molar Chemicals, Hungary) was added and mixed thoroughly. After this, the incubation and phase-separation steps were repeated. The supernatants were eliminated, and the pellets were washed with 750 µL 75% EtOH-DEPC. The samples were centrifuged at 7,500 *g* at 4°C for 5 min, then the supernatants were discarded, and the samples were dried at 45°C for 20 min. The pellets were suspended in RNase-free water and incubated at 55°C for 10 min. The concentration was measured using an IMPLEN N50 UV/Vis Nanophotometer (Implen GmbH, Munich, Germany), and RNA samples were stored at −80°C until use.

High-throughput mRNA sequencing analysis was implemented on the Illumina sequencing platform to achieve global transcriptome data. The total RNA sample quality was investigated using the Eukaryotic Total RNA Nano Kit according to the manufacturer's guidelines on Agilent BioAnalyzer. Samples with an RNA integrity number (RIN) value >7 were accepted for the library preparation. RNA-Seq libraries were prepared from total RNA using the Ultra II RNA Sample Prep kit (New England BioLabs) according to the manufacturer's protocol. In short, poly-A RNAs were captured by oligo-dT conjugated magnetic beads, and then mRNAs were eluted and fragmented at 94°C. First-strand cDNA was created by random priming reverse transcription; then, double-stranded cDNA was made in the second-strand synthesis step. After the reparation of ends, A-tailing and adapter ligation took place. The adapter-ligated fragments were amplified in enrichment PCR, and finally, sequencing libraries were produced. Sequencing runs were performed on the Illumina NextSeq 500 instrument, applying single-end 75-cycle sequencing.

## 2.6 Data analysis

Raw RNA-seq reads were fed into a pipeline to quantify reads mapping to each genomic feature. Quality control (QC) steps were built in at each step of the pipeline, and QC was carried out with FastQC and MultiQC. To remove low-quality bases, short reads, and adapters, Trimmomatic was used. We relied on Illumina's "Considerations for RNA Seq read length and coverage" (https://knowledge.illumina.com/library-preparation/rna-library-prep/library-preparation-rna-library-prep-reference_material-list/000001243) to determine if the reads were appropriate for further analysis. The next step consisted of aligning the reads to the human genome (GRCh38) using Bowtie2, whereas samples with an alignment percentage over 90% were accepted. This was followed by read quantification using FeatureCounts, a highly efficient general-purpose read summarization program that counts mapped reads for genomic features such as genes, exons, promoters, gene bodies, genomic bins, and chromosomal locations. The resulting count's table was used for further downstream analysis. For the methods of differential gene expression, PCA analysis, generating the heatmaps of the differentially expressed genes and the pre-selected pathways, and generating volcano plots, see previous article (Szucs et al., 2023). Pathway analysis was conducted using the ViSEAGO package (Brionne et al., 2019). The input for the analysis was a ranked gene list of the differentially expressed genes with $p$-value <0.05 and log2foldchange > |1|. Functional Gene Ontology enrichment was performed with the fgsea package (Korotkevich et al., 2021) using the ViSEAGOrunfgsea command with the "fgseaMultilevel" method (parameters: scoreType = "std", minSize = 5). Enrichment results were merged (Supplementary Table S1), and semantic similarity measures were made using Wang distance measures, which are based on graph topology. The clustering of the enrichment results was based on the Ward D2 method, and the dendrogram was split into 20 categories (Yu et al., 2010). The heatmap showing these results was made with the ComplexHetamap package (Gu et al., 2016).

## 2.7 Quanterix multi-plex ELISA

For the cytokine assay, we used the Quanterix SP-X digital biomarker analyzer (Quanterix). The system detected simultaneously 10 cytokines in a multiplex assay with Simoa Corplex Cytokine Panel 1 10-Plex Kit (REF: 85-0329, Quanterix). The assay was performed according to the manufacturer's protocol. Supernatants were thawed, centrifuged, and 4-times diluted with assay diluent. Calibration standards were prepared freshly and measured in triplicates samples in duplicates. After the measurement, results were analyzed and visualized in GraphPad.

## 2.8 *In vitro* scratch assay

AD-MSC cells from three donors were collected and counted using an EVE automatic cell counter (NanoEntek, Hwaseong, Republic of Korea). The *in vitro* scratch assay measures the cell proliferation and migration. The required $1.5\times10^4$ cells per well seeded in E-Plate WOUND 96 plates (REF: 300,600,970, Agilent/BioTek, Santa Clara, CA, United States) in maintenance media. The cells were cultured for 24 h under standard conditions (37°C, 5% $CO_2$), and then the protocol was separated into two different directions. (I.) Upon 24 h incubation, the scratch was created, and the media was changed immediately to media containing inflammatory agents. It is followed by 48 h of impedance measurement by xCELLigence Real-Time Cell Analyzer (RTCA) device (Agilent/BioTek, Santa Clara, CA, United States). (II.) After 24 h incubation, the media was replaced with media containing inflammatory agents, and the cells were incubated 24 h under standard conditions; then, the scratch was made, and the media was changed immediately to agents-free upkeeping media, followed by 48 h impedance measurement. The scratches were generated using the AccuWound 96 Scratch Tool (Agilent/BioTek, Santa Clara, CA, United States) wound-making device.

## 2.9 RNA isolation and real-time PCR

Upon inflammation-inducing treatments (described above), the Macherey-Nagel NucleoSpin RNA Mini kit (740,955.250, Dueren, Germany) was applied according to the manufacturer's instructions. All work with RNA and cDNA samples was performed in BioSan UVT-B-AR DNA/RNA UV-Cleaner box (Riga, Latvia). After RNA was extracted and their quality and quantity were verified by IMPLEN N50 UV/Vis nanophotometer, the cDNA synthesis was

performed using High-Capacity cDNA Reverse Transcription Kit (4,368,813, Applied Biosystems™, Thermo Fisher Scientific, Waltham, MA, United States) according to the protocol of the manufacturer. Analytik Jena qTOWER$^3$ G Touch Real-Time Thermal Cycler (Jena, Germany) was utilized for reverse transcription.

## 2.10 qPCR

The Xceed qPCR Probe 2x Mix No-ROX kit (NPCR10502L, Institute of Applied Biotechnologies, Prague, Czech Republic) and TaqMan probes (4,331,182, 250 rxns, FAM-MGB, Thermo Fisher Scientific, Waltham, MA, United States) were used for quantitative PCR. Three biological and three technical replicates were applied in all cases, and data were analyzed by $2^{-\Delta\Delta CT}$ method. The protocol was executed according to the manufacturer's instructions.

## 2.11 ELISA

For measurement of cytokine/chemokine levels in cells upon inflammation induction, the Human IL-6 ELISA set (555220), Human IL-8 ELISA set (555244), Human IP-10 ELISA set (550926), and Reagent Set B (550534) were applied from BD OptEIA™ (BD Biosciences, Franklin Lakes, NJ, United States) according to the guidelines of the manufacturer.

## 2.12 Cytotoxic effect of inflammatory agents on AD-MSCs

To measure the cytotoxicity of the given treatment, the Cytotoxicity Detection Kit (LDH) (REF: 11644793001, Roche, Basel, Switzerland) was applied according to the manufacturer's instructions. Cell supernatants were collected upon 24 h of inflammation induction (described above), and the colorimetric absorbance measurement was executed by Synergy HTX multiplate reader (Agilent/BioTek, Santa Clara, CA, United States) on 490 nm, reference wavelength was 620 nm.

## 2.13 Cell proliferation and metabolism

Effects on proliferation were measured with BrdU Cell Proliferation ELISA Kit (Ref: 11647229001, Roche, Basel, Switzerland). The thymidine analog 5-bromo-2′-deoxyuridine (BrdU) is incorporated into the DNA, thus allowing the determination of the inhibitory or stimulatory effect on the proliferation of the activator molecules. $1{,}5 \times 10^4$ cells per well were seeded into a 96-well plate. The inflammatory environment was simulated with the materials and concentrations mentioned above. The treatment lasted 24 h, and the assays were performed according to the manufacturer's protocol. Measurement was performed on Synergy HTX multiplate reader (Agilent/BioTek, Santa Clara, CA, United States) at 550 nm, with reference at 650 nm for MTT assay, on 450 nm, with reference at 690 nm.

Changes in metabolism due to an inflammatory environment were examined by Cell Proliferation Kit (MTT) (Ref: 11465007001, Roche, Basel, Switzerland) according to the manufacturer's guidelines. The bioreduction of tetrazolium salt to formazan gives information about cellular metabolism and viability. $1.5 \times 10^4$ cells per well were seeded into a 96-well plate, then the cells were incubated for 24 h under standard conditions (37°C, 5% $CO_2$). Next, the 24 h induction of inflammation was taken place (described above), and the colorimetric absorbance measurement was carried out by Synergy HTX multiplate reader (Agilent/BioTek, Santa Clara, CA, United States) on 550 nm, reference wavelength was 650 nm.

# 3 Results

## 3.1 Overall transcriptomic profile of treated cells

The Venn diagrams illustrate the extensive impact of the treatments on gene expression, revealing both upregulation and downregulation of numerous genes, along with significant intersections (Figure 1A). Specifically, the treatments exhibited downregulation of genes as follows: LPS (104 genes), TNF-α (87 genes), IL-1β (50 genes), IFN-γ (56 genes), and PolyI:C (83 genes), with a collective influence on 25 shared genes. Conversely, the treatments led to the upregulation of multiple genes: LPS (14 genes), TNF-α (34 genes), IL-1β (26 genes), IFN-γ (38 genes), and PolyI:C (14 genes), with a common effect observed in 109 genes. These findings underscore the intricate and multifaceted impact of the treatments on the transcriptomic profile, revealing both shared and unique regulatory responses across the treated conditions. The Volcano plot illustrates extensive alterations in gene expression induced by the treatments, encompassing up and downregulation of genes' expression (Figure 1B). Notably, among the top 10 most significantly altered genes, a majority exhibition.

## 3.2 ViSEAGO and clustered pathways

The heatmap generated through ViSEAGO analysis delineates treatments into two primary clusters, with PolyI:C, TNF-α, and IFN-γ forming one cluster and IL-1β and LPS constituting the other (Figure 2A). There is a difference between the two groups in defense and immune response, signal transduction, chemotaxis, cellular response to chemical stimulus, biological regulation, and T-cell activation. They have common effects on organelle organization, mitotic cell cycle, primary metabolic process, DNA repair, system development, ion transmembrane transport, lipid transport, cellular process, meiotic cell cycle, and cell cycle regulation.

The treatments exert distinct effects on multiple pathways: LPS impacts two pathways, TNFα influences eight pathways, IL-1β affects one pathway, IFN-γ modulates three pathways, and PolyI:C impacts five pathways (Figure 2B). This differential influence on various molecular pathways underscores the complexity of the treatments' interactions with cellular processes. The treatments

10.3389/fcell.2024.1367242

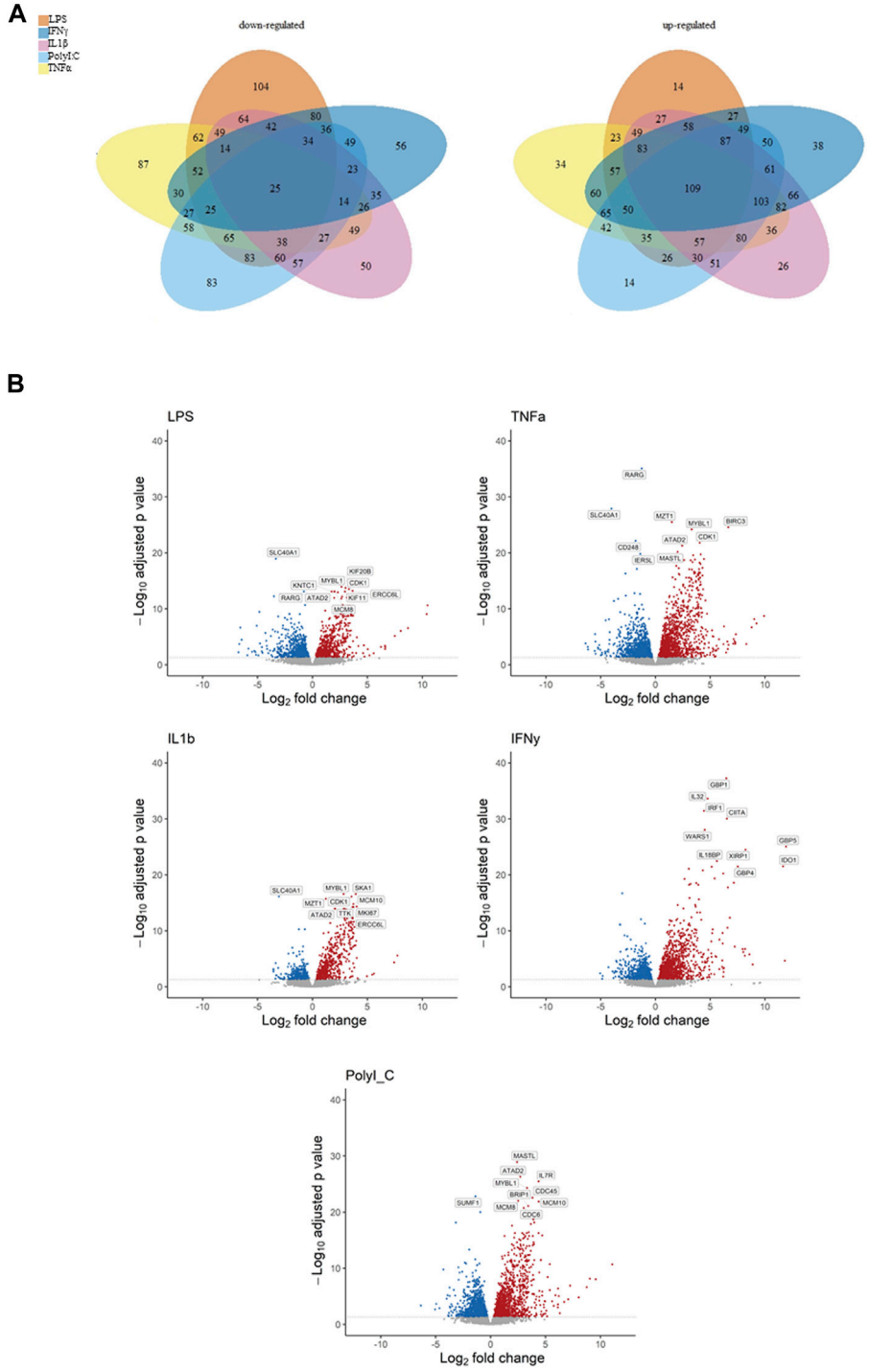


FIGURE 1
Representation of down- and upregulated DEGs after pro-inflammatory treatment compared to the control condition, **(A)** Venn diagrams illustrating overlapping gene numbers between the treatments, and Volcano plots **(B)** depicting the most significantly altered genes, where p adjusted < 0.05 are shown in red, significantly downregulated genes p adjusted < 0.05 are shown in blue.

also elicit shared alterations in multiple pathways. Specifically, LPS and TNFα affect four common pathways, while IFNγ and PolyI:C induce changes in three overlapping pathways. Additionally, LPS and IFN-γ influence one common pathway, as do LPS and PolyI:C, and TNFα and PolyI:C. Notably, the combined treatment of LPS, TNFα, and PolyI:C results in concurrent modifications in three pathways, whereas the combination of LPS, TNFα, and IL-1β influences one shared pathway. Furthermore, TNFα, IFNγ, and PolyI:C collectively impact one common pathway. Lastly, the joint influence of LPS, TNFα, IL-1β, and PolyI:C is reflected in

10.3389/fcell.2024.1367242

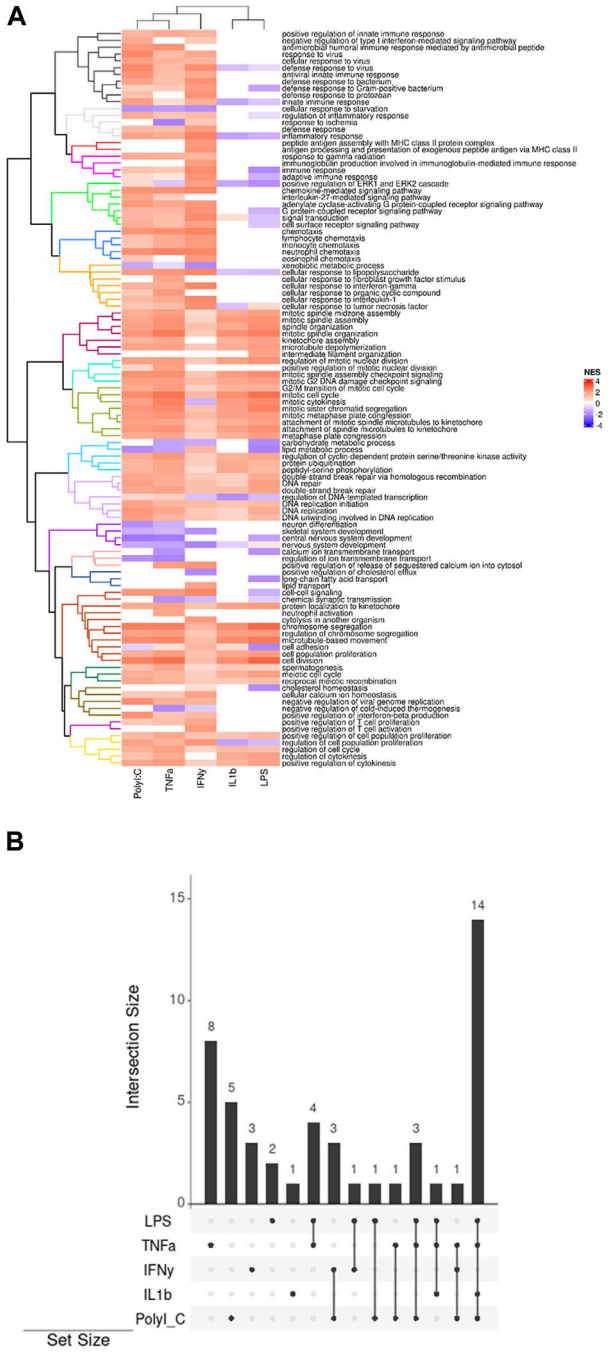


FIGURE 2
**(A)** Display of clustered pathways heatmap generated by ViSEAGO. The different colors represent uniform groups, including several pathways and biological processes **(B)** The UpSet plots visually represent the gene intersections within various pathways in the AD-MSC following treatment with pro-inflammatory agents. The vertical bars highlight the number of shared genes, denoting the intersection size, among specific pathway sets, indicated by bottom-filled connected circles.

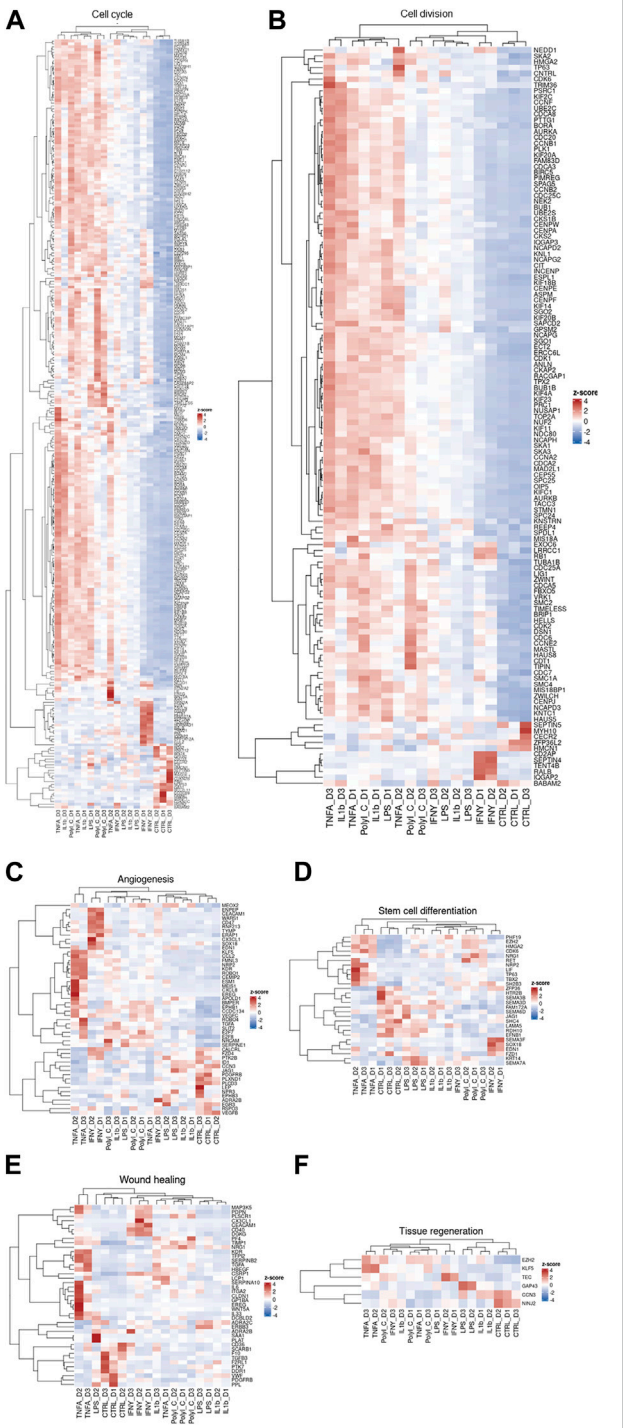


FIGURE 3
Clustered heatmaps depicting various processes: **(A)** Cell cycle, **(B)** Cell division, **(C)** Angiogenesis, **(D)** Stem cell differentiation, **(E)** Wound healing, and **(F)** Tissue regeneration. These biological processes are crucial for AD-MSC tissue regeneration, healing, and immunomodulation of the microenvironment.

alterations in 14 pathways, emphasizing the intricate interplay of these treatments in affecting cellular processes.

Our transcriptomic dataset has been visualized through a series of heatmaps, categorized based on predefined pathways (Figure 3). Across all heatmaps, the distinction is evident between the transcriptional patterns of treated and control samples, albeit with notable inter-donor variations. This dataset is an illustrative exemplar of the diverse cellular responses induced by treatments, each reflecting the unique molecular landscape of individual patients. Notably, genes

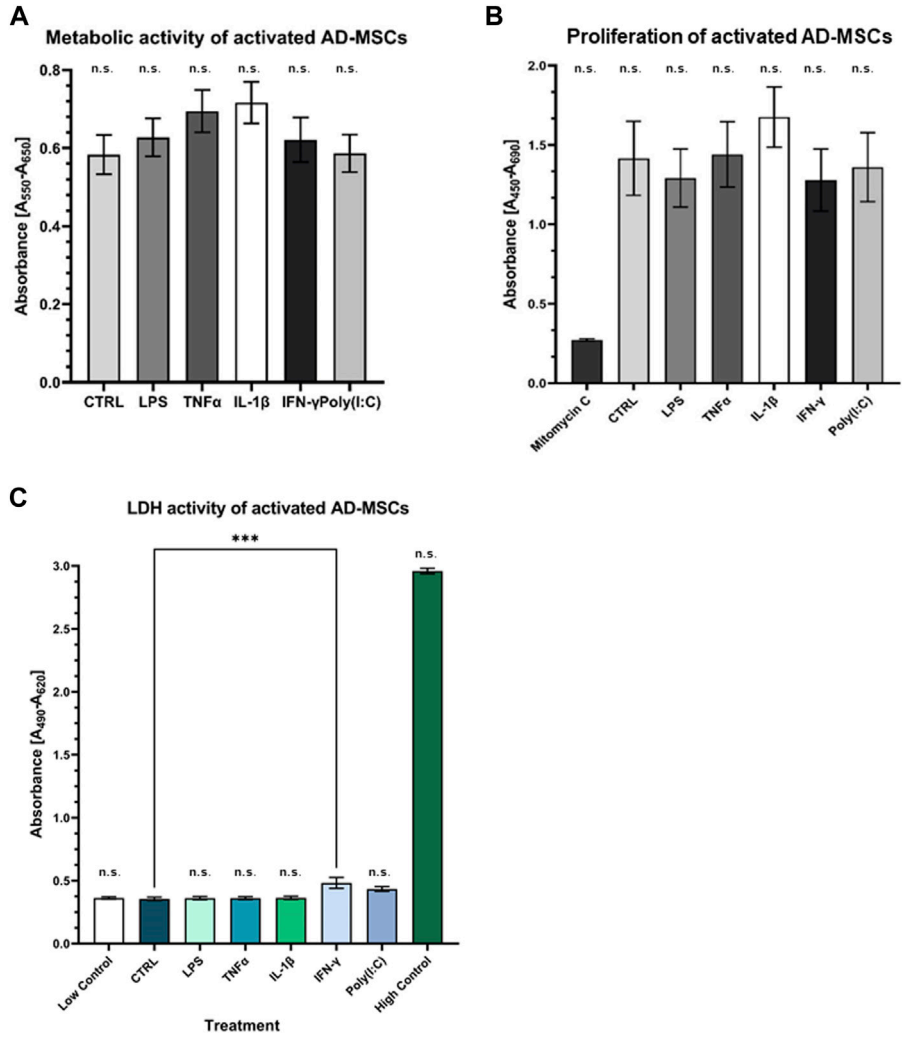


FIGURE 4
Assessment of metabolic and proliferation activity of treated AD-MSCs **(A)** The metabolic activity of the treated cells was detected by MTT assay. There is no significant change compared to the control. **(B)** BrdU incorporation indicated the proliferative capacity of cells, which was not significantly affected by treatments. **(C)** Cell viability was not affected by any treatments, indicating that our results were not caused by dead cells. (N = 3 donors, each measurement performed in triplicates).

modulated by TNF-α and IFN-γ in the angiogenesis pathway heatmap tend to cluster together. In the context of cell cycle and cell division pathways, TNF-α, IL-1β, and PolyI:C appear to share analogous effects, whereas IFN-γ delineates a distinct grouping. Regarding stem cell differentiation, the impact of LPS and IL-1β aligns closely with that of the control group. TNF-α exhibits similarity with PolyI:C and IFN-γ manifests as an independent cluster.

Furthermore, the heatmap of tissue regeneration reveals that LPS and IL-1β treatments display comparable profiles to the control group, whereas TNF-α delineates discrete gene clusters. LPS and IL-1β treatments diverge from the control group in wound healing pathways, whereas TNF-α, IFN-γ, and PolyI:C treatments segregate into distinct clusters. These observations highlight the nuanced and pathway-specific effects of the treatments on cellular responses, underlining the complexity of treatment outcomes across diverse biological contexts.

## 3.3 Perform cellular characterization and evaluate the safety of treatment

Primary cell cultures were maintained, and their differentiation potential was assessed. Remarkably, these cells demonstrated tri-lineage differentiation capacity, encompassing adipogenic, chondrogenic, and osteogenic lineages (Supplementary Figure S1). This differentiation was verified through microscopic examination of distinct cell type-specific features, reinforcing the suitability of these cultures as a valuable model for our study. The FACS analysis revealed crucial cell characteristics and verified their mesenchymal origin, bolstering their identity and facilitating further exploration of their unique traits and functions in our study [data not shown; see previous article by (12)]. Cytotoxicity and viability tests showed that the cells did not receive a cytotoxic amount of inflammatory agents, and their metabolism and viability were preserved during treatment, underscoring the safety and potential

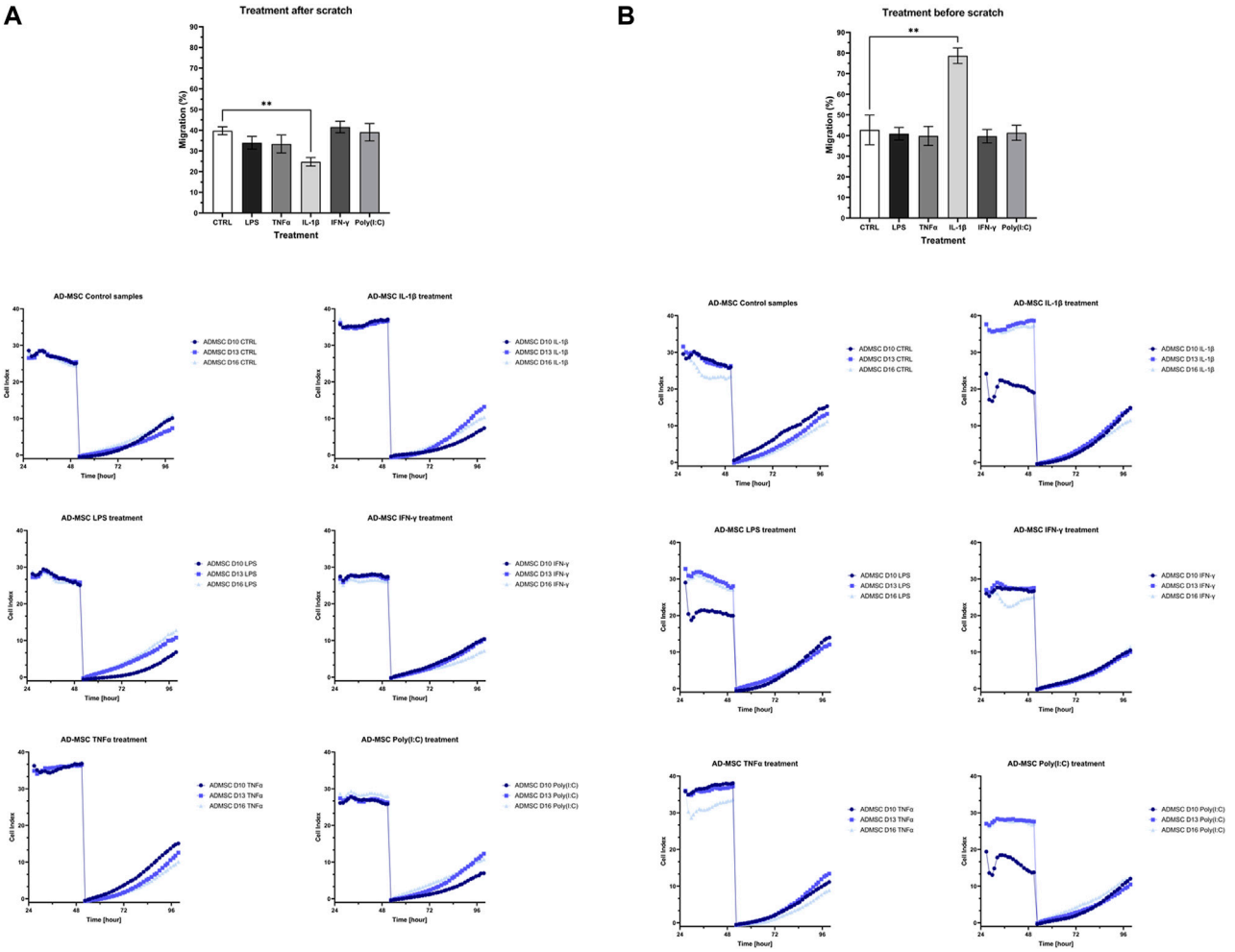


FIGURE 5
The bar charts and diagrams show the results of the cell proliferation and migration studies with two visualized layouts. The impedance-based method measured the re-population of the direct wound size. **(A)** "treatment before scratch", which is intended to model that the wound is initially in an inflammatory environment, and **(B)** "treatment after scratch", which is designed to model an infected wound. Both of these cases have a clinical manifestation in chronic non-healing wounds and, e.g., infectious wounds associated with diabetes.

therapeutic relevance of the administered agents in cellular health and function (Figure 4).

## 3.4 Influence of treatments on the cell proliferation and migration

The cell proliferation and migration assay utilized impedance measurements to assess the rate of cell migration during wound closure in treated samples relative to a control group after the injury. Two experimental conditions were examined: one where the wound was introduced before treatment (Figure 5A) and another where treatment preceded wound induction (Figure 5B). In both cases, distinct variations in wound closure dynamics were evident between cells subjected to IL-1β treatment and the control group. Specifically, when applied before wound initiation, IL-1β significantly hastened wound closure, whereas its post-wound application decelerated the process.

## 3.5 Gene and protein expression analysis by qPCR and ELISA

The quantitative polymerase chain reaction (qPCR) analysis results unveiled distinct gene expression patterns in response to various treatments (Figure 6). Notably, CXCL-8 demonstrated a robust upregulation in response to all treatments, with a marked increase following exposure to LPS, TNFα, and IL-1β. Conversely, both NAGS and STAT6 exhibited consistent downregulation across all treatment conditions. Interestingly, while TNFα treatment had no appreciable effect on IL-6 expression, the other administered treatments induced a significant reduction in IL-6 mRNA levels.

Furthermore, CXCL-10 displayed an elevated expression profile in response to TNFα treatment and a modest increase following IFNγ exposure. Conversely, ASGR1 exhibited a notable decrease in expression levels following treatment with LPS, TNFα, and IFNγ, while it demonstrated an elevation in response to IL1β and PolyI:C. In the case of ICAM1, its expression slightly increased following

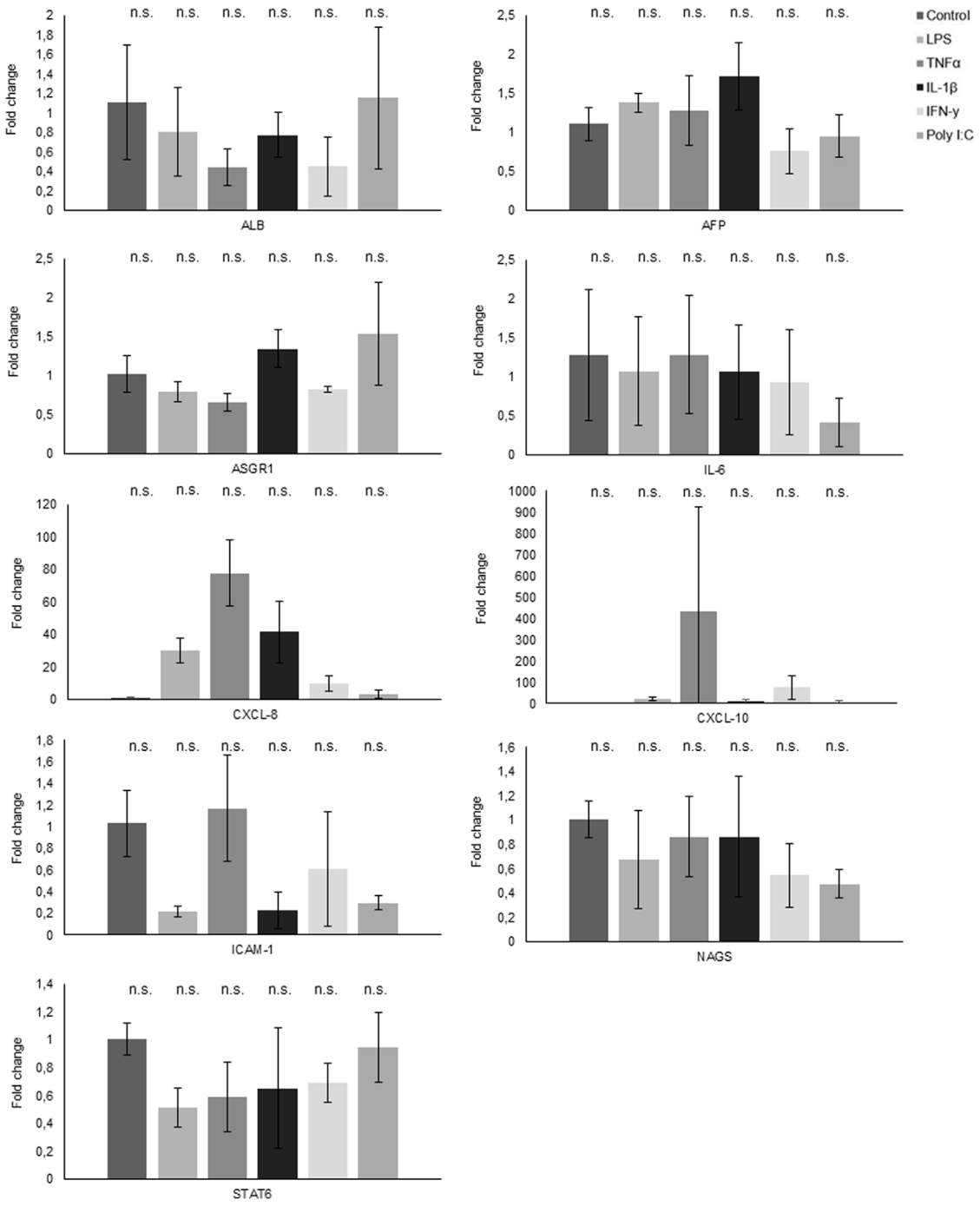


FIGURE 6
Gene expression analysis through qPCR reveals the fold change in various genes following treatments.

TNFα treatment, but conversely, it experienced a decrease when subjected to all other treatments.

At the protein level, noteworthy distinctions emerge (Figure 7A). Specifically, the treatments with LPS, TNFα, and IL-1β resulted in a notable upsurge in IL-6 levels, whereas IFNγ and Poly I:C treatments led to a discernible reduction in IL-6 protein concentrations. CXCL-8 exhibited an augmentation in response to LPS and TNFα treatments, contrasted by a diminishment observed following the remaining treatment regimens. Interestingly, CXCL-10 demonstrated an elevation in protein levels across all administered treatments, with particularly significant peaks observed following TNFα and IFNγ treatments. The multiplex ELISA findings reveal notable changes in the IFNγ, IL-5, IL-12p70, and IL-22 levels. Specifically, IL-5, IL-12p70, and IL-22 significantly increased following IL-1β treatment (Figure 7B).

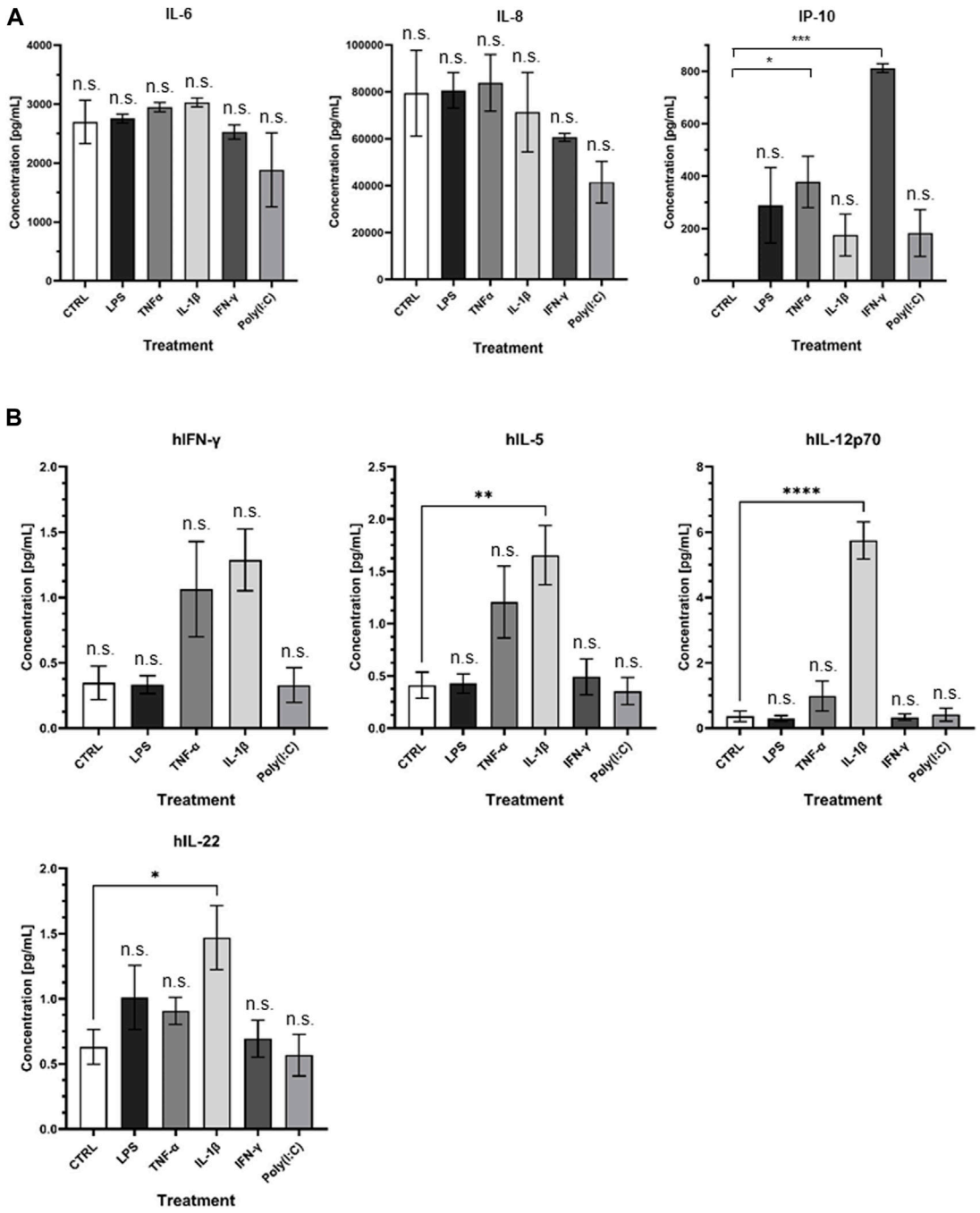


FIGURE 7
**(A)** Visual representation of ELISA results and **(B)** presentation of Quanterix findings.

## 4 Discussion

Mesenchymal stem cells (MSCs) are crucial in various immunological processes. They actively regulate their microenvironment and influence the differentiation of different cells, including immune cells, by producing cytokines and growth factors (Saparov et al., 2016). In their basal state, MSCs exhibit antiangiogenic properties. The immunomodulatory effectiveness of MSCs is contingent upon the nature and intensity of inflammatory signals received, such as interferon-γ (IFN-γ), tumor necrosis factor-α (TNF-α), and Toll-like receptor (TLR)-mediated activation. Under specific inflammatory stimuli (IFN-γ, TNF-α, TLR-mediated activation), MSCs transform, becoming antiapoptotic, proangiogenic, and immunosuppressive (Meisel et al., 2004; Krampera et al., 2006; Ghannam et al., 2010; Saparov et al., 2016; Vereb et al., 2020). They contribute to inflammation reduction through the secretion of factors like interleukin-6 (IL-6), indoleamine 2,3-dioxygenase (IDO), HLA G5 (human leukocyte antigen G5), interleukin-10 (IL-10), transforming growth factor beta-1 (TGFb1), hepatocyte growth factor (HGF), HOX-1, IL-1Ra

(IL-1 receptor antagonist), prostaglandin E2 (PGE2), and through cell-cell contact (Bartholomew et al., 2002; Meisel et al., 2004; Aggarwal SP and Pittenger, 2005; Saparov et al., 2016). The immunomodulatory potential of MSCs thus hinges on their response to specific inflammatory cues (Renner et al., 2009; Li et al., 2012). Mesenchymal stem cells (MSCs) actively produce a diverse array of chemokines and adhesion molecules, including ligands for CXC chemokine receptor 3 (CXCR3), C-C chemokine receptor type 5 (CCR5), intercellular adhesion molecule 1 (ICAM-1/CD54), and vascular cell adhesion molecule 1 (VCAM-1) (Vereb et al., 2016; Vereb et al., 2020). The pronounced expression of CXCR3 in effector and memory T cells underscores the pivotal significance of MSC-generated chemokines, particularly CXCL9 (chemokine ligand 9), CXCL10 (chemokine ligand 10), and CXCL11 (chemokine ligand 11). These chemokines play a critical role in orchestrating the recruitment of lymphocytes to the site of tissue damage, thereby ensuring optimal functionality of immunosuppression (Crop et al., 2010; Wang et al., 2014; Saparov et al., 2016). The ability of MSCs to influence the immune system and the effects are intricately tied to variables such as the tissue origin (whether from fat, bone marrow, *etc.*), the specific microenvironment they inhabit, and the nature of their interactions with other cellular partners. The role of adipose-derived mesenchymal stem cells (AD-MSCs) in wound healing is a subject of considerable significance. These cells exhibit a wide array of regenerative, anti-apoptotic, antifibrotic, anti-oxidative, and immunomodulatory properties, rendering them invaluable for therapeutic applications, particularly in wound healing (Neuss et al., 2004; Fu et al., 2009; DelaRosa and Lombardo, 2010; Trayhurn et al., 2011; Shohara et al., 2012; Konno et al., 2013; Cao et al., 2015; Ti et al., 2015; Furuta et al., 2016; Carelli et al., 2018; Feldbrin et al., 2018; Mushahary et al., 2018; Ridiandries et al., 2018; Sahu et al., 2019; Al-Ghadban and Bunnell, 2020; Kuca-Warnawin et al., 2020; Kurte et al., 2020; Munir et al., 2020; Xiao et al., 2020; Bunnell BA, 2021; Krampera and Le Blanc, 2021; Nieto-Nicolau et al., 2021; Krawczenko and Klimczak, 2022; Skibber et al., 2022; Wiese et al., 2022; Cheng et al., 2023; Huerta et al., 2023).

Moreover, the secretome of AD-MSCs, the array of substy release, has positively affected various diseases. Research has focused on the impact of priming or pre-conditioning AD-MSCs with pro-inflammatory cytokines, such as interferon-gamma (IFN-γ) and tumor necrosis factor-alpha (TNFα), on their immunomodulatory capabilities. This treatment enhances their potential to suppress the immune response by upregulating specific genes associated with signaling proteins, immune molecules, and cell surface markers (Heo et al., 2011; Konno et al., 2013; Cao et al., 2015; Saparov et al., 2016; Chinnadurai et al., 2017; Carvalho et al., 2019; Al-Ghadban and Bunnell, 2020; Bunnell BA, 2021). However, the precise balance between immunosuppressive and pro-inflammatory effects remains an area of ongoing exploration. Mesenchymal stem cell (MSC) therapy has experienced substantial growth over the last two decades, with over 1,000 trials conducted.

Nevertheless, only a tiny fraction has progressed to industry-sponsored phase III trials, primarily due to the relative novelty of this field. Challenges persist in optimizing cell quantity delivery methods and comprehending the importance of MSC localization at the injury site. Licensing AD-MSCs with IFN-γ is suggested to enhance their immunomodulatory potential, with clinical experiences showing potential for treating immune-related diseases (Waterman et al., 2010; Heo et al., 2011; Konno et al., 2013; Cao et al., 2015; Saparov et al., 2016; Chinnadurai et al., 2017; Hu and Li, 2018; Carvalho et al., 2019; Al-Ghadban and Bunnell, 2020; Bunnell BA, 2021; Lu and Qiao, 2021). Immunoglobulin kappa chains in various cancer cell types have also garnered attention in recent studies (Chen et al., 2009; Zhao et al., 2021). These investigations underscore the significance of key proteins like RAG1, RAG2, and AID, which are pivotal for immunoglobulin production and rearrangement (Zhao et al., 2021). Although emerging evidence suggests a potential role of immunoglobulin expression in promoting cancer cell growth, the functional consequences remain unclear. Given the vital roles of immunoglobulins in human physiology and disease management, in-depth research is crucial to uncover their multifaceted functions, particularly in cancer etiology and therapeutic strategies. In conclusion, these studies collectively emphasize the importance of AD-MSCs in wound healing, their licensing with pro-inflammatory cytokines, and the intriguing role of immunoglobulins in various cellular contexts, particularly in cancer. Ongoing research holds promise for further advancements in regenerative medicine and cancer biology (Chen et al., 2009; Zhao et al., 2021).

The immense potential of adipose-derived mesenchymal stem cells (AD-MSCs) in regenerative medicine is undeniable. Their regenerative, anti-apoptotic, antifibrotic, anti-oxidative, and immunomodulatory qualities offer substantial promise for clinical therapy (DelaRosa and Lombardo, 2010; Konno et al., 2013; Cao et al., 2015; Carelli et al., 2018; Qi et al., 2018; Pittenger et al., 2019; Song et al., 2020; Bunnell BA, 2021; Szucs et al., 2023). Additionally, our evolving comprehension of AD-MSCs has unveiled the dynamic role played by their secretome and the substances they release (Trayhurn et al., 2011). This secretome can be customized through specific pretreatments, enhancing its therapeutic adaptability. Investigations into the paracrine effects of AD-MSCs have yielded compelling findings. For instance, pre-conditioning AD-MSCs with tumor necrosis factor-alpha (TNFα) and applying their secretome to cutaneous wounds in rats has remarkably expedited wound healing, proliferation, angiogenesis, epithelialization, and macrophage recruitment (Heo et al., 2011; Saparov et al., 2016). Notably, pro-inflammatory cytokines like IL-6 and IL-8 have been recognized as contributors to this acceleration (Saparov et al., 2016; Heo et al., 2011) Similarly, AD-MSCs subjected to pre-treatment with lipopolysaccharides (LPS) have demonstrated their potential in promoting wound healing and angiogenesis, coupled with an increased release of growth factors associated with tissue regeneration and immune responses (Wang et al., 2022). AD-MSCs have showcased their immunomodulatory capabilities in a mouse model of atopic dermatitis, effectively suppressing B-lymphocyte proliferation and maturation (Shin et al., 2017). These promising findings underscore the diverse applications of AD-MSCs and their secretome in regenerative medicine. The varying roles of cytokines, the impact of factors such as MMP-9 and MMP-8 on wound healing, and identifying potential therapeutic targets collectively enrich the landscape of AD-MSC therapy. The intricate interplay of these elements highlights their critical significance in advancing regenerative medicine (Chang and Nguyen, 2021). Croitoru-Lamoury and others explored how the

proinflammatory cytokines TNF-α and IFN-γ influence the gene expression of chemokines and their receptors in human mesenchymal stem cells (HuMSCs). HuMSCs were exposed to TNF-α, IFN-γ, or a combination of both for up to 72 h, and gene expression was examined using RT-PCR at various time points (Croitoru-Lamoury et al., 2007). The findings revealed that TNF-α increased the expression of the receptor CXCR4, while both TNF-α and IFN-γ boosted the gene transcription of multiple chemokines (CCL2/MCP-1, CCL3/MIP-1α, CCL4/MIP-1β, CCL5/RANTES, CXCL8/IL-8, CXCL10/IP-10) and cytokines (IL-1β and IL-6). IFN-γ specifically heightened the gene expression of specific chemokines (CXCL9/MIG, CX3CL1/fractalkine) and IL-6. Notably, the combined treatment of TNF-α and IFN-γ synergistically increased the expression of several genes, including CCL3/MIP-1α, CCL4/MIP-1β, CCL5/RANTES, CXCL9/MIG, CXCL10/IP-10, CX3CL1/fractalkine, IL-1β, and IL-6 (Croitoru-Lamoury et al., 2007). One of the most important anti-inflammatory cytokines is IL-10. MSCs can act on macrophages or dendritic cells to produce IL-10, but whether or not MSCs can secret IL-10 by themselves is still controversial (Yagi et al., 2010).

In a very comprehensive and detailed comparative study, it has been demonstrated that MSC from various tissues secreted MCP-1, IL-8, VEGF, IL-6, IL-5, IFNγ, and MIP-1β influenced by the age of the culture (Croitoru-Lamoury et al., 2007). In the studies, MSCs from different tissues were tested without treatment, where it was found that fat-derived MSCs secrete the highest levels of IL-6. The pro-inflammatory cytokines TNF-α, IL-2, IL-9, and IL-17, expressed in the supernatant, were associated with myogenic differentiation (Croitoru-Lamoury et al., 2007). The collaborative application of IFN-γ and TNF-α significantly amplifies MSCs' ability to produce factor H, a pivotal molecule crucial for impeding complement activation (Tu et al., 2010; Saparov et al., 2016). Similar to our result, IL-1b induced TNF-α, IL-6, IL-8, IL-23A, CCL5, CCL20, CXCL10, CXCL11 cytokine secretion along with increased expression of adhesion molecules (VCAM-1, ICAM-1, ICAM-4) (Saparov et al., 2016). When MSC was subjected to multi-cytokine priming involving TNF-α, IL-1β, and IFN-γ, the presence of IL-1β further amplified the well-established immunoregulatory activity initiated by TNF-α/IFN-γ (Hackel et al., 2021). Prolonged treatment of TNFa resulted in similar gene expression and cytokine secretion (IL-4, IL-8, IL6, and IL10 to our findings (Lee et al., 2010; Ting et al., 2021).

However, how these treatments affect the real wound healing ability was not tested. TLR receptors are one of the most ancient components of defense against pathogens and innate immunity. Tests with LPS (TLR4) and PolyI:C (TLR3) showed that MSC lifted their IL-6 and IL-8 expression (Fuenzalida et al., 2016; Park et al., 2016; Vereb et al., 2016; Vereb et al., 2020; Szucs et al., 2023), and the TLR3 manifest a more potent immunosuppressive phenotype (Fuenzalida et al., 2016; Park et al., 2016).

In summary, AD-MSCs have emerged as formidable allies in pursuing effective treatments for non-healing, chronic, and inflamed wounds, even in prolonged inflammation. While these diverse treatments may activate distinct pathways, their cumulative potential in fostering tissue healing, remodeling the extracellular matrix, and promoting regeneration within clinical settings is undeniably remarkable (Hu and Li, 2018; Naji et al., 2019; Pittenger et al., 2019; Mazini et al., 2020; Szucs et al., 2023).

## Data availability statement

The original contributions presented in the study are included in the article/Supplementary Material, further inquiries can be directed to the corresponding author.

## Ethics statement

The studies involving humans were approved by National Public Health and Medical Officer Service (NPHMOS) and the National Medical Research Council (16821-6/2017/EÜIG, STEM-01/2017. The studies were conducted in accordance with the local legislation and institutional requirements. The participants provided their written informed consent to participate in this study.

## Author contributions

DS: Data curation, Investigation, Methodology, Visualization, Writing–original draft, Writing–review and editing. TM: Data curation, Investigation, Methodology, Visualization, Writing–original draft. VM: Data curation, Formal Analysis, Investigation, Methodology, Software, Validation, Visualization, Writing–original draft, Writing–review and editing. ZP: Writing–original draft, Data curation. SP: Investigation, Methodology, Resources, Writing–original draft, Writing–review and editing. LK: Funding acquisition, Visualization, Writing–review and editing. ZV: Conceptualization, Funding acquisition, Investigation, Methodology, Project administration, Resources, Supervision, Writing–original draft, Writing–review and editing.

## Funding

The author(s) declare that financial support was received for the research, authorship, and/or publication of this article. This work was supported by the National Research, Development, and Innovation Office (NKFI PD 132570 to ZV) and GINOP_PLUSZ-2.1.1-21-2022-00043 project (co-financed by the European Union and the European Regional Development Fund) ZV was supported by the Bolyai János Postdoctoral Fellowship (BO/00190/20/5). Project no. TKP2021-EGA-28 has been implemented with support from the Ministry of Innovation and Technology of Hungary from the National Research, Development and Innovation Fund, financed under the TKP2021-EGA funding scheme. LK has received funding from the EU's Horizon 2020 research and innovation program under grant agreement No. 739593. The Biobank Competence Centre of the Life Sciences Cluster of the Centre of Excellence for Interdisciplinary Research, Development, and Innovation of the University of Szeged supported the research. SP was supported by Project no. TKP2021-NKTA-34 has been implemented with the support provided by the Ministry of Culture and Innovation of Hungary from the National Research, Development and Innovation Fund, financed under the TKP2021-NKTA funding scheme.

## Acknowledgments

We would like to express our very great appreciation to Katalin Boldog for her administrative and technical support during our research work.

## Conflict of interest

The authors declare that the research was conducted in the absence of any commercial or financial relationships that could be construed as a potential conflict of interest.

## Publisher's note

All claims expressed in this article are solely those of the authors and do not necessarily represent those of their affiliated organizations, or those of the publisher, the editors and the reviewers. Any product that may be evaluated in this article, or claim that may be made by its manufacturer, is not guaranteed or endorsed by the publisher.

## Supplementary material

The Supplementary Material for this article can be found online at: https://www.frontiersin.org/articles/10.3389/fcell.2024.1367242/full#supplementary-material

**SUPPLEMENTARY FIGURE S1**
Successful tri-lineage differentiation of AD-MSCs is demonstrated, with microscopic images illustrating the characteristic features of each tissue type.

**SUPPLEMENTARY TABLE S1**
The result of Functional Gene Ontology enrichment performed by ViSEAGO.

## References

Aggarwal Sp, M. F., and Pittenger, M. F. (2005). Human mesenchymal stem cells modulate allogeneic immune cell responses. *Blood* 1054, 1815–1822. doi:10.1182/blood-2004-04-1559

Al-Ghadban, S., and Bunnell, B. A. (2020). Adipose tissue-derived stem cells: immunomodulatory effects and therapeutic potential. *Physiology* 352, 125–133. doi:10.1152/physiol.00021.2019

Anton, K., Banerjee, D., and Glod, J. (2012). Macrophage-associated mesenchymal stem cells assume an activated, migratory, pro-inflammatory phenotype with increased IL-6 and CXCL10 secretion. *Plos One* 74, e35036. doi:10.1371/journal.pone.0035036

Bartholomew, A., Sturgeon, C., Siatskas, M., Ferrer, K., McIntosh, K., Patil, S., et al. (2002). Mesenchymal stem cells suppress lymphocyte proliferation *in vitro* and prolong skin graft survival *in vivo*. *Exp. Hematol.* 301, 42–48. doi:10.1016/s0301-472x(01)00769-x

Brembilla, N. C., Vuagnat, H., Boehncke, W. H., Krause, K. H., and Preynat-Seauve, O. (2023). Adipose-derived stromal cells for chronic wounds: scientific evidence and roadmap toward clinical practice. *Stem Cell Transl. Med.* 121, 17–25. doi:10.1093/stcltm/szac081

Brionne, A., Juanchich, A., and Hennequet-Antier, C. (2019). ViSEAGO: a Bioconductor package for clustering biological functions using Gene Ontology and semantic similarity. *BioData Min.* 12, 16. doi:10.1186/s13040-019-0204-1

Bunnell Ba, (2021). Adipose tissue-derived mesenchymal stem cells. *Cells* 10, 3433. doi:10.3390/cells10123433

Cao, W., Cao, K., Cao, J., Wang, Y., and Shi, Y. (2015). Mesenchymal stem cells and adaptive immune responses. *Immunol. Lett.* 1682, 147–153. doi:10.1016/j.imlet.2015.06.003

Carelli, S., Colli, M., Vinci, V., Caviggioli, F., Klinger, M., and Gorio, A. (2018). Mechanical activation of adipose tissue and derived mesenchymal stem cells: novel anti-inflammatory properties. *Int. J. Mol. Sci.* 191, 267. doi:10.3390/ijms19010267

Carvalho, A. E. S., Sousa, M. R. R., Alencar-Silva, T., Carvalho, J. L., and Saldanha-Araujo, F. (2019). Mesenchymal stem cells immunomodulation: the road to IFN-gamma licensing and the path ahead. *Cytokine and growth factor Rev.* 47, 32–42. doi:10.1016/j.cytogfr.2019.05.006

Chang, M., and Nguyen, T. T. (2021). Strategy for treatment of infected diabetic foot ulcers. *Accounts Chem. Res.* 545, 1080–1093. doi:10.1021/acs.accounts.0c00864

Chen, Z., Qiu, X., and Gu, J. (2009). Immunoglobulin expression in non-lymphoid lineage and neoplastic cells. *Am. J. pathology* 1744, 1139–1148. doi:10.2353/ajpath.2009.080879

Cheng, H. Y., Anggelia, M. R., Lin, C. H., and Wei, F. C. (2023). Toward transplantation tolerance with adipose tissue-derived therapeutics. *Front. Immunol.* 14, 1111813. doi:10.3389/fimmu.2023.1111813

Chinnadurai, R., Rajan, D., Ng, S., McCullough, K., Arafat, D., Waller, E. K., et al. (2017). Immune dysfunctionality of replicative senescent mesenchymal stromal cells is corrected by IFNγ priming. *Blood Adv.* 111, 628–643. doi:10.1182/bloodadvances.2017006205

Croitoru-Lamoury, J., Lamoury, F. M., Zaunders, J. J., Veas, L. A., and Brew, B. J. (2007). Human mesenchymal stem cells constitutively express chemokines and chemokine receptors that can be upregulated by cytokines, IFN-beta, and Copaxone. *J. Interferon Cytokine Res.* 271, 53–64. doi:10.1089/jir.2006.0037

Crop, M. J. B., Korevaar, C. C., Ijzermans, S. S., Pescatori, J. N., et al. (2010). Inflammatory conditions affect gene expression and function of human adipose tissue-derived mesenchymal stem cells. *Clin. Exp. Immunol.* 1623, 474–486. doi:10.1111/j.1365-2249.2010.04256.x

DelaRosa, O., and Lombardo, E. (2010). Modulation of adult mesenchymal stem cells activity by toll-like receptors: implications on therapeutic potential. *Mediat. Inflamm.* 2010, 865601. doi:10.1155/2010/865601

Feldbrin, Z., Omelchenko, E., Lipkin, A., and Shargorodsky, M. (2018). Osteopontin levels in plasma, muscles, and bone in patient with non-healing diabetic foot ulcers: a new player in wound healing process? *J. Diabetes Complicat* 328, 795–798. doi:10.1016/j.jdiacomp.2018.05.009

François, M., Romieu-Mourez, R., Li, M. Y., and Galipeau, J. (2012). Human MSC suppression correlates with cytokine induction of indoleamine 2,3-dioxygenase and bystander M2 macrophage differentiation. *Mol. Ther.* 201, 187–195. doi:10.1038/mt.2011.189

Fu, X., Han, B., Cai, S., Lei, Y., Sun, T., and Sheng, Z. (2009). Migration of bone marrow-derived mesenchymal stem cells induced by tumor necrosis factor-alpha and its possible role in wound healing. *Wound repair Regen.* 172, 185–191. doi:10.1111/j.1524-475X.2009.00454.x

Fuenzalida, P., Kurte, M., Fernandez-O'ryan, C., Ibanez, C., Gauthier-Abeliuk, M., Vega-Letter, A. M., et al. (2016). Toll-like receptor 3 pre-conditioning increases the therapeutic efficacy of umbilical cord mesenchymal stromal cells in a dextran sulfate sodium-induced colitis model. *Cytotherapy* 185, 630–641. doi:10.1016/j.jcyt.2016.02.002

Furuta, T., Miyaki, S., Ishitobi, H., Ogura, T., Kato, Y., Kamei, N., et al. (2016). Mesenchymal stem cell-derived exosomes promote fracture healing in a mouse model. *Stem Cell Transl. Med.* 512, 1620–1630. doi:10.5966/sctm.2015-0285

Ghannam, S., Bouffi, C., Djouad, F., Jorgensen, C., and Noel, D. (2010). Immunosuppression by mesenchymal stem cells: mechanisms and clinical applications. *Stem Cell Res. Ther.* 11, 2. doi:10.1186/scrt2

Gu, Z., Eils, R., and Schlesner, M. (2016). Complex heatmaps reveal patterns and correlations in multidimensional genomic data. *Bioinformatics* 3218, 2847–2849. doi:10.1093/bioinformatics/btw313

Guasti, L., New, S. E., Hadjidemetriou, I., Palmiero, M., and Ferretti, P. (2018). Plasticity of human adipose-derived stem cells - relevance to tissue repair. *Int. J. Dev. Biol.* 62, 431–439. doi:10.1387/ijdb.180074pf

Hackel, A., Aksamit, A., Bruderek, K., Lang, S., and Brandau, S. (2021). TNF-α and IL-1β sensitize human MSC for IFN-γ signaling and enhance neutrophil recruitment. *Eur. J. Immunol.* 512, 319–330. doi:10.1002/eji.201948336

Heo, S. C., Jeon, E. S., Lee, I. H., Kim, H. S., Kim, M. B., and Kim, J. H. (2011). Tumor necrosis factor-alpha-activated human adipose tissue-derived mesenchymal stem cells accelerate cutaneous wound healing through paracrine mechanisms. *J. investigative dermatology* 1317, 1559–1567. doi:10.1038/jid.2011.64

Hu, C., and Li, L. (2018). Preconditioning influences mesenchymal stem cell properties *in vitro* and *in vivo*. *J. Cell. Mol. Med.* 223, 1428–1442. doi:10.1111/jcmm.13492

Huerta, C. T., Voza, F. A., Ortiz, Y. Y., Liu, Z. J., and Velazquez, O. C. (2023). Mesenchymal stem cell-based therapy for non-healing wounds due to chronic limb-threatening ischemia: a review of preclinical and clinical studies. *Front. Cardiovasc. Med.* 10, 1113982. doi:10.3389/fcvm.2023.1113982

Konno, M., Hamabe, A., Hasegawa, S., Ogawa, H., Fukusumi, T., Nishikawa, S., et al. (2013). Adipose-derived mesenchymal stem cells and regenerative medicine. *Dev. Growth Differ.* 553, 309–318. doi:10.1111/dgd.12049

Korotkevich, G., Sukhov, V., Budin, N., Shpak, B., Artyomov, M. N., and Sergushichev, A. (2021). Fast gene set enrichment analysis. *bioRxiv*. doi:10.1101/060012

Krampera, M., Cosmi, L., Angeli, R., Pasini, A., Liotta, F., Andreini, A., et al. (2006). Role for interferon-gamma in the immunomodulatory activity of human bone marrow mesenchymal stem cells. *Stem Cells* 242, 386–398. doi:10.1634/stemcells.2005-0008

Krampera, M., and Le Blanc, K. (2021). Mesenchymal stromal cells: putative microenvironmental modulators become cell therapy. *Cell stem Cell* 2810, 1708–1725. doi:10.1016/j.stem.2021.09.006

Krawczenko, A., and Klimczak, A. (2022). Adipose tissue-derived mesenchymal stem/stromal cells and their contribution to angiogenic processes in tissue regeneration. *Int. J. Mol. Sci.* 23, 2425. doi:10.3390/Ijms23052425

Kuca-Warnawin, E., Janicka, I., Szczesny, P., Olesinska, M., Bonek, K., Gluszko, P., et al. (2020). Modulation of T-cell activation markers expression by the adipose tissue-derived mesenchymal stem cells of patients with rheumatic diseases. *Cell Transplant.* 29, 963689720945682. doi:10.1177/0963689720945682

Kurte, M., Vega-Letter, A. M., Luz-Crawford, P., Djouad, F., Noël, D., Khoury, M., et al. (2020). Time-dependent LPS exposure commands MSC immunoplasticity through TLR4 activation leading to opposite therapeutic outcome in EAE. *Stem Cell Res. Ther.* 111, 416. doi:10.1186/s13287-020-01840-2

Lee, M. J., Kim, J., Kim, M. Y., Bae, Y. S., Ryu, S. H., Lee, T. G., et al. (2010). Proteomic analysis of tumor necrosis factor-alpha-induced secretome of human adipose tissue-derived mesenchymal stem cells. *J. Proteome Res.* 94, 1754–1762. doi:10.1021/pr900898n

Li, N., and Hua, J. L. (2017). Interactions between mesenchymal stem cells and the immune system. *Cell Mol. Life Sci.* 7413, 2345–2360. doi:10.1007/s00018-017-2473-5

Li, W., Ren, G., Huang, Y., Su, J., Han, Y., Li, J., et al. (2012). Mesenchymal stem cells: a double-edged sword in regulating immune responses. *Cell death Differ.* 199, 1505–1513. doi:10.1038/cdd.2012.26

Lu, S., and Qiao, X. (2021). Single-cell profiles of human bone marrow-derived mesenchymal stromal cells after IFN-γ and TNF-α licensing. *Gene* 771, 145347. doi:10.1016/j.gene.2020.145347

Mazini, L., Rochette, L., Admou, B., Amal, S., and Malka, G. (2020). Hopes and limits of adipose-derived stem cells (ADSCs) and mesenchymal stem cells (MSCs) in wound healing. *Int. J. Mol. Sci.* 214, 1306. doi:10.3390/Ijms21041306

Meisel, R., Zibert, A., Laryea, M., Gobel, U., Daubener, W., and Dilloo, D. (2004). Human bone marrow stromal cells inhibit allogeneic T-cell responses by indoleamine 2,3-dioxygenase-mediated tryptophan degradation. *Blood* 10312, 4619–4621. doi:10.1182/blood-2003-11-3909

Munir, S., Basu, A., Maity, P., Krug, L., Haas, P., Jiang, D. S., et al. (2020). TLR4-dependent shaping of the wound site by MSCs accelerates wound healing. *Embo Rep.* 215, e48777. doi:10.15252/embr.201948777

Mushahary, D., Spittler, A., Kasper, C., Weber, V., and Charwat, V. (2018). Isolation, cultivation, and characterization of human mesenchymal stem cells. *Cytom. Part A* 93A1, 19–31. doi:10.1002/cyto.a.23242

Naji, A., Eitoku, M., Favier, B., Deschaseaux, F., Rouas-Freiss, N., and Suganuma, N. (2019). Biological functions of mesenchymal stem cells and clinical implications. *Cell Mol. Life Sci.* 7617, 3323–3348. doi:10.1007/s00018-019-03125-1

Neuss, S., Becher, E., Wöltje, M., Tietze, L., and Jahnen-Dechent, W. (2004). Functional expression of HGF and HGF receptor/c-met in adult human mesenchymal stem cells suggests a role in cell mobilization, tissue repair, and wound healing. *Stem Cells* 223, 405–414. doi:10.1634/stemcells.22-3-405

Nieto-Nicolau, N., Martinez-Conesa, E. M., Fuentes-Julian, S., Arnalich-Montiel, F., Garcia-Tunon, I., De Miguel, M. P., et al. (2021). Priming human adipose-derived mesenchymal stem cells for corneal surface regeneration. *J. Cell. Mol. Med.* 2511, 5124–5137. doi:10.1111/jcmm.16501

Park, K. S., Kim, S. H., Das, A., Yang, S. N., Jung, K. H., Kim, M. K., et al. (2016). TLR3-/4-Priming differentially promotes Ca(2+) signaling and cytokine expression and Ca(2+)-dependently augments cytokine release in hMSCs. *Sci. Rep.* 6, 23103. doi:10.1038/srep23103

Pittenger, M. F., Discher, D. E., Peault, B. M., Phinney, D. G., Hare, J. M., and Caplan, A. I. (2019). Mesenchymal stem cell perspective: cell biology to clinical progress. *NPJ Regen. Med.* 4, 22. doi:10.1038/s41536-019-0083-6

Qi, K., Li, N., Zhang, Z., and Melino, G. (2018). Tissue regeneration: the crosstalk between mesenchymal stem cells and immune response. *Cell. Immunol.* 326, 86–93. doi:10.1016/j.cellimm.2017.11.010

Renner, P., Eggenhofer, E., Rosenauer, A., Popp, F. C., Steinmann, J. F., Slowik, P., et al. (2009). Mesenchymal stem cells require a sufficient, ongoing immune response to exert their immunosuppressive function. *Transplant. Proc.* 416, 2607–2611. doi:10.1016/j.transproceed.2009.06.119

Ridiandries, A., Tan, J. T. M., and Bursill, C. A. (2018). The role of chemokines in wound healing. *Int. J. Mol. Sci.* 1910, 3217. doi:10.3390/Ijms19103217

Sahu, A., Foulsham, W., Amouzegar, A., Mittal, S. K., and Chauhan, S. K. (2019). The therapeutic application of mesenchymal stem cells at the ocular surface. *ocular Surf.* 172, 198–207. doi:10.1016/j.jtos.2019.01.006

Saparov, A., Ogay, V., Nurgozhin, T., Jumabay, M., and Chen, W. C. (2016). Preconditioning of human mesenchymal stem cells to enhance their regulation of the immune response. *Stem Cells Int.* 2016, 3924858. doi:10.1155/2016/3924858

Shin, T. H., Lee, B. C., Choi, S. W., Shin, J. H., Kang, I., Lee, J. Y., et al. (2017). Human adipose tissue-derived mesenchymal stem cells alleviate atopic dermatitis via regulation of B lymphocyte maturation. *Oncotarget* 81, 512–522. doi:10.18632/oncotarget.13473

Shohara, R., Yamamoto, A., Takikawa, S., Iwase, A., Hibi, H., Kikkawa, F., et al. (2012). Mesenchymal stromal cells of human umbilical cord Wharton's jelly accelerate wound healing by paracrine mechanisms. *Cytotherapy* 1410, 1171–1181. doi:10.3109/14653249.2012.706705

Skibber, M. A., Olson, S. D., Prabhakara, K. S., Gill, B. S., and Cox, C. S. (2022). Enhancing mesenchymal stromal cell potency: inflammatory licensing *via* mechanotransduction. *Front. Immunol.* 13, 874698. doi:10.3389/Fimmu.2022.874698

Song, N., Scholtemeijer, M., and Shah, K. (2020). Mesenchymal stem cell immunomodulation: mechanisms and therapeutic potential. *Trends Pharmacol. Sci.* 419, 653–664. doi:10.1016/j.tips.2020.06.009

Szucs, D., Miklos, V., Monostori, T., Guba, M., Kun-Varga, A., Poliska, S., et al. (2023). Effect of inflammatory microenvironment on the regenerative capacity of adipose-derived mesenchymal stem cells. *Cells* 1215, 1966. doi:10.3390/cells12151966

Ti, D., Hao, H., Tong, C., Liu, J., Dong, L., Zheng, J., et al. (2015). LPS-preconditioned mesenchymal stromal cells modify macrophage polarization for resolution of chronic inflammation via exosome-shuttled let-7b. *J. Transl. Med.* 13, 308. doi:10.1186/s12967-015-0642-6

Ting, H. K., Chen, C. L., Meng, E., Cherng, J. H., Chang, S. J., Kao, C. C., et al. (2021). Inflammatory regulation by TNF-alpha-activated adipose-derived stem cells in the human bladder cancer microenvironment. *Int. J. Mol. Sci.* 228. doi:10.3390/ijms22083987

Trayhurn, P., Drevon, C. A., and Eckel, J. (2011). Secreted proteins from adipose tissue and skeletal muscle - adipokines, myokines and adipose/muscle cross-talk. *Archives physiology Biochem.* 1172, 47–56. doi:10.3109/13813455.2010.535835

Tu, Z., Li, Q., Bu, H., and Lin, F. (2010). Mesenchymal stem cells inhibit complement activation by secreting factor H. *Stem Cells Dev.* 1911, 1803–1809. doi:10.1089/scd.2009.0418

Vereb, Z., Mazlo, A., Szabo, A., Poliska, S., Kiss, A., Litauszky, K., et al. (2020). Vessel wall-derived mesenchymal stromal cells share similar differentiation potential and immunomodulatory properties with bone marrow-derived stromal cells. *Stem Cells Int.* 2020, 8847038. doi:10.1155/2020/8847038

Vereb, Z., Poliska, S., Albert, R., Olstad, O. K., Boratko, A., Csortos, C., et al. (2016). Role of human corneal stroma-derived mesenchymal-like stem cells in corneal immunity and wound healing. *Sci. Rep.* 6, 26227. doi:10.1038/srep26227

Wang, K. X., Chen, Z. Y., Jin, L., Zhao, L. L., Meng, L. B., Kong, F. T., et al. (2022). LPS-pretreatment adipose-derived mesenchymal stromal cells promote wound healing in diabetic rats by improving angiogenesis. *Injury* 53 (5312), 3920–3929. doi:10.1016/j.injury.2022.09.041

Wang, Y., Chen, X., Cao, W., and Shi, Y. (2014). Plasticity of mesenchymal stem cells in immunomodulation: pathological and therapeutic implications. *Nat. Immunol.* 1511, 1009–1016. doi:10.1038/ni.3002

Waterman, R. S., Tomchuck, S. L., Henkle, S. L., and Betancourt, A. M. (2010). A new mesenchymal stem cell (MSC) paradigm: polarization into a pro-inflammatory MSC1 or an Immunosuppressive MSC2 phenotype. *Plos One* 54, e10088. doi:10.1371/journal.pone.0010088

Wiese, D. M., Wood, C. A., Ford, B. N., and Braid, L. R. (2022). Cytokine activation reveals tissue-imprinted gene profiles of mesenchymal stromal cells. *Front. Immunol.* 13, 917790. doi:10.3389/fimmu.2022.917790

Wu, L., Cai, X., Zhang, S., Karperien, M., and Lin, Y. (2013). Regeneration of articular cartilage by adipose tissue derived mesenchymal stem cells: perspectives from stem cell biology and molecular medicine. *J. Cell. physiology* 2285, 938–944. doi:10.1002/jcp.24255

Xiao, K., He, W., Guan, W., Hou, F., Yan, P., Xu, J., et al. (2020). Mesenchymal stem cells reverse EMT process through blocking the activation of NF-kappaB and Hedgehog pathways in LPS-induced acute lung injury. *Cell death Dis.* 1110, 863. doi:10.1038/s41419-020-03034-3

Yagi, H., Soto-Gutierrez, A., Kitagawa, Y., Tilles, A. W., Tompkins, R. G., and Yarmush, M. L. (2010). Bone marrow mesenchymal stromal cells attenuate organ injury induced by LPS and burn. *Cell Transplant.* 196, 823–830. doi:10.3727/096368910X508942

Yu, G., Li, F., Qin, Y., Bo, X., Wu, Y., and Wang, S. (2010). GOSemSim: an R package for measuring semantic similarity among GO terms and gene products. *Bioinformatics* 267, 976–978. doi:10.1093/bioinformatics/btq064

Zhao, J., Peng, H., Gao, J., Nong, A., Hua, H. M., Yang, S. L., et al. (2021). Current insights into the expression and functions of tumor-derived immunoglobulins. *Cell Death Discov.* 7, 148. doi:10.1038/s41420-021-00550-9

Zwick, R. K., Guerrero-Juarez, C. F., Horsley, V., and Plikus, M. V. (2018). Anatomical, physiological, and functional diversity of adipose tissue. *Cell metab.* 271, 68–83. doi:10.1016/j.cmet.2017.12.002